

SYNTHESIS AND CHARACTERIZATION OF POLYURETHANE NANOCOMPOSITES

A THESIS

Submitted in partial fulfillment of the
Requirements for the award of the degree of

DOCTOR OF PHILOSOPHY

IN

Chemistry

BY

POOJA PURI

(Enrollment No.: 950809001)



School of Chemistry and Biochemistry
Thapar University, Patiala-147004, Punjab, INDIA

MAY 2016

अनेकसंशयोच्छेदि, परोक्षार्थस्य दर्शकम् ।
सर्वस्य लोचनं शास्त्रं, यस्य नास्ति अन्धैव सः ॥

it blasts many doubts, foresees what is not obvious |
science is the eye of everyone, one who hasn't got it, is like blind ||

CERTIFICATE

This is to certify that the thesis entitled “**Synthesis and Characterization of Polyurethane Nanocomposites**” being submitted by Ms. Pooja Puri in fulfillment of the requirements of the degree of **DOCTOR OF PHILOSOPHY**, in School of Chemistry and Biochemistry, Thapar University, Patiala is a record of the candidate’s own work carried out by her under our supervision and guidance. The matter embodied in this thesis has not been submitted in part or full to any other university or institution for the award of any degree.



Prof. Rajeev Mehta
(SUPERVISOR)

Professor
Department of Chemical Engineering,
Thapar University,
Patiala, (INDIA).



Prof. Sunita Rattan
(SUPERVISOR)

Professor
Department of Chemistry,
Amity Institute of Applied Sciences,
Amity University Uttar Pradesh, (INDIA).

To Shri Shri 108 Vishnu Dass Ji Maharaj

&

To Loving Memories of My Departed Father Pawan Kumar Puri

ACKNOWLEDGMENT

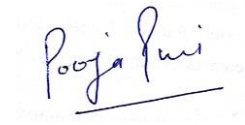
I sincerely express my gratitude to my supervisor and co-supervisor, Professor Rajeev Mehta and Professor Sunita Rattan, for consistent guidance in this research work. I am fortunate to have blessings of almighty, brought closer to my advisors, is always interested in exploring new research directions and ideas with deep vision, encouragement and dimension. They gave freedom in performing research activities and ensured that my various contents are neatly tied together. One can easily feel friend and philosopher in their disposition. I express my gratitude to Professor and Head, Bonamali Pal, and Professor S. D. Tiwari, my doctoral committee members, for the inspiring words and suggestions during my progress report presentations, which helpful in realization of the ultimate target of this project. I am deeply grateful to Professor O.P Pandey, Dean of Research and Sponsored Projects, for his excellent professional guidance and sincere advice to complete this research work.

This research has benefited from the ideas and suggestions of many well-wishers. Special thanks to Management, Jaypee University of Information Technology, Wagnaghat, for providing excellent research environment, learning ambiance at the campus and facilities for research activities on High-end Nano and Material Science Laboratories. A very special Thanks to Dr. G. D. Tyagi, Director – Shivalik Agro Poly Products Ltd. (SAP), Himachal Pradesh, for giving me an opportunity to work towards my Doctor of Philosophy (Ph.D.) research work.

I am eternally grateful to my respected in-law family members, Mother, and affectionate Sisters. Without their sustained moral support, it would have been impossible to succeed in writing this wonderful thesis. Words elude me expressing my sincere thanks to my husband Vivek, who offered every possible help and supported the long hours of preparation, that went into this effort. I feel greatly indebted to my daughter Prishi, for her love and patience, without which, it was impossible to complete this Ph.D. work.

I strongly commit and dedicate this achievement to his holiness, Shri Shri 108 Vishnu Dass Ji Maharaj, who is always transcendental entity to me and my departed Father, though they are

no more in worldly sense but their living guidance never left my spirit to work more and more and reach ultimate heights of the knowledge.

A handwritten signature in black ink that reads "Pooja Puri". The signature is written in a cursive style and is positioned above a horizontal line.

DATE: May 25, 2016

POOJA PURI

PLACE: Patiala

ABSTRACT

Current enthusiasm in the field of the nanotechnology leads to the development of nanocomposites as one of the rapidly evolving areas of composites research. Nanocomposites are multiphase materials, where one of the phases has nanoscale dimensions. Most nanocomposites composed of just two phases, one continuous phase called matrix and other nanophase dispersed in the matrix.

The objective to fabricate such nanocomposite materials is to obtain distinct properties evolved from the synergistic effects of the component materials. This may include improved physical or chemical properties, enhanced environmental stabilities that may be exploited for various applications such as military equipments, safety, protective garments, automotive, aerospace, electronics and optical devices.

At present, although nanocomposites employing CNTs as carbon based fillers are dominating but graphene and graphite nanoplatelets (GNPs) are considered to open a new area of functionalized nanocomposite systems in the near future. Graphene have high enormous surface area (up to $2630 \text{ m}^2 \text{ g}^{-1}$), high aspect ratio (200–1500), and high electrical ($10^6 \text{ (ohm cm)}^{-1}$) and thermal ($400 \text{ W m}^{-1} \text{ K}^{-1}$) conductivities . GNPs are small stacks of graphene and exhibits similar exceptional properties to pure monolayer graphene sheet as well as CNTs.

However, though the GNPs improve the electrical properties but there is not significant change in the mechanical properties of the prepared nanocomposites. Therefore, attempts were made to use a second filler with GNPs to retain/enhance the mechanical properties of PU along with its electrical properties. Using montmorillonite (MMT) clay to reinforce polymer-based composites have raised much attention to academic and industrial sectors due to the addition of small amount of clay could substantially enhance the mechanical properties of pristine polymers. Strong interfacial interactions between the dispersed clay layers and the

polymer matrix lead to enhanced mechanical, thermal and barrier properties of the virgin polymer.

The thesis entitled “Synthesis and Characterization of Polyurethane Nanocomposites” deals with the preparation of polymer graphite nanocomposites using GNPs and the montmorillonite clay as the nanofillers and polyurethane as the matrix material. Attempts have been made to synthesize composites using GNPs and polymers because the dispersion of GNPs in polymers shows various applications such as in solar cells, EMI shielding materials, LEDs, energy storage materials, electrochemical cells, sensors etc . The synthesis of polyurethane /organically modified montomoriillonite has also been attempted to study the effect of clay on mechanical properties of the nanocomposites. Finally, to study the synergic effect of both the fillers, GNPs and the clay in polyurethane, ternary nanocomposites based on GNPs, OMMT and polyurethane were prepared using in-situ polymerization.

PU/OMMT (Polyurethane/Organically Modified Montmorillonite) nanocomposites were prepared by in situ polymerization Technique. The structure of prepared nanocomposites and dispersion state of filler was studied and characterized by XRD and TEM. An intercalation type of morphology was observed by TEM. The mechanical properties of these nanocomposites at different loading levels of OMMT were also investigated using the Universal testing machine. The tensile strength, elongation at break and hardness shore were enhanced with the increase in the loading level of OMMT as compared to pure polyurethane. The obtained properties may be used in MEMS applications like pressure diaphragm, where the mechanical properties on nanoscale are crucial.

Further, the incorporation of GNPs was attempted in polyurethane. The polyurethane/graphite composites have been synthesized with the aim of using them for electromagnetic shielding applications. The polyurethane/graphite composites were prepared through in situ polymerization method in the presence of graphite nanoparticles. The prepared composites were characterized by scanning electron microscope, transmission electron microscope (TEM), and x-ray diffraction techniques. The shifting of the major peak of GNPs in prepared nanocomposites towards the left from 26.336 (d-spacing = 3.381 Å) to 25.374 (d-spacing = 3.507 Å) a 2θ scale indicates the intercalation type of dispersion in the prepared nanocomposites. This was further validated with the TEM characterization. The introduction of GNPs in PU during in situ polymerization creates an electrical network in the resulting composite, which therefore makes it highly conductive. The prepared nanocomposite showed an electrical network at 2.2 vol.% of the percolation threshold in DC condition and a similar

percolation threshold was found at 100 Hz in AC conditions. The maximum conductivity found at 6.5 vol.% of filler loading was 0.01 S/cm. The resulting composites were evaluated for electromagnetic interference (EMI) shielding at different filler loadings. The prepared PU/GNPs composites were found to be highly effective with shielding effectiveness of 19.34 dB, and with electromagnetic interference shielding materials at 0.9–1 GHz.

Finally, to study the synergic effect of both the fillers, GNPs and the clay in polyurethane, ternary nanocomposites based on GNPs, OMMT and polyurethane were prepared using in-situ polymerization with the aim of achieving low percolation threshold and improving the electrical and mechanical properties. The nanocomposites were evaluated for their electrical and mechanical properties and the results were compared with the corresponding binary systems, i.e., PU having GNP as the only filler. It was observed that the addition of OMMT at a concentration of around 2 wt%, significantly enhances the electrical and mechanical properties of the nanocomposites with the percolation threshold at much lower concentration of the GNPs. The excellent electrochemical properties arise due to formation of new 3D network (clay-graphite-clay or graphite-clay-graphite) and the synergistic effect between the three components.

LIST OF FIGURES

Figure No.	Title	Page No.
Figure 2.1	Schematic view of graphite layer structure	10
Figure 2.2	Schematic diagram illustrating the staging phenomenon in GIC.	12
Figure 2.3	SEM image of EG	13
Figure 2.4	Horn type sonicator	14
Figure 2.5	Schematic view of graphite layer structure (a) reduction of GO (b) various oxygen functionalities on edges and plans of GO	16
Figure 2.6	Layer structure of montmorillonite	20
Figure 2.7	Urethane linkage	21
Figure 2.8	Extension of (a) prepolymer with (b) diol chain extender	22
Figure 2.9	Chemical structure of different isocyanates	24
Figure 2.10	Formation of polyether	25
Figure 2.11	Structure of BDO	26
Figure 2.12	Structure of TMP	27
Figure 2.13	Different carbon based nanofillers used to prepare polymer nanocomposites	29
Figure 2.14	Different types of morphologies of polymer layer silicates nanocomposites	34
Figure 3.1	Graphite nanoparticles: (a) TEM, (b) particle size estimation from XRD, (c) particle size distribution in the TEM image (a).	43
Figure 3.2	Schematic diagram of whole synthesis process of polyurethane/graphite composites	44
Figure 3.3	X-ray diffraction of expanded graphite, graphite nanoparticles and prepared samples of composites.	46
Figure 3.4	X-ray diffraction of prepared samples of composites with different loadings.	47
Figure 3.5	SEM images of prepared PU/GNPs 1.5 vol.% composites with (a, b, e) low magnification at 1 μm , (f) high magnification at 1 μm , (c) low magnification at 10 μm , (d) high magnification at 10 μm .	49
Figure 3.6	HRTEM images of prepared PU/GNPs 0.5 vol.% composites with (a) SAED pattern of composite and lattice fringes of dispersed GNP, (b) number of graphene layers forming a thin graphene stack, (c) graphene layers in GNP and intercalation dispersion along with agglomeration of GNPs, (d) agglomerated part of GNP's at different edges, (e) GNPs clusters.	50
Figure 3.7	HRTEM images of prepared PU/GNPs 1.5 vol.% composites with (a) live FFT, (b) clusters of GNPs, (c)	51

	graphite nanoparticles size distribution in composite material, (d) high-resolution lattice fringes.	
Figure 3.8	Fringes profile of Figure 3.6d.	51
Figure 3.9	Interparticle distance (IPD) model for PU/graphite composite.	53
Figure 3.10	Geometrical orientations measurement for IPD using Matlab.	53
Figure 3.11	Surface morphology of composite material using image J.	54
Figure 3.12	Electrical conductivity of PU/graphite composites as a function of GNP content under DC conditions.	56
Figure 3.13	Electrical conductivity of PU/graphite composites as a function of GNP content under AC conditions.	57
Figure 3.14	Resistivity variations with temperature on different loadings of filler in composites.	58
Figure 3.15	Voltage, current characteristics of composite at percolation threshold.	60
Figure 3.16	Voltage, current characteristics of composite above percolation threshold.	61
Figure 3.17	Electrical conductivity of PU/graphite composites calculated from V I characteristics compared with experimental data.	62
Figure 3.18	Experimental setup for electromagnetic shielding effectiveness measurement.	64
Figure 3.19	SE of PU/graphite composites with different loadings of GNPs.	65
Figure 3.20	Schematic of (a) A typical RLC model for nano scaled interconnects, and (b) A transmission line circuit model for a driver-PU/GNPs interconnect-load configuration.	66
Figure 3.21	Time and frequency responses of PU/GNP composites based interconnects using (a) Impulse response, (b) Step response, (c) Bode plot, (d) Nyquist plot, (e) Nichols chart, (f) Pole zero map.	67
Figure 4.1	Schematic diagram of whole synthesis process of polyurethane/OMMT composites	73
Figure 4.2	X-ray Diffraction of pure Cloisite [®] 30B, and prepared samples of polyurethane/clay nanocomposites.	74
Figure 4.3	TEM images of prepared samples of polyurethane/clay nanocomposites.	75
Figure 4.4	Characterization of nanocomposite with universal testing machine.	76
Figure 4.5	Mechanical properties of PU/OMMT nanocomposites (a) tensile strength (b) elongation % (c) hardness shore A.	77-78
Figure 4.6	PU/OMMT as pressure MEMS (a) comsol simulation snapshots (b) deflection of round diaphragm (c) radial and tangential characteristics.	78-80
Figure 5.1	Schematic diagram of whole synthesis process of ternary PU/GNP/OMMT composites	85
Figure 5.2	X-ray Diffraction of GNPs, Cloisite 30B, and Prepared	87

	Samples of Ternary Composites	
Figure 5.3	SEM images of prepared PU/GNPs/Cloisite-30B composites: (a, b) Clay particles are anchored on the surface of GNPs, (c, d) The bundles of GNPs at high magnification.	89
Figure 5.4	TEM images of prepared PU/GNPs/Cloisite-30B composites, (a) Intercalated GNPs, (b) Intercalated OMMT, (c) Stacked graphene layers with high resolution lattice fringes, (d) Live FFT.	90
Figure 5.5	Profile of fringes to calculate d spacing.	91
Figure 5.6	Electrical conductivity of PU/GNPs and PU/GNPs/Cloisite-30B composites as a function of GNP content.	93
Figure 5.7	Geometrical orientations measurement for IPD using Matlab	94
Figure 5.8	Effect of clay concentration on electrical conductivity of ternary nanocomposite.	94
Figure 5.9	Tensile strength of pure PU, PU/GNPs, and PU/Cloisite-30B.	96
Figure 5.10	Elongation % of pure PU, PU/GNPs, and PU/Cloisite-30B.	97
Figure 5.11	Hardness Shore A of pure PU, PU/GNPs, and PU/Cloisite-30B.	98

LIST OF TABLES

Table No.	Title	Page No.
Table 2.1	Different types of modifiers used to modify clay particles	20
Table 2.2	Conductive polyurethane composites used for various applications	23
Table 3.1	Summary of the percolation threshold and maximum conductivity of various GNPs/polymer nanocomposites	55

Special Thanks To

Thapar University, INDIA

and

Jaypee University of Information Technology, INDIA

TABLE OF CONTENTS

	PAGE NO.
CERTIFICATE	iii
ACKNOWLEDGEMENT	v–vi
ABSTRACT	vii–ix
LIST OF FIGURES	x–xii
LIST OF TABLES	xiii
TABLE OF CONTENTS	xv–xvii
CHAPTER 1	1–9
INTRODUCTION AND MOTIVATION	1
1.1 Background	1
1.2 Problem Statement and Contributions	2
1.2.1 Objectives of dissertation	4
1.2.2 Contribution	5
1.3 Outline of the Thesis	8
CHAPTER 2	10–38
LITERATURE REVIEW	10
2.1 Graphite as Nanofiller	10
2.1.1 Structure of Graphite	10
2.1.2 Formation of GICs and their Expansion	11
2.1.3 Preparation of Graphite Nanoplatelets (GNPs) by Ultrasonication.	13
2.1.4 Preparation of Graphite Nanoplatelets via Graphite Oxide(GO)	15
2.1.5 Preparation of Graphite Nanoplatelets by Microwave Irradiation- Ultrasonication Method	17
2.1.6 Graphene	17
2.2 Clay as Nanofiller	18
2.2.1 Structure of Clay Particles	18
2.2.2 Modification of Clay Particles	19
2.3 Polyurethane(PU) as Matrix for Nanocomposites	21
2.3.1 Monomers to form Polyurethane(PU)	24
2.3.1.1 Diisocyanates	24
2.3.1.2 Polyols	25
2.3.2 Chain Extenders	26
2.3.2.1 Monols	26
2.3.2.2 Diols	26
2.3.2.3 Triols	27
2.4 Processing of Polymer/ Graphite Nanocomposites	27
2.4.1 Methods of Synthesis of Polymer/Graphite Nanocomposites	27
2.4.2 Electrical Properties of Polymer/Graphite Nanocomposites	28
2.5 Processing of Polymer/Clay Nanocomposites	33

2.5.1 Methods of Synthesis and Mechanical Properties of Polymer/Clay Nanocomposites	33
2.6 Ternary Nanocomposites	36
CHAPTER 3	39–69
SYNTHESIS OF CONDUCTIVE POLYURETHANE/GRAPHITE COMPOSITES FOR ELECTROMAGNETIC INTERFERENCE SHIELDING	39
3.1 Introduction	39
3.2 Experimental Section	41
3.2.1 Materials	41
3.2.2 Preparation of Expanded Graphite and Graphite Nanoplatelets	42
3.2.3 Preparation of Polyurethane Graphite Composites by <i>In-situ</i> Polymerization	42
3.2.4 Characterization	45
3.3 Results and Discussion	46
3.3.1 XRD Analysis	46
3.3.2 SEM and TEM Analysis	48
3.3.3 Electrical Conductivity and Percolation Threshold Measurement	52
3.4 EMI Shielding of Polyurethane Graphite Composites	62
3.5 Interconnect Track at Nanoscale in Integrated Circuits	66
3.6 Conclusion	68
CHAPTER 4	70–81
SYNTHESIS AND MECHANICAL PROPERTIES OF POLYURETHANE/CLAY NANOCOMPOSITES	70
4.1. Introduction	70
4.2. Experimental Section	71
4.2.1 Materials	71
4.2.2 Preparation of Polyurethane OMMT Nanocomposites by In-situ Polymerization	72
4.2.3 Characterization	72
4.3. Results and Discussion	74
4.3.1 XRD and TEM Analysis	74
4.3.2 Mechanical Properties	76
4.4. Conclusion	81
CHAPTER 5	82–99
SYNERGISTIC EFFECTS OF CLAY AND GNPS ON ELECTRICAL AND MECHANICAL PROPERTIES OF PU/GNP/OMMT TERNARY COMPOSITE	82
5.1. Introduction	82
5.2 Experimental Section	83
5.2.1 Materials	83
5.2.2 Preparation of Expanded Graphite and Graphite Nano Sheets	84
5.2.3 Preparation of Polyurethane Graphite Clay Composites by <i>In-Situ</i> Polymerization	84

5.2.4 Characterization	86
5.3 Results and Discussion	86
5.3.1 XRD Analysis	86
5.3.2 SEM and TEM Analysis	88
5.3.3 Electrical Conductivity and Percolation Threshold Measurement	91
5.4 Mechanical Properties	95
5.5 Conclusion	99
CHAPTER 6	100-101
CONCLUSION AND FUTURE SCOPE	100
6.1 Conclusion	100
6.2 Future Scope	101
REFERENCES	102-118
LIST OF PUBLICATIONS	119

CHAPTER 1

INTRODUCTION AND MOTIVATION

1.1 *Background*

In today's technological era there is a continuous demand of a multifunctional high performance materials with desirable mechanical, thermal, electricals, and chemical properties which can broaden their use to target or achieve a specific application. A lot of efforts are being in progress to create such noble materials by focusing on the area of polymer nanocomposites. The various properties of a polymer can be improved by adding inorganic nanofillers as a second phase in it. Polymer nanocomposites are the materials which are created by adding some nanoscale fillers to some microscopic sample material often referred to as matrix.

In other words, polymer nanocomposites the two phase material, where one of the phase has at least one dimension in nanometre range (10^{-9} m). The key factor which contributes to the improved properties of polymer is the uniform dispersion of nanofillers in it. The nanoscale dimensions of the filler produce ultra large interfacial area per unit volume responsible for improving the inherent properties of the polymer. In spite of improving the new properties, some properties may also be generated, which are not present in the neat polymer. Nanocomposites also provide opportunities to combine the diverse properties which otherwise may not be possible to achieve within a single material e.g. mechanical properties and conducting properties. Recently the conducting polymers have drawn attention towards them due to having many potential applications in areas like antistatic coatings, electromagnetic shielding, smart sensors, electrochemical display and so on. Conductive polymer nanocomposite can be prepared by incorporating the conductive nanofillers either in an insulating matrix or in a conductive one. In the present study polyurethane (PU) has been used as a matrix due to its myriad applications and which is insulating in nature. Various carbon based conductive nanofillers like CNTs, carbon black, carbon nanofibers, GNPs have been used for a long time to prepare polymer nanocomposites. Among these conductive fillers, the GNPs have attracted a great deal of attention

towards them due to their superior mechanical, electrical, and thermal properties. Moreover, the GNPs are highly cost effective and present abundantly in nature in the form of natural graphite flakes having layered structure. The other best combination of properties of GNPs like high modulus (1060 GPa) excellent electrical conductivity (104 S/cm at ambient temperature), thermal conductivity ($\sim 3000 \text{ W m}^{-1} \text{ K}^{-1}$), low dielectric constant (3 at ambient temperature), high aspect ratio (200 -1500) and enormous specific surface area ($\sim 2630 \text{ m}^2/\text{g}$), make it the preferred nanofiller to be used in synthesis of nanocomposites. The graphite lattice consists of many graphite layers stacked over one another. The challenge is how to separate these stacked graphene layers to nano meter range. A lot of research is going on to separate a single layer graphene to exploit the full benefit of graphite. The conductivity of nanocomposite is mainly varied as a function of filler concentration. The minimum amount of filler which must added to matrix, so that it starts to conduct due to formation of continuous conductive network throughout the matrix is called percolation threshold. The value of this percolation threshold is different for different conducting nanocomposites, because it is effected by many parameters like choice of filler and polymer matrix, processing methods, and dispersion of the filler in the matrix.

In the present study, the second filler, which has been reinforced into PU matrix, are the organically modified clay particles often referred as OMMT. The clays are used blended with PU to form the PU nanocomposite with enhanced mechanical properties. Beside primerly improving the mechanical properties of prepared nanocomposites, the clay particles are also supposed to enhance the thermal, barrier, and flame retardant properties of the neat polymer. But in the present study only mechanical properties of prepared nanocomposites of PU, are studied.

1.2 *Problem Statement and Contributions*

A number of polymers have been studied for a long time to prepare their nanocomposites, but conducting polymers are in great demand as they find their applications in many fields like high sensitive electromechanical MEMS, smart sensors, and high speed interconnects in modern integrated circuits. To prepare the conductive polymer nanocomposite, a conductive nanofiller is added either in a conductive polymer or an insulating one. The present study involves the

incorporation of, GNPs as conducting filler into PU, an insulating matrix to prepare their nanocomposites and evaluate them for EMI shielding applications.

Since PU is an insulator and has high abrasion resistance, tear resistance, shock absorption, resistance to weather and even hydrocarbons, so it has been one of the promising polymers to be used in nanocomposites synthesis. PU covers the advantages of rubbers and plastics both which make it a versatile material in a number of applications such as automotive, construction, electronics, glazing, footwear, many consumer products and from industrial components to biomedical area. PU can be synthesized by addition polymerization between a diisocyanate and a diol by using either a polyether or polyester as chain extender. The nanofillers can be dispersed into this matrix via various routes to prepare its nanocomposites. The major issue associated with the processing of these conducting polymer nanocomposites, is the degree of dispersion of conductive filler like GNPs and CNTs into the matrix. These fillers have the drawback to get agglomerated as their concentration approaches the percolation threshold. Moreover, for the conventional macrocomposite a large quantity of filler is required to reach the percolation threshold which leads to high density and deteriorate the mechanical properties of the composite. The challenge is, how to retain the mechanical properties of a composite along with its electrical properties at low percolation threshold. Various attempts are in progress to overcome this challenge by lowering down the percolation threshold as much as possible. More recently ternary nanocomposite have been prepared to retain the mechanical properties along with the conductivity by improving the degree of dispersion and lowering down the percolation threshold. In the present study three types of nanocomposites namely: PU/GNPs, PU/OMMT, and PU/GNPs/OMMT, were prepared with the aim to retain the mechanical properties by lowering down the percolation threshold.

The requirement of high performance multifunctional nanocomposite materials, which do have good electrical properties along with retained mechanical properties, to be used in applications especially in MEMS and smart sensors. One of the possible solution to enhance the mechanical properties of PU/GNPs nanocomposite is the addition of a nanofiller like clay. In order to optimize the properties of nanocomposite, an effort has been made in the present study to observe the effect of addition of clay nano particles along with GNPs to the PU matrix, on the

percolation threshold and mechanical properties of the prepared ternary nanocomposites, in comparison to neat PU, PU/GNPs, and PU/OMMT nanocomposites. Ternary nanocomposites obtained from PU/OMMT/GNPs offer the possibility to combine diverse properties which would not be possible otherwise in single material.

1.2.1 *Objectives of dissertation*

In view of the above discussion, the research problem was divided into three stages along with following objectives:

Stage I

- i. Synthesis of polyurethane/graphite nanocomposites by using *in-situ* polymerization technique at different loading levels of GNPs.
- ii. Study of electrical properties and calculation of percolation threshold of prepared nanocomposites.
- iii. The characterization of prepared nanocomposites by using XRD, SEM, and TEM.

Stage II

- i. Synthesis of polyurethane/OMMT nanocomposites by using *in-situ* polymerization technique at different loading levels of OMMT.
- ii. Study of mechanical properties (tensile strength, elongation at break, hardness Shore A) of the prepared nanocomposites.
- iii. The characterization of prepared nanocomposites by using XRD, SEM, and TEM.

Stage III

- i. Synthesis of polyurethane/OMMT/GNPs ternary nanocomposites by using *in-situ* polymerization technique at different loading levels of GNPs and of OMMT.

- ii. Study of electrical properties and calculation of percolation threshold of the prepared nanocomposites at fixed weight fraction of OMMT.
- iii. Study of mechanical properties (tensile strength, elongation at break, hardness Shore A) of the prepared nanocomposites at fixed weight fraction of GNPs.
- iv. The characterization of prepared nanocomposites by using XRD, SEM, and TEM.

1.2.2 Contribution

The contribution towards this research work, has been published in SCI journals, and is as follows:

1. *Pooja Puri, Rajeev Mehta, and Sunita Rattan “Synthesis of Conductive Polyurethane/Graphite Composites for Electromagnetic Interference Shielding” Journal of Electronic Materials, Springer, November 2015, Vol. 44, No. 11, pp 4255-4268*

The main findings of this contribution are:

- i. The PU/GNPs nanocomposites were prepared using *in-situ* polymerization.
- ii. The prepared nanocomposites showed an impartation of electrical network at 2.2 vol% as percolation threshold in DC condition and a similar percolation threshold was found at 100 Hz in AC conditions.
- iii. The percolation threshold was also validated with analytical methods. The prepared nanocomposites showed an impartation of electrical network at 2.2 vol% of the percolation threshold in DC condition and a similar percolation threshold was found at 100 Hz in AC conditions.
- iv. The variation of resistivity was studied at different loading of GNPs.
- v. The resulting composites were evaluated for electromagnetic interference (EMI) shielding at different filler loadings. The prepared PU/GNPs composites were found to be highly effective with shielding effectiveness of 19.34 dB.

- vi. The RLC model of a transmission line of PU/GNPs. interconnects made of N Parallel PU/GNP tracks of the same lengths L and widths W, is the possible application of these nanocomposites in integrated circuits.
- vii. The time and frequency responses of PU/GNP tracks were also studied for their stability at different loadings of GNPs.
- viii. The good EMI shielding is the additional benefit for crosstalk free tracks in integrated circuits.

2. Pooja Puri, Rajeev Mehta, and Sunita Rattan “Synthesis and Mechanical Properties of Polyurethane/Clay Nanocomposites” *Journal of Optoelectronics and Advanced Materials*, Vol. 16, No. 9-10, September - October 2014, pp 1126 – 1130.

The main findings of this contribution are:

- i. The introduction of nanoclay during the polymerization of PU enhanced the mechanical properties resulting nanocomposites.
- ii. The effect of loading level of OMMT 0.5wt%, 1.0wt%, and 1.5wt% on mechanical properties of PU was experimentally determined.
- iii. The same *in-situ* polymerization technique and the monomers were used to prepare these nanocomposites.
- iv. The tensile strength of nanocomposite samples was found to increase with the increase in wt% loading levels as compared to pristine PU because of good interfacial interaction between the OMMT layers and the polymer matrix.
- v. Also, expectedly the elongation % decreased with the clay (a ceramic) loading, however this downfall was very less as compared to pure PU and was maintained at a level close to that of pure PU.

- vi. The hardness shore A, values were also increased with the increase in % loading levels as compared to pristine PU.
 - vii. The improved mechanical properties were used for MEMS modeling for pressure measurement. A pressure diaphragm was simulated by using these properties as simulation parameters.
 - viii. The high sensitivity with good precision of pressure MEMS make them use in integrated circuits with signal conditioning and processing circuitry.
3. *Pooja Puri, Rajeev Mehta, and Sunita Rattan “Synergistic Effects of Clay and GNPs on Electrical and Mechanical Properties of PU/GNP/OMMT Ternary Composite” Journal of Optoelectronics and Advanced Materials, Vol. 17, No. 3-4, March - April 2015, pp 477-483.*

The main findings of this contribution are:

- i. Ternary PU nanocomposite were prepared using two nanofillers OMMT and GNPs by *in-situ* polymerization technique.
- ii. The percolation threshold was lowered to 0.6 vol% with addition of 2 wt% of OMMT. This was much lower as compared to percolation threshold of nanocomposite containing only GNPs as filler (2.2 vol%).
- iii. The reduction in the percolation threshold was due to the high degree of dispersion in the presence of clay particles.
- iv. With this improvement in percolation threshold, the electrical conductivity also increased as compare to PU/GNPs nanocomposites.
- v. Along with electrical properties, the effect of addition of OMMT was also studied for mechanical properties. It was observed that tensile strength and hardness shore

A increased as compared to PU/GNP nanocomposites but were lower than PU/OMMT nanocomposites

- vi. An opposite trend was found for elongation %. The elongation % decreased with an increase in loading levels of clay at constant fraction of GNPs (0.5wt %) in ternary nanocomposites.

4. *Pooja Puri, Rajeev Mehta, and Sunita Rattan “Polymer Nanocomposite with High Conductivity and Mechanical Strength” ICPPC-2010 Second International Conference on Polymer Processing and Characterization Kottayam, Kerala, India 2010.*

- i. Since the interconnect is a graphene based polymer nanocomposite, we can neglect the interlayer resistance of interconnect layers. Ion and Ioff currents varies linearly with thickness of interconnect and Ion/Ioff remains constant.
- ii. The conductive behavior can be explained by the percolation transition of the conductive network formation. In most cases, relatively large quantities of filler were needed to reach the critical percolation value, as the particle size is at micro- and millimeter scales.
- iii. The transition in conductive particle containing polymers was greatly affected by the aggregation, structure, average size and size distribution of the graphene.

1.3 *Outline of the Thesis*

The thesis has been organized into 6 chapters and out of that CHAPTER 1 presents Introduction comprises problem statement and contributions. CHAPTER 2 presents the history of polymer nanocomposites with different combinations of fillers and polymer matrices. This chapter also discussed the various methods of polymerization, characterization techniques, and applications of resultant nanocomposites. The preliminary notations are introduced to keep the clarity of usage

throughout the thesis, CHAPTER 3 presents the synthesis of PU/graphite nanocomposites by using *in-situ* polymerization technique at different loading levels of GNPs, CHAPTER 4 presents the synthesis of PU/OMMT nanocomposites by using *in-situ* polymerization technique at different loading levels of OMMT with the study of mechanical properties (tensile Strength, elongation at break, hardness Shore A) of the prepared nanocomposites, CHAPTER 5 presents the synthesis of PU/OMMT/GNPs ternary nanocomposites by using *in-situ* polymerization technique at different loading levels of GNPs and of OMMT. Finally, followed by the conclusion and future scope of the research work for further research are provided in CHAPTER 6.

CHAPTER 2

LITERATURE REVIEW

2.1 Graphite as Nanofiller

2.1.1 Structure of Graphite

Graphite is a well-known allotrope of carbon present abundantly in nature in the form of flakes. These natural graphite flakes are conductive in nature and have a layered structure. In layered structure of graphite 2s, 2px, and 2py electrons of carbon atom form three sp^2 hybridized orbitals, whereas the 2pz electron form a delocalized orbital of π symmetry, which is responsible for high conductivity of graphite [Chung *et al.* (2002); Dresselhaus *et al.* (2001)]. So, layered structure of natural graphite flakes is consist of number of graphite sheets having Interlayer spacing of 3.35 Å. Each sheet is further consisting of number of graphite nanosheets, which need to be separated from each other at nano level, so as to use them as nanofillers. In order to use the graphite as nanofillers in polymer nanocomposites synthesis, the first step is to separate or exfoliate the layers of graphite as thin as possible, because the high molecular weight polymers cannot be diffused into the small galleries of pristine Graphite [Mai *et al.* (2006)].

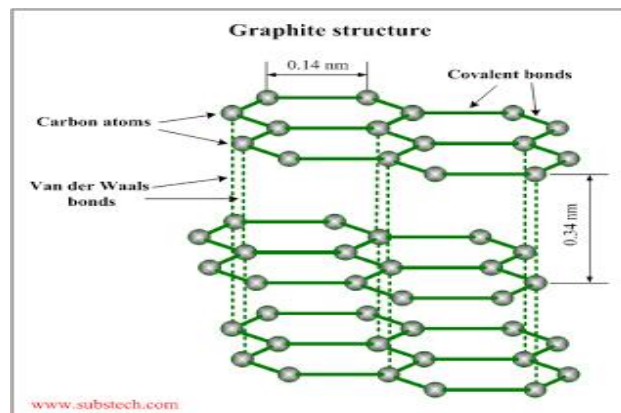


Figure 2.1: Schematic view of graphite layer structure [Chung *et al.* (2002)]

Unlike several laminar silicates, the Ion exchange reaction is not possible in graphite because the layers do not wear any net charges on them. Moreover, no any exchangeable ion group is present in the interlayer spacing of graphite, so direct intercalation of any organic polymeric molecule is not possible into the gallery of layers, as do layered silicates. But due to presence of weak Vander wall forces between the successive layers, the different species of atoms, ions, and molecules can be intercalated into the interlayer space, forming graphite intercalation compounds (GICs) also known as expandable graphite [Hwang *et al.* (2013)].

2.1.2 Formation of GICs and their Expansion

Generally, two types of GICs are formed during intercalation of chemical species in the gallery of graphite layers. One is donor type GIC formed by intercalation of donor species like alkali metals (potassium, sodium), and the other is acceptor type GIC formed by intercalation of electron acceptor species halogen, halide ions, and acids [Geng *et al.* (2013)]. Therefore, the formation of GIC is of great importance as it is the first step to prepare the GNPs from natural graphite. GICs can be formed by various synthesis methods (vapor phase transportation, liquid intercalation, intercalation by electrochemical technology, co-intercalation and sequential intercalation approaches). In vapor phase transportation method, the alkali metal compound is heated and passed through a tube to intercalate into the interlayer space of graphite [Dresselhaus *et al.* (2001)]. But this method needs some extreme precautions to be taken due explosive nature of pure alkali metals (like K) as they come in contact with moisture. When some intercalant enters into interlayer space of graphite, the staging phenomenon occurs. The term stage is the number of graphitic layers between two intercalate layers and is denoted by n. Generally, the stage1- stage5 GICs are formed as shown in Figure 2.2 [Chen *et al.* (2001); Yoshida *et al.* (2001)]. Various acids like nitric acid, sulphuric acid, perchloric acid, and selenic acid can be used to prepare GICs but the most commonly used GIC to prepare polymer nanocomposites is H₂SO₄-GIC (graphite bisulphate) [Stankovich *et al.* (2006); Xiao *et al.* (2002)]. Typically, the synthesis of H₂SO₄-GIC involves the chemical interaction of graphite with mixture of highly concentrated sulphuric acid and fuming nitric acid serving as oxidizing agents. GIC formed by this method still possess a layered structure

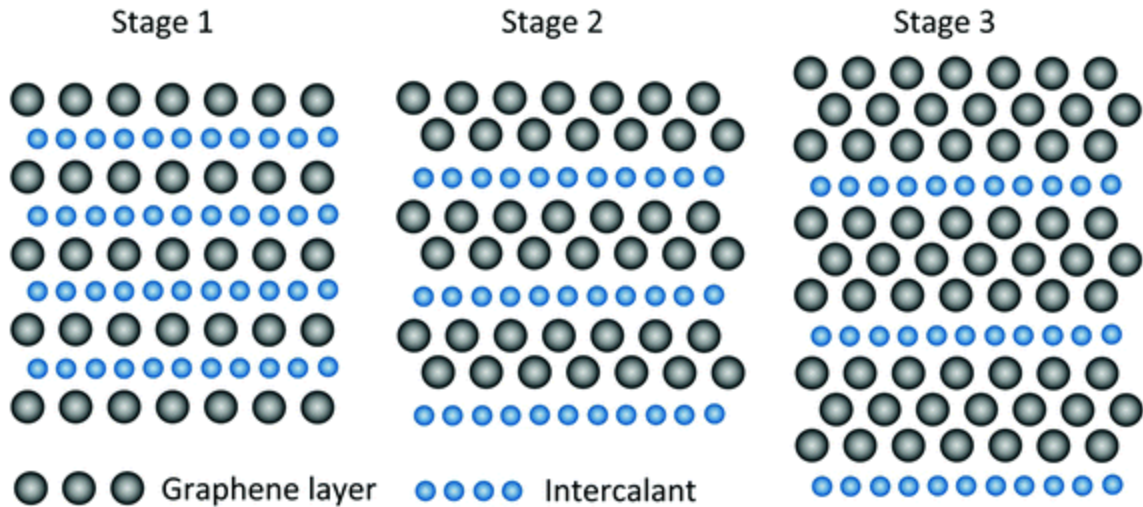
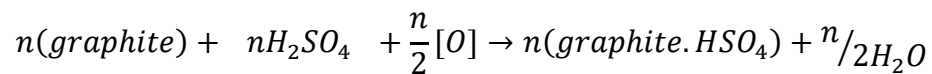


Figure 2.2: Schematic diagram illustrating the staging phenomenon in GIC.

like pristine graphite, but much lighter in color than it. This is due to loss of electronic conjugation brought about during the oxidation process. The reaction between graphite and concentrated sulphuric acid can be express as follows:



Where O is oxidant agent and *graphite.HSO₄* is GIC formed.

GICs have an extra ordinary properties of large expansion (up to hundreds of times) along the c – axis or thickness direction than in the in-plane direction. It can be expanded at elevated temperature by number of heating methods such as giving a thermal shock in muffle furnace at high temperature for few seconds and microwave irradiations. Generally, the exfoliation or expansion is carried out at 900°C or high temperature [Pawar *et al.* (2013); Raulo *et al.* (2015)]. As the GIC (any kind of GIC) is heated at high temperature, the intercalants which are trapped between the layers get volatilized, which push the layers apart from each other leading to expansion of layers along the c-direction, and a puffed up material having worm like shape with low density and high temperature resistance is obtained known as expanded graphite (EG). [Geng *et al.* (2013); Chen *et al.* (2003)] prepared EG by subjecting GICs to microwave irradiation in a microwave oven for 30 seconds and proved that microwave irradiation results into a more explosive expansion than heated

in a furnace. Microwave irradiation is more efficient than conventional heating in a furnace as it involves short reaction time and obtained EG particles can be easily handled.

2.1.3 Preparation of Graphite Nanoplatelets (GNPs) by Ultrasonication.

EG has a porous structure with worm like shape. The surface of EG exhibits many pores of different sizes, 10 nm – 10 μm and appears like a loose porous vermicular material having a honeycomb structure. It still possesses a layered structure as that of pristine graphite, but much larger interlayer spacing than pristine graphite and GICs. EG also offers a great compatibility with many organic polymers to form their nanocomposites, because it consists of many delaminated graphite sheets in nm thickness. However, the EG is not the fully exfoliated form of graphite and many stacks of graphite are still interlocked into expanded graphite.

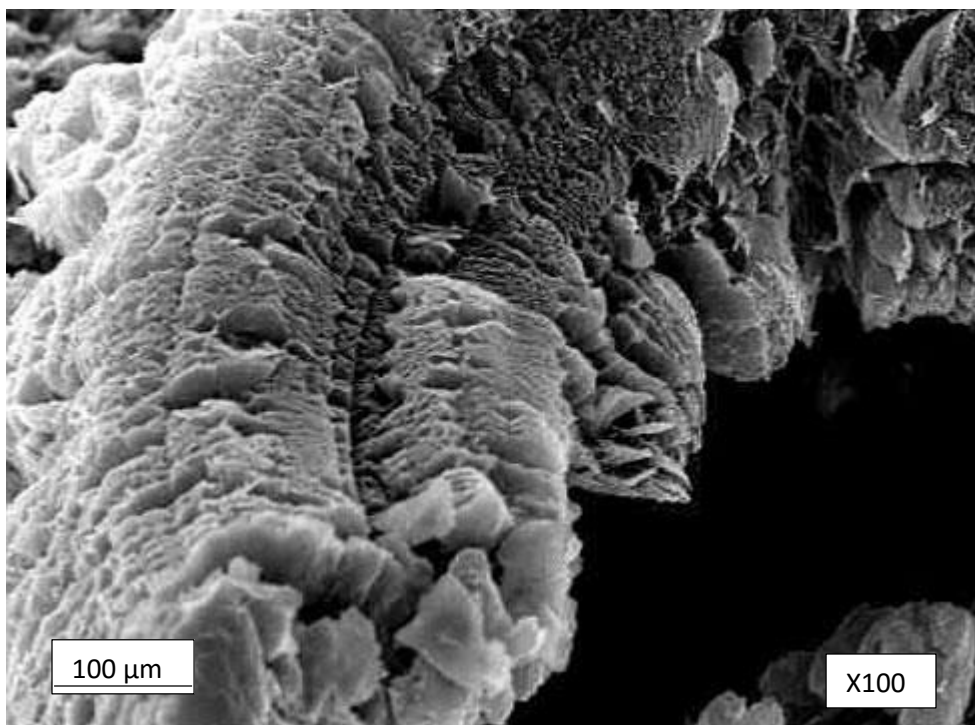


Figure 2.3: SEM image of EG



Figure 2.4: Horn type sonicator

In order to fully utilize the potential of graphite to prepare polymer nanocomposites, the EG has to be further breakdown to the thin graphite nanoplatelets or even individual graphene layers, which opens the windows to prepare the GNPs. Various methods are available in the literatures to prepare the GNPs and single layer graphene. The most common method is, “chemical intercalation - hot expansion – ultrasonication”. In this method first of all, GICs are prepared by treating the natural graphite flakes with concentrated acids (H_2SO_4 , HNO_3) and then followed by expansion of prepared GICs at high temperature to form EG. The EG particles are then sonicated in an ultrasonic bath or horn type sonicator for various time intervals in a particular solvent. [Chen *et al.* (2003)] prepared GNPs with this approach by sonicating the EG into alcohol solution for 8 hours and separated nanosheets with thickness of 32-80 nm and diameter of 0.5-20 μm were obtained. Similarly, [Fukuda *et al.* (1997)] prepared GNP is of thickness 70 nm thickness by the same approach. [Chen *et al.* (2004)] prepared the GNPs with same technique of sonication. The sonication was done for 10 hours and GNPs of thickness 52 nm as revealed by BET measurements, and diameter 13 μm , were obtained. The average thickness of nanoplatelets was found to be 50 nm based on the average value of 50 graphite sheets. It was also concluded that diameter of GNPs decreased with increase in irradiation time. [Li *et al.* (2009)]. also prepared the GNPs by sonicating

the expanded graphite in acetone for 8 hours. The thickness and average diameter of prepared GNPs were 4.5 nm revealed by TEM analysis and 46 μm measured by particle size analyzer. Ultrasonication is an efficient technique to exfoliate EG into GNPs with high aspect ratio

2.1.4 Preparation of Graphite Nanoplatelets via Graphite Oxide(GO)

The second approach used to prepare GNPs of very small thickness is via the formation of graphite oxide (GO). By adopting the GO approach, the single layer graphene (1nm thickness) could be obtained [Geng *et al.* (2009)]. Go was first prepared by Brodie about 150 years back. It can also be synthesized using method laid down by Staudenmaier or Hummer [Hummers *et al.* (1958)], which involves the oxidation of graphite using strong oxidants such as KMnO_4 , KClO_3 , and NaNO_2 in the presence of nitric acid or its mixture with sulphuric acid [Kim *et al.* (2010)]. Typically, this approach involves the treatment of natural graphite flakes with highly concentrated acids. In this way GO layers are obtained which are decorated with many oxygenated functional groups on the edges and planes [Cai *et al.* (2008)]. The oxide layers are then reduced by some reducing agents followed by ultrasonication in an aqueous media. The interlayer spacing of GO can vary from 6 to 10 Å depending upon the amount of water content. The exfoliation of GO is the efficient way to produce the graphene layers in bulk quantities. A lot of work has been reported on this route of preparation of graphene nanosheets by [Potts *et al.* (2011); Kuilla *et al.* (2010); Stankovich *et al.* (2010)].

GO is hydrophilic in nature due to presence of oxygen functionalities on the layers, so it can be dispersed in aqueous media only and not in organic solvents or polymers. [Park *et al.* (2009); Stankovich *et al.* (2006)], introduced the concept of chemical functionalization of GO by treating it with organic isocyanates. This treatment reduces the hydrophilic character and make GO possible to be dispersed in polar solvents like DMF. It leads to complete exfoliation of GO sheets with about 1nm thickness. Due to chemical functionalization of layers, GO is insulator in nature, so the reduction is carried out to restore back the sp^2 bonds of graphite. Out of many reducing agents, they found the hydrazine-hydrate is the best one to produce the thin graphene like sheets. [Stankovich *et al.* (2007)], proposed the following mechanism for reduction of graphite oxide using hydrazine.

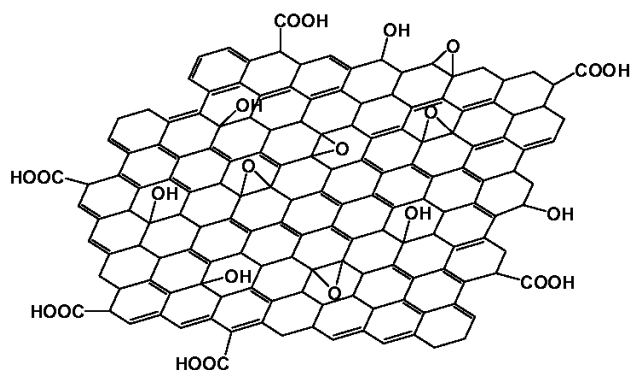
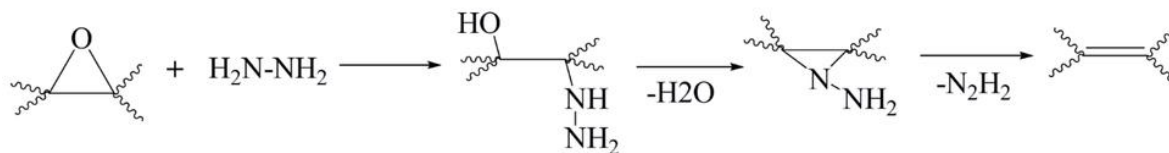


Figure 2.5: Schematic view of graphite layer structure (a) reduction of GO (b) various oxygen functionalities on edges and plans of GO

This type of reduction of GO involves the hazardous nature and high cost of chemicals used in the process, so limits its applicability to produce graphene sheets in bulk quantities. To overcome this issue, another route called thermal exfoliation and reduction can be used by heating the dry GO at high temperature in an inert environment. The so called graphite oxide sheets obtained by this method are known as thermally reduced graphene oxide sheets. This type of reduction results into formation of highly wrinkled graphene oxide sheets due to structural defects caused by evolution of CO_2 , after decomposition of oxygen functionalities of GO. [Compton *et al.* (2010)] has prepared the partially reduced graphene based sheets from GO by Hummer's method with the help of sonication in aqueous media followed by reduction with hydrazine-hydrate at 100°C . These partially reduced graphene based sheets were converted to fully reduced graphene sheets by annealing at 250°C for 2 hr under N_2 .

[Dikin *et al.* (2007)], concluded in one of their studies that just like CNTs graphene oxide sheets can be assembled into a paper like material under a directional flow. The thickness of obtained free standing graphene oxide paper was from 1-30 μm . This was achieved by vacuum filtration of

colloidal dispersion of graphene oxide sheets with anodisc membrane, filter. [Wang *et al.* (2008)] has further proved in one of his studies that chemically converted graphene obtained by reduction of GO have the tendency to precipitate as irreversible agglomerates due to their hydrophobic nature, so their dispersion become difficult in the aqueous and organic solvents [Park *et al.* (2009)]. [Li *et al.* (2008)], overcame this issue and concluded in one of their studies that surfactant and polymeric materials are not required to ensure the stability of colloidal solution of graphene sheets rather they achieved their stability by maximize the charge density with addition of ammonia to increase the pH. around 10. The resulting electrostatic forces acted to stabilized the aqueous suspension.

2.1.5 Preparation of Graphite Nanoplatelets by Microwave Irradiation-Ultrasonication Method

Besides above mentioned methods, the GNPs can also be prepared by microwave irradiation [Zhang *et al.* (2010); Falcao *et al.* (2007)] and sometime followed by ultra-sonication [Srivastava *et al.* (2008)]. By using this approach, many researchers have successfully prepared GNPs of thickness 10-30nm with various intercalants trapped between the layers. Recently [Kumar *et al.* (2015)]. have successfully prepared GNPs from expandable graphite of nitric acid and sulfuric acid by first microwave irradiations for three minutes followed by second microwave irradiations for three minutes after socking the expandable graphite into strong oxidizing agents. [Menendez *et al.* (2010); Hu *et al.* (2011); Wei *et al.* (2009)] have found this method of producing GNPs more versatile and efficient one due to having many advantages such as ecofriendly nature, short reaction time with energy transfer instead of heat transfer, and higher safety.

2.1.6 Graphene

The single layer graphene which is only one atom thick is attracting attention day by day due to having a potential of providing extraordinary thermal, electrical and mechanical properties in the field of material science, nanoelectronics and condensed matter physics. Until 2004, it was believed that graphene sheets cannot exist in free state, because they are thermodynamically unstable in nature [Sengupta *et al.* (2011); Novoselov *et al.* (2005); Viculis *et al.* (2005)]. But with the discovery of free standing graphene in 2004, the total scenario about graphene was changed. It gave a boost up to many researchers to produce graphene in bulk quantities. In 2010 [Geim *et al.*

(2011)], Geim and Novoselov received noble price in physics for discovery of graphene. In 2004 first of all graphene was prepared by [Geim *et al.* (2011)], using scotch-tape method. This method involved the peeling of graphene from highly oriented pyrolytic graphite (HOPG) using scotch-tape. Then this monolayer of graphene was captured on a silicon wafer with SiO₂ layer in its top, by dipping the scotch-tape in acetone. This method is also known as micromechanical cleavage method. The other methods used to prepare graphene are chemical vapor deposition (CVD), epitaxial growth of graphene on electrically insulated substrates like silicon carbide.

2.2 Clay as Nanofiller

2.2.1 Structure of Clay Particles

The present work is dealing with addition of clay as nanofiller in PU matrix with primary aim of improving its mechanical properties so it is worthwhile to give a brief account of these nanoparticles.

The addition of clay nanoparticles in polymer matrix not only improve its mechanical properties but some other properties may also be enhanced which include, gas barrier properties, increased heat distortion temperature, flame retardancy, increased thermal stability, chemical resistance, electrical conductivity. The polymer/ clay nanocomposites are optically transparent in comparison to conventionally filled polymers due to very small thickness of clay nanolayers as compared to wavelength of visible light. The clay particles are most commonly used layered silicate to synthesize polymer nanocomposites due to their unique structure and properties [Zeng *et al.* (2005)]. Clay particles are present abundantly in nature and are cost effective. Their rich intercalation chemistry, high strength and stiffness and high aspect ratio make them a suitable filler to be used as in preparation of polymer nanocomposites. The most commonly used nanoclay is Montmorillonite(MMT) which belongs to smectite family of clays. Although the clay minerals like talc and mica are used for so many years as fillers to prepare composites but they are non-expendable in nature. MMT is not present as nanoparticles in nature but it can be easily exfoliated or delaminated to nano platelets with a thickness of about 1nm and an aspect ratio of 100 to 1500 and surface areas of 700 - 800-meter square per gram [Goettler *et al.* (2007)]. MMT is a layered silicate which has 2:1 type structure. it consists of two layers of silica tetrahedral and one layer of

Alumina octahedral or magnesia octahedral. The two tetrahedral layers sandwich the octahedral layer sharing their apex oxygen with the later. These three layers form one clay sheet which has thickness near about 1 nm. The layers are held together by weak vander- wall forces, so the layers can be easily delaminated to increase the interlayer spacing called gallery between them. Due to isomorphic substitution of aluminium (Al) with magnesium(Mg), iron(Fe) and Lithium(Li) in octahedral sheet and silicon(Si) with aluminium (Al), a negative charge of charge density between 0.5 and 1.3 occurs on each sheet [Mou *et al.* (2007)]. Due to presence of positive charge metal ions like sodium, calcium and magnesium in the interlayer space, the layers are held together to each other by compensating the charges. These charge compensating cations provide a route for rich intercalation reach chemistry and surface modifications of clay layers required to disperse them into polymer matrices.

2.2.2 *Modification of Clay Particles*

The silicate clay layers are hydrophilic in nature, but polymers tend to be hydrophobic so both are incompatible to each other. The challenge is to disperse the clay particles effectively and uniformly into polymers due to their different nature. Due to this drawback of clay particles, the surface modification of these particles is required to disperse them properly in the polymer matrix. A lot of methods are available in Literature to modify the surface of clay particles such as adsorption, Ion Exchange with inorganic cations, grafting of organic compounds, reaction with acids ultrasound, intraparticle and interparticle polymerization etc. [de Paivaet *et al.* (2008)]. Ion exchange reaction is most commonly used to modify the clay particles. The exchange reaction could be used to replace the inorganic exchangeable ions present in galleries between the layers with alkyl ammonium surfactants. This opens the galleries enough and make them hydrophobic, so that a polymer can be intercalated between the layers. Such types of modified clays are known as organophilic clays. The number of ammonium surfactant ions that can exchange the positive charge cations in the galleries depends on charge density on the clay particles. At lower charge densities, the surfactant packs in monolayers and as the charge density increases, bilayers and trilayers can be formed [Navratilova *et al.* 2007]. Such a modified clay is referred as organoclay and denoted by OMMT. The OMMT are named as Cloisite 15A, 20A, 25A, and Cloisite 30B etc. depending upon the type of modifier used to modify them as described in the table.

Table 2.1: Different types of modifiers used to modify clay particles

MMT clay	Organic modifier	Chemical structure of Modifier
Cloisite Na+	None	None
Cloisite 15A	2M2HT: dimethyl, dehydrogenated tallow, quaternary ammonium	$\begin{array}{c} \text{CH}_3 \\ \\ \text{HT}-\text{N}^+-\text{CH}_3 \\ \\ \text{HT} \end{array} \quad \text{Cl}^-$ <p>Where HT is Hydrogenated Tallow (~65% C18; ~30% C16; ~5% C14) Anion: Chloride</p>
Cloisite 20A	2M2HT: dimethyl, dehydrogenated tallow, quaternary ammonium	$\begin{array}{c} \text{CH}_3 \\ \\ \text{HT}-\text{N}^+-\text{CH}_3 \\ \\ \text{HT} \end{array} \quad \text{Cl}^-$ <p>Where HT is Hydrogenated Tallow (~65% C18; ~30% C16; ~5% C14) Anion: Chloride</p>
Cloisite 30B	MT2EtOH: methyl, tallow, bis-2-hydroxyethyl, quaternary ammonium	$\begin{array}{c} \text{CH}_2\text{CH}_2\text{OH} \\ \\ \text{H}_3\text{C}-\text{N}^+-\text{T} \\ \\ \text{CH}_2\text{CH}_2\text{OH} \end{array}$ <p>Where T is Tallow (~65% C18; ~30% C16; ~5% C14) Anion: Chloride</p>

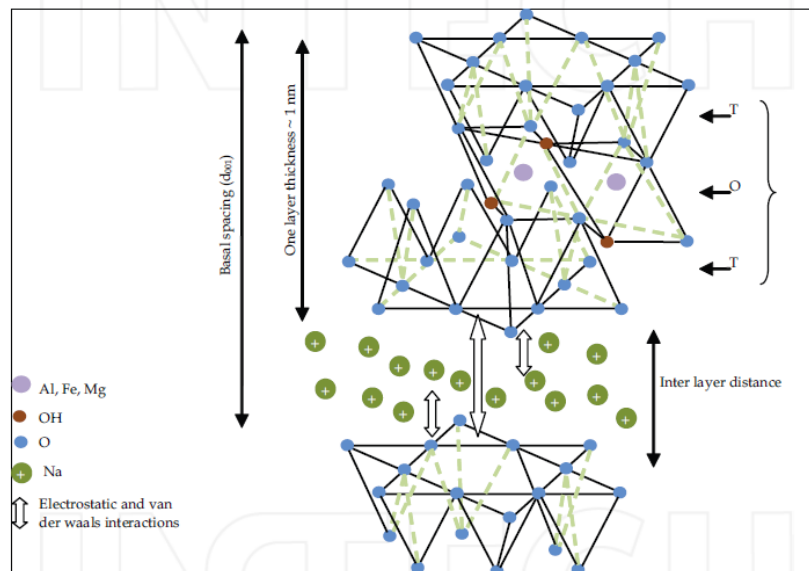


Figure 2.6: Layer structure of montmorillonite [Zeng et al. (2005)]

2.3 Polyurethane(PU) as Matrix for Nanocomposites

Nanoparticles incorporated into PU is the object of active experimental investigation, so it is worthwhile to give a brief account of this polymer. The discovery of polyurethane(PU) dates back to the Year 1937 by Otto Bayer and his coworkers at the laboratories of I.G. Farben in Leverkusen, Germany. The commercial scale production of PU was started with toluene diisocyanate(TDI) and polyester polyols in around 1952, when polyisocyanates were commercially available. lycra was the first Spandex fiber produced by DuPont by reacting PTMG poly (tetra methylene ether) glycol and 4,4- diphenyl methane diisocyanate(MDI) and ethylene diamine. After this PU was available from flexible PU foams to rigid PU foams.

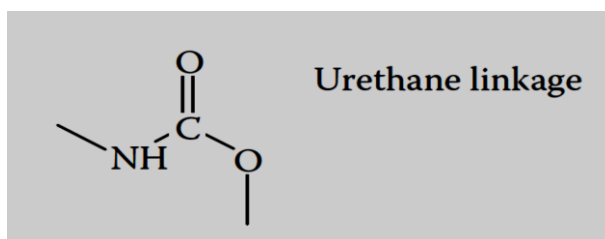
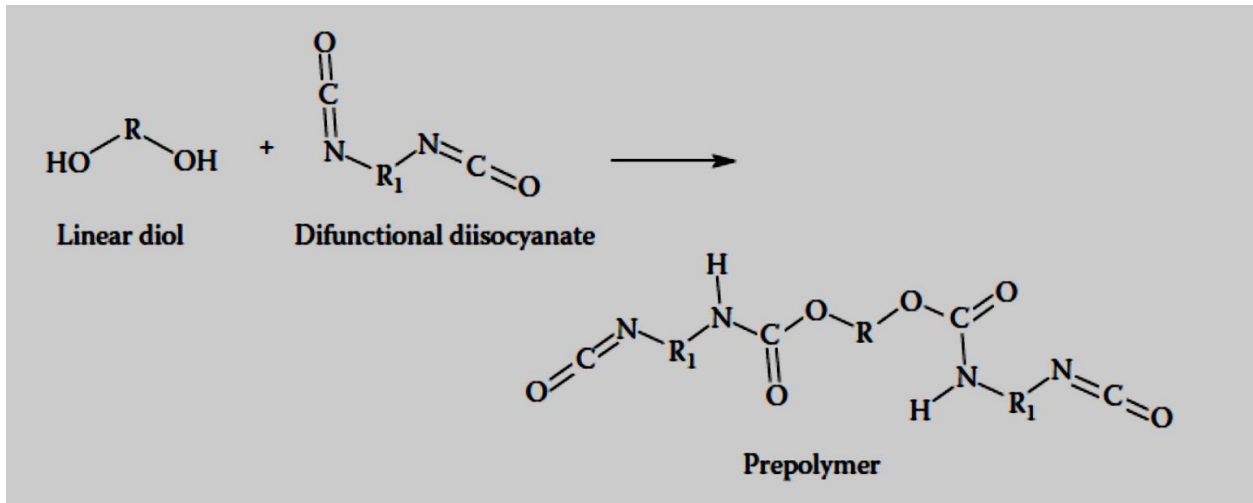


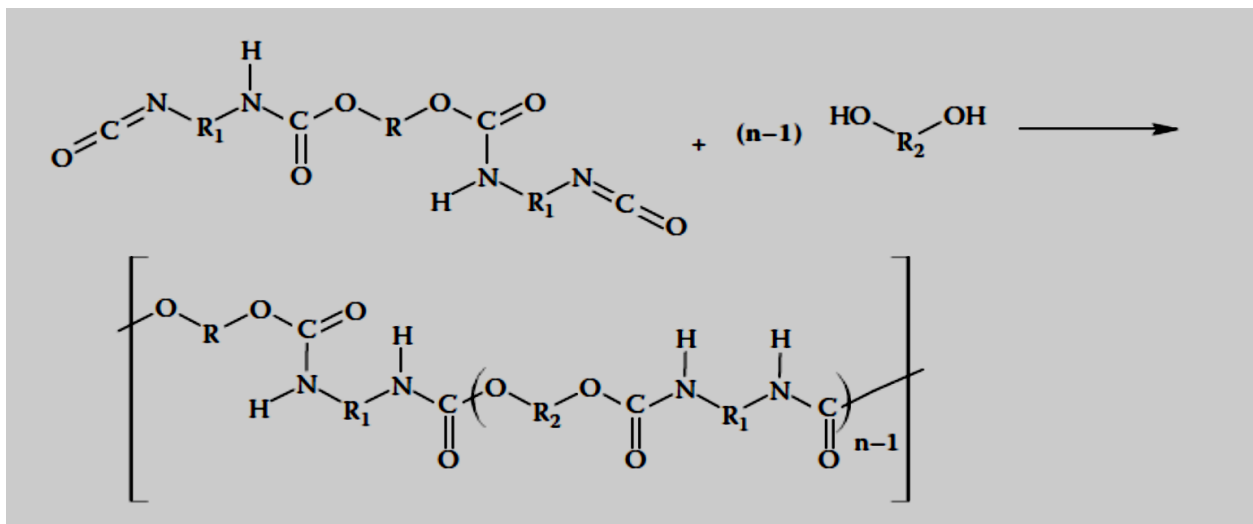
Figure2.7: Urethane linkage

polyurethanes are the organic Polymers that contain urethane linkage in their structure as shown in Figure 2.7. They are typically made by the reaction of a polyol with a diisocyanate followed by the addition of additives such as chain extenders, catalysts. and blowing agents. The initial step in the synthesis of PU is the formation of a prepolymer by reacting a suitable linear diol with difunctional isocyanate as shown in Figure 2.8 a. The prepolymer is formed by addition polymerization reaction and no any by product is formed during the reaction. The molecular weight of the prepolymer is too low to form the polymer, so the overall molecular weight is increased by addition of chain extender to the prepolymer as shown in Figure 2.8 b. The whole synthesis of PU should be carried out in an inert atmosphere and free of moisture. If water is present in the surrounding, it will react with isocyanate group liberating carbon dioxide, which will make the whole reactants spongy and processing would be difficult to carry out. The resulting polymer may be a liquid form or a solid form with various advantages and limitations, mainly depends upon the different isocyanates and polyols constituents. The potential applications of PU varies from

domestic level to industrial level [Gurunathan *et al.* (2015)]. The different kinds of PU can be used in different applications for example; the flexible form in upholstered furniture, transportation,



(a)



(b)

Figure2.8: Extension of (a) prepolymer with (b) diol chain extender

packing, rigid foam in insulation in walls and roofs. Thermoplastic PU are used in medical devices and footwear to coatings, adhesives, sealants and elastomers used in floors and automotive interiors. In industries PUs find their uses in rollers of all shapes and sizes. Due to excellent wear resistance of PUs the find their applications in the mining industries also. Conductive PU in its composite form is used in many applications as listed in Table 2.2

Table 2.2: Conductive polyurethane composites used for various applications [Gurunathan *et al.* (2013)].

S.No	Conductive material used (wt%)	Conductivity of the composite(S/cm)	Demonstrated/suggested application	References
1	PAni (30 wt%)	4×10^{-4}		[Rodrigues <i>et al.</i> (2003)]
2	PAni (34 wt%)	8×10^{-2}	Antistatic	[Kwon <i>et al.</i> (2004)]
3	PAni (1–75 wt%)	3.3×10^{-1}	Antistatic	[Kwon <i>et al.</i> (2004)]
4	PAni (10 wt%)	1.7×10^{-5} – 2.4×10^{-5}	Fuel cells, dialysis	[Amado <i>et al.</i> (2006)]
5	SPAni	1.1×10^{-2} – 2.2×10^{-5}		[Li <i>et al.</i> (2007)]
6	PAni (30 wt%)	1.7×10^{-6} – 1.5×10^{-2}		[Vicentini <i>et al.</i> (2007)]
7	PAni (10.6–26.4 wt%)	1×10^{-8}	Antistatic	[Wang <i>et al.</i> (2009)]
8	PAni (2 wt%)	1×10^{-4}	Corrosion protection	[Ahmad <i>et al.</i> (2009)]
9	PTh	10^{-4} – 10^{-2}		[Sari <i>et al.</i> (2003)]
10	PPy	10^{-7} – 10^{-2}	Pressure sensing	[Brady <i>et al.</i> (2005)]
11	PPy-30 wt%	2.6×10^{-1}	Sensors, packaging materials	[Kotal <i>et al.</i> (2011)]
12	PPV		Photoelectrochemical cells	[Wang <i>et al.</i> (2003)]
13	Carbon black		VOC sensor, shape-memory	[Chen <i>et al.</i> (2004)]
14	SWCNTs (3 wt%)	5.9×10^{-3}	Shape-memory	[Lee <i>et al.</i> (2011)]
15	MWCNTs (10 %)	5.3	Flexible electronic displays	[Shang <i>et al.</i> (2011)]
16	SWNTs (5 wt%)		Microwave absorption	[Liu <i>et al.</i> (2007)]
17	Opt. active MWCNTs (0.5 wt%)	1.58×10^{-3}	Intelligent textiles	[Jung <i>et al.</i> (2007)]
18	MWCNTs (5 wt%)	1×10^{-3}	Shape-memory	[Cho <i>et al.</i> (2005)]
19	SWCNT ? PPy	9.8×10^{-3}	Shape-memory	[Sahoo <i>et al.</i> (2007)]
20	CNTs with azo ggroup		Photonic devices	[Yang <i>et al.</i> (2007)]
21	CNTs with Ni–Fe nano		Removal of trichloro-ethylene	[Krause <i>et al.</i> (2010)]
22	MWCNTs		Biomedical	[Meng <i>et al.</i> (2005)]
23	Graphene (2 wt%)	10^{-5} , 10^{-8}	Various applications	[Kim <i>et al.</i> (2010)]

2.3.1 Monomers to form Polyurethane (PU)

2.3.1.1 Diisocyanates

The isocyanate constitutes the major part of PU. It forms the hard or rigid part of it. Mainly three types of isocyanates are used to prepare PU namely toluene diisocyanate (TDI), 4,4 diphenyl methyl diisocyanate (MDI), and 1,5-naphthalene diisocyanate (NDI). The aromatic diisocyanates may also be used, but they are less reactive as compared to aliphatic ones. TDI exists in two types of isomers namely 2,4 and 2,6 TDI. It can be used in two ways to synthesize PU, either it can be used as 80:20 mixtures of 2,4 and 2,6 isomers or pure 100 % 2,4 TDI can also be used.

In the present study we have used pure 2,4 isomers because it results in formation of high performance polyurethane material. The second reason to choose TDI over MDI is that MDI has tendency to get dimerize readily so it has to be stored at a temperature of - 4 degree Celsius which is practically not possible.

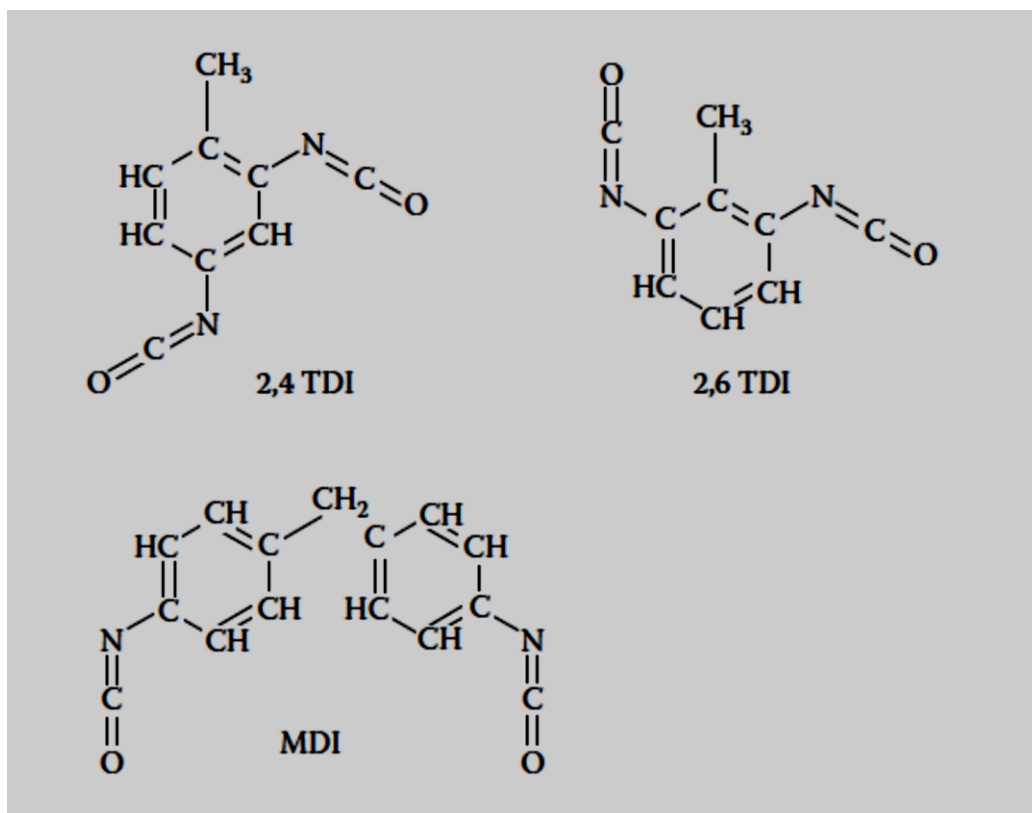


Figure 2.9: Chemical structure of different isocyanates

2.3.1.2 Polyols

These form the soft segment of PUs and provide flexibility to them. These are the linear molecules with molecular weight ranging from 400 – 7000. Two types of polyols namely polyethers and polyesters are generally used to synthesize polyurethane depending upon their advantages and limitations [Sahay *et al.* (1980); Bhushan *et al.* (2008)].

Polyethers have good hydrolytic stability than polyester polyols due to presence of ether group in their structure. Commonly two types of polyether are used to synthesize polyurethane. These are polypropylene glycol(C3) and polytetramethylene glycol(C4). These two types of polyethers are formed by addition polymerization reaction of some monomeric epoxide in the presence of a catalyst as shown in Figure 2.10.

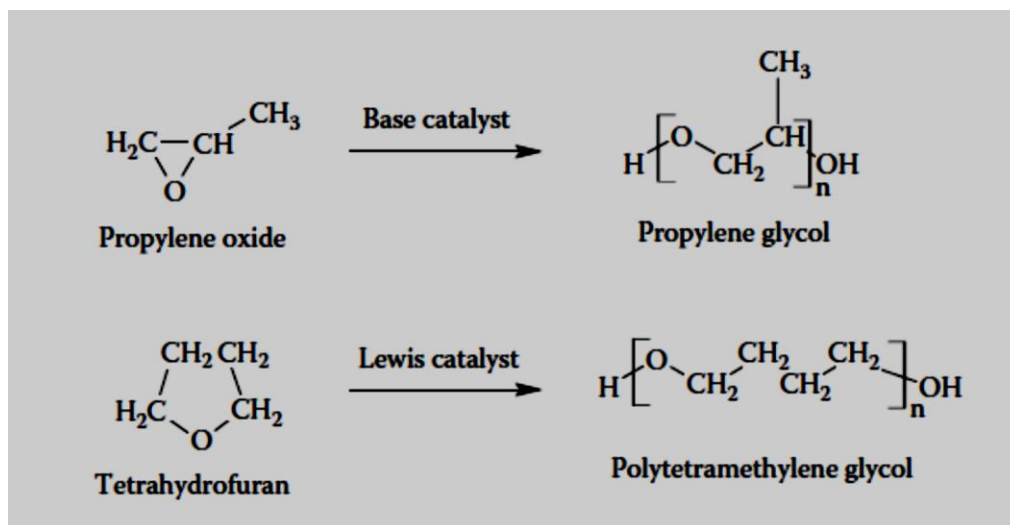


Figure 2.10: Formation of polyether

the polyesters have lower hydrolytic stability than polyether polyols but better oil resistance. These are also prone to fungal attack. The various types of polyesters used to form polyurethane are, the dibasic acid reacted with diol, polycaprolactone materials and polycarbonate based materials. The esterification reaction conditions during the synthesis of polyesters should be such, that the terminal groups should be hydroxyl groups at the end of reaction. Polycaprolactone are formed by ring opening of caprolactone. The various polycarbonates which can be used to form PU are poly (ethylene ether carbonate) and poly (propylene ether carbonate).

2.3.2 Chain Extenders

The two types of chain extenders which can be added to the prepolymer during the synthesis of PU are diamines and hydroxyl compounds (monol, diol and triols). Aromatic diamines are generally used as chain extenders in TDI based polyurethane, but one major drawback with aromatic diamine is the rate of reaction. The rate of reaction with aromatic diamine is too fast to control for normal use and some substitutes are required to add in the aromatic ring to control the rate of reaction. The PU formed by amines chain extender have better mechanical properties, but low temperature resistance than formed with diol chain extenders.

Hydroxyl compounds are also frequently used as chain extenders during synthesis of PU. These are classified as:

2.3.2.1 Monols

The water and alcohol can be used as chain extender under this category, but these have disadvantage of liberating CO₂ during their reaction with diisocyanates, which is not desirable for the strength of polyurethane formed.

2.3.2.2 Diols

diols have the advantages of no liberation of CO₂ due to formation of urethane linkage during the reaction. The various diols have been ranked in following order to obtain the desirable properties in formed polyurethane

Ethylene glycol > 1,3 propane diol > 1, 4 butanediol > 1,5 pentanediol > 1,6 hexane diol.

among these diols the most commonly used diol is 1, 4 butanediol(BDO).

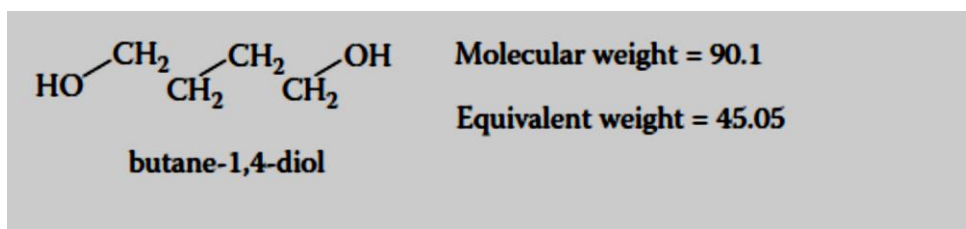


Figure 2.11: Structure of BDO

2.3.2.3 Triols

Trimethylol propane(TMP) can also be used as chain extender, but they lead to cross -linking in the polyurethane chains. Glycerol can also be used, but due to its hygroscopic nature it causes problem in processing.

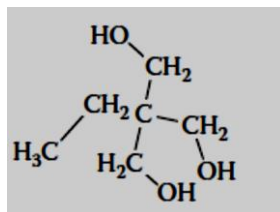


Figure 2.12: Structure of TMP

2.4 Processing of Polymer/ Graphite Nanocomposites

2.4.1 Methods of Synthesis of Polymer/Graphite Nanocomposites

inorganic fillers have been used for a long time for the modification of polymers in various aspects. But as the size of filler has decreased from microscale to nanoscale, it has brought a revolutionary change in the production of low cost, light weight, high performance and multifunctional composites. The nanoscale fillers have high aspect ratio and less structural defects as compared to their microscale counterparts, so are more efficient in improving and generating the new properties in a neat polymer. The polymer graphite nanocomposites are in great demand because they find their applications in many fields like antistatic coating, electrochemical displays, sensors, catalysis, redox capacitors, electromagnetic shielding and in secondary batteries.

There are generally three methods to prepare polymer graphite nanocomposites; solution processing or compounding, melt processing or mixing and in-situ polymerization technique . The solution processing method involves the use of a polymeric solution and the graphite nanoparticles are mixed and dispersed in a particular solvent. The polymer should also be soluble in the same solvent. Due to presence of weak van der Waals forces between graphite nanoplatelets, they can be easily dispersed in adequate solvent and in the meantime the polymer adsorbs onto the delaminated sheets. When the solvent is evaporated, all the mixture precipitated out and the polymeric chains are kinetically trapped in the layers of graphite nanoparticles forming an intercalated or exfoliated

type of nanocomposite. A strong stirring environment such as a sonication is required in this process to break down the graphite nanoplatelets as thin as possible. This method has certain limitations such as it requires a large amount of solvent and high temperature to dissolve the polymers, so this method may pose some serious environmental pollution. In the melt blending process, exfoliated graphite nanoplatelets are mixed with the polymer matrix in the molten state. Due to the neutral nature of graphite, the polymeric chains can easily be diffused into the galleries of GNPs, forming an intercalated or exfoliated nanocomposite. This technique is solvent-free but requires many dispersing agents like twin screw extruder, injection molding, twin roller, etc. The in-situ polymerization technique involves the use of monomers instead of polymers. The monomers are polymerized in the presence of the filler. The generated polymer chains, as they grow, separate the graphite nanosheets and enter the interlayer space to form the polymer nanocomposites. The polymerization can be initiated by heat or radiation, by a suitable initiator and some particular catalyst. The catalyst is generally prefixed inside the interlayer space of GNPs after the swelling step by the monomers. This method ensures strong interaction between the filler and the polymer matrix, and a well-dispersed intercalated or exfoliated nanocomposite is obtained. Although this technique facilitates the good dispersion of the filler in the matrix, this technique has certain limitations also. This method is not suitable for gaseous monomers such as polyethylene, polystyrene. Since heating is required in this method during the processing of nanocomposites, it is also an electrical energy-consuming process. Sometimes the molecular weight of the generated polymers may be low due to the termination of active centers responsible for chain growth. The active centers may be terminated due to the formation of reactive species such as radicals and ions generated from the treatment of graphite. It leads to the formation of low molecular weight polymers, which is not desirable to improve the mechanical properties of the composites.

2.4.2 Electrical Properties of Polymer/Graphite Nanocomposites

Conductive polymer composites have been started to be prepared during the early 1970s by dispersing graphite as a conductive filler into various polymer matrices. But the micro-scale size of these graphite filler particles leads to high density and reduced mechanical properties of the prepared composites. Since then, efforts are in progress to synthesize polymer-graphite nanocomposites by using graphite as a filler in the nanometer scale [Khanam *et al.* (2015)]. The conducting polymer

nanocomposites are synthesized by incorporation of conductive filler like GNPs, carbon nanotubes (CNTs), graphene, and fullerenes into the polymer matrix as shown in Figure 2.x.

These are the promising materials which are currently and in future be applied in many applications, examples are antistatic materials, electromagnetic interference shielding for electronic devices, electrochemical displays and sensors etc. The conductive behavior of polymer graphite nanocomposites is explained by percolation theory which has been explained in the successive chapter 3. Also, according to percolation theory, there occurs insulator- conductor transition in polymer nanocomposites, when a continuous conductive network is formed by the filler particles for the first time in the polymer matrix. Initially when a small amount of filler content is added in the polymer matrix, the resistivity does not show much variation and it closely matches to that of pure polymer.

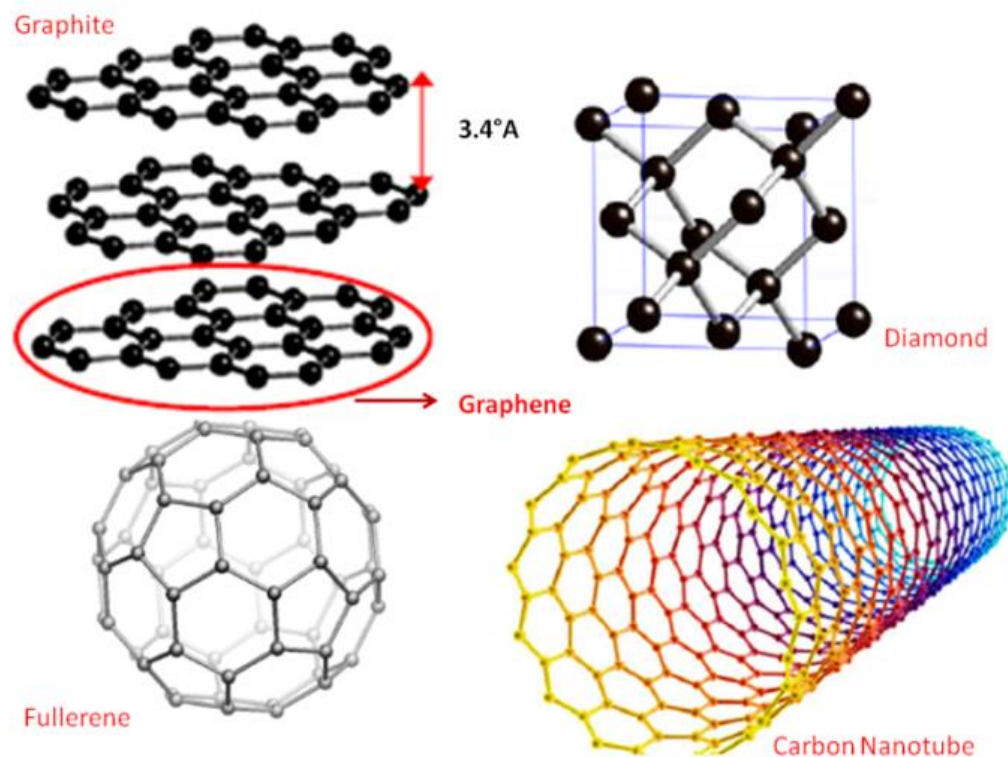


Figure 2.13: Different carbon based nanofillers used to prepare polymer nanocomposites

But as the quantity of filler is increased further, the resistivity starts showing variation and a stage is reached when there is a sharp decrease in resistivity due to formation of a continuous conductive network of filler particles. This minimum amount of filler at which the insulator- conductor transition occurs is called percolation threshold and denoted by P_c . The value of P_c is different for different polymer matrices. During early 1990 with the development of expanded graphite, efforts were put to prepare polymer graphite nanocomposites by using expanded graphite as nanofiller by in situ polymerization technique. [Celzard *et al.* (1996)]. successfully prepared epoxy resin/expanded graphite nanocomposites by in situ polymerization technique by incorporating expanded graphite flakes of thickness 100nm. The percolation threshold for these prepared nanocomposites was found to be 1.3vol%. Similarly, [Chen *et al.* (2001)]. successfully prepared polystyrene/expanded graphite nanocomposites by the same technique and they found that percolation threshold was achieved at 1.8 wt.%. Several other polymer matrices like poly (methyl methacrylate) (PMMA), poly (vinyl chloride) (PVC), poly (styrene- methyl methacrylate) have been successfully reinforced with expanded graphite by the same technique. [Chen *et al.* (2003)] and co-workers have successfully prepared nanocomposites of methyl methacrylate (MMA) and styrene(St) monomers using GNPs and conventional graphite powder(7500 mesh) as fillers by in-situ polymerization technique. Ultrasonication was carried out to ensure the good dispersion of both the fillers in the matrix . They made a comparison of percolation thresholds of two types of composites prepared and found that composite filled with GNPs exhibits percolation threshold at 1.0 wt % and other composite containing conventional graphite powder filler exhibits percolation threshold at 7.0 wt.%. Similarly in their another study they successfully prepared polystyrene/ GNP nanocomposites by in situ polymerization technique and good dispersion of GNPs was achieved indicated by TEM. The percolation threshold for these prepared nanocomposites was found to be 1.0 wt % . Another approach of preparing nanocomposites based on anhydride cured epoxy resin with graphite nanoparticles was proposed by [Yasmin *et al.* (2003)] They used various processing techniques like direct, sonication, shear and combined sonication and shear to prepare the nanocomposites. They reported that nanocomposites formed by shear mixing showed good dispersion of GNPs and have best modulus improvement as compared to other processing techniques. [Wei *et al.* (2009)] prepared two types of nanocomposites based on vinyl chloride/vinyl acetate copolymer using graphene nanosheets formed from GO and graphene nanosheets formed from EG by ultrasonication in acetone for 20h . They used in situ reduction-

extractive dispersion technique to prepare these nanocomposites. The GO was reduced by hydrazine and better dispersion was obtained by using GO due to reduction extractive technique as revealed by optical microscopy. The percolation threshold of nanocomposites based on GO was found to be 0.15 vol % which was much lower than achieved by incorporation of EG (0.7 vol. %). [Wakabayashi *et al.* (2008)], proposed another approach of preparing polypropylene/ graphite nanocomposites by using solid-state shear pulverization(SSSP) method and single- screw melt extrusion process. The graphite used was not given any pretreatment and was used as such as received. Shear and compressive forces helped for good dispersion of graphite in the matrix at nanometre scale as indicated by TEM. Nanocomposites made by SSSP technique indeed showed better mechanical properties as compared to composites made by single- screw melt extrusion process. [Stankovich *et al.* (2006)], prepared well dispersed polystyrene/ graphene nanocomposites by complete exfoliation of GO followed by reduction with dimethyl hydrazine. The polymer was added before the reduction step so it was a key factor and helped to prevent the agglomeration of sheets. The percolation threshold for prepared nanocomposites was found to be 0.1vol.% , which is the lowest reported value of p_c for any carbon based composite except for those involving carbon nanotubes. [Uhl *et al.* (2005)], prepared nanocomposites based on Polyamide-6(PA-6) using virgin graphite, expandable graphite and expanded graphite through melt blending process and their mechanical properties were studied. The tensile modulus of PA-6 was improved on addition of graphite but at the same time elongation at break and strength were decreased. The flame retardant properties were also enhanced on addition of graphite as compared to PA-6/ clay nanocomposites. [Du *et al.* (2004)], have successfully prepared poly (4,4 prime-oxybis (benzene) disulfide)/ graphite nanocomposites by using in situ- ring opening polymerization of cyclo(4,4- oxybis(benzene) disulfide oligomers. The graphite nanosheets were dispersed at 200°C. The GNPs were well dispersed and an intercalated type of morphology was formed in prepared nanocomposites indicated by TEM. The percolation threshold for prepared nanocomposites was found to be app. 4wt % GNPs [Stankovich *et al.* (2006)], synthesized first time the nanocomposites based on polystyrene using individual graphene sheets as filler via the route of GO using solution compounding technique. Dimethylformamide (DMF) was used as a solvent to incorporate these graphene sheets into polystyrene matrix. GO was given a chemical treatment with phenyl-isocyanate in order to increase its compatibility with organic polymer. Another study reported by [Kim *et al.* (2010)], compared first time the use of two types of graphene

sheets derived from GO. They exfoliated the layers of graphene sheets from GO firstly by giving organic isocyanate treatment to GO in dimethylformamide (DMF) and secondly by thermal reduction of GO at high temperature. They also compared first time the three different types of methods of dispersion of graphene sheets in thermoplastic((TPU). The good Dispersion of graphene sheets were achieved by solvent blending technique as compare to melt processing technique. The electrical and mechanical properties of prepared nanocomposites by three different methods were also compared. The percolation threshold of 0.5wt % was observed by solvent blending technique using thermally reduced graphene sheets(TRG). The increased tensile modulus and decreased nitrogen permeation of TPU was achieved at 3 wt % of isocyanated treated GO by using in-situ polymerization technique. In the recent study reported by [Kim *et al.* (2015)], various conducting polymers (polythiophene, polyethylene and polypropylene) have been reinforced with few layer graphene sheets derived from GO by in- situ polymerization technique. In this study GO was used as chemical oxidant. The study reported by [Yousefi *et al.* (2015)], concluded that a good dispersion of reduced graphene oxide sheets was achieved in aq. emulsion of polyurethane(PU) by ultrasonication. The graphene sheets of GO were highly oriented and well dispersed at about 2 wt.% of GO loading level. The percolation threshold was found to be 0.07 vol.% for the prepared nanocomposites. The improved mechanical properties were also obtained at loading level of 3 wt% of graphene sheets of GO. A recent study on synthesis of thermoplastic polyurethane (TPU) reinforced with exfoliated graphite(EG) via melt mixing and compression molding has been proposed by [Valentina *et al.* (2015)]. The shielding effectiveness of about 20 DB was reported at loading level of 20 wt % of EG [Quan *et al.* (2015)]. synthesized nanocomposites based on thermoplastic polyurethane (TPU) and graphene nanoplatelets (GNPs) using a single solvent throughout the process. The uniform dispersion of GNPs was achieved in the matrix, which resulted in improved mechanical properties, thermal stability and flame retardant behaviour of polyurethane(PU). [Li *et al.* (2007)], reported a study, where they tried to improve the electrical conductivity of GNPs by their vapor phase bromination treatment . These bromine(Br) treated GNPs were dispersed into epoxy resin by high shear mixer and ultrasonication. Due to bromination treatment, two types of bonds (ionic and covalent bonds) were induced between carbon and bromine. The fraction of ionic bonds reached to maximum at 3h bromination exposure, which accounted for the maximum conductivity (from 353 S/cm to maximum of 540 S/cm). On the other hand the formation of covalent bonds displaced some of carbon atom from the highly

planner structure of pristine graphite. This lead to decrease in carrier concentration and hence the electrical conductivity was also decreased. The percolation threshold of prepared nanocomposite with untreated GNPs was found to be 1wt % (app. 0.5 vol %). The bromination treatment did not affect the percolation threshold value of prepared nanocomposites. They concluded that percolation threshold mainly depends upon the aspect ratio of filler and bromination treatment is not expected to have a significant effect on aspect ratio of GNPs. In their another study, they reported the synthesis of epoxy nanocomposites based on UV/ O₃ treated GNPs. The UV/O₃ treatment had a significant effect on morphology, mechanical and electrical properties of prepared nanocomposites. The electrical resistivity of nanocomposite with treated GNPs was reduced much faster than the nanocomposites prepared with GNPs of without treatment by eliminating unbonded gaps or microvoids. The percolation threshold of prepared nanocomposite was about 1.0 wt %.(0.5 vol %) and this value is lower than those reported in Literature. [Chen *et al.* (2003)] have reported a lot of studies on synthesis and percolation threshold of polymer graphite nanocomposites. Some examples are PMMA (P_c 0.31 vol %), P_c for unsaturated polyester 0.64 vol%(1.65 wt %), nylon 6(P_c 0.75 vol %), SR (P_c 0.9 vol %) respectively.

2.5 Processing of Polymer/Clay Nanocomposites

2.5.1 Methods of Synthesis and Mechanical Properties of Polymer/Clay Nanocomposites

The same three basic approaches are used to synthesize polymer- clay nanocomposites as discussed in previous section. polymer clay nanocomposites are organic/ inorganic hybrid polymers containing clay platelets as nanofillers. The nanoclay platelets are characterized by high aspect ratio and high surface area/ volume ratio and ease of modification of their surfaces in order to make them compatible with organic polymers. If these clay platelets are properly dispersed in a polymer matrix at a loading level of 1-5 wt%, they can impart unique combinations of properties such as enhancement in mechanical properties (strength, modulus and toughness), physical properties (thermal and barrier), chemical resistance, fire resistance and along with maintaining high degree of optical clarity.

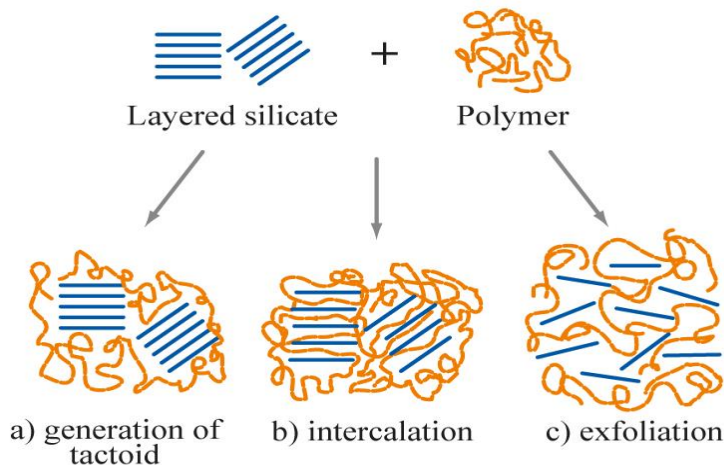


Figure 2.14: Different types of morphologies of polymer layer silicates nanocomposites

The enhancement in properties is directly related to degree of exfoliation and dispersion of platelets in the polymer matrix. Greater the separation of layers of clay platelets while dispersing in polymer matrix, more the chances of obtaining an exfoliated type of morphology in the prepared nanocomposites. The two typical types of morphologies (intercalated, exfoliated) formed in polymer nanocomposites are shown in Figure2.14

The enhancement in mechanical properties of a particular polymer may find their applications in fields like automotive and aerospace industry due to significant weight reduction. Due to improved barrier properties, the polymer/ clay nanocomposites may find their applications as packaging materials and being optically transparent in nature these may be used in packaging industries as wrapping films, beverage containers, packing for processed meat, cheese and dairy products etc . Recently a study has been reported where nylon - 6 exfoliated nanocomposite have been used to prepare or new grade of plastic film for food packaging. Polymer/ clay nanocomposites may also be used as electro material in biosensors, smart windows, and may also find their applications in biomedical fields in drug delivery and in medical devices.

The first mention of polymer- clay nanocomposites goes back to 1949 when [Bower *et al.* (1949)] carried out the adsorption of DNA by using montmorillonite clay. In 1963, Greenland prepared polyvinyl alcohol montmorillonite nanocomposite in aqueous [Anadão *et al.* (1949)]. medium. In 1976, Fujiwara and Sakomoto of the Unitika Co. described the first organoclay hybrid polyamide nanocomposite. However the first industrial application of clay nanocomposites was reported by [Kato *et al.* (2005); Ahmadi *et al.* (2005)] researchers at the Toyota Central research laboratory in

1988. They synthesized nylon 6/OMMT nanocomposites by using in-situ polymerization technique with ϵ -caprolactam as monomer. This group reported a significant enhancement in tensile strength, tensile modulus, flexural strength, flexible modulus and heat distortion temperature as compare to neat nylon 6. Timing belt having good rigidity and excellent thermal stability was the first commercial product made by this group by using these prepared nylon 6/OMMT nanocomposites [Shanmuganathan *et al.* (1998)]. The in-situ polymerization technique got a boost up to prepare different kinds of polymer clay nanocomposites after the pioneer work reported by Toyota group. [Wang *et al.* (1998)], reported the first prepared polyurethane /clay nanocomposite in 1998. These nanocomposites had improved strength, toughness and modulus as compared to the neat polyurethane(PU). [Cheng *et al.* (1998)], prepared polyurethane (PU) nanocomposites by solution blending technique using OMMT and modified OMMT named as MOMMT. OMMT was modified by grafting 4,4-Diphenylmethane diisocyanate (MDI) on the surface of OMMT. The grafting was favored due to interaction of hydroxyl groups (OH) present on the surface of montmorillonite and isocyanate groups (NCO) present on MDI. They reported that PU/MOMMT nanocomposites exhibit increased tensile strength and tear strength but decreased elongation at break as compared to PU/ OMMT nanocomposites. [Yu *et al.* (2008)], synthesized PU/ OMMT nanocomposites by using in-situ polymerization technique. They used to modify the clay with Octadecylammonium salt and PU was polymerized with poly(propylene glycol) PPG, 4,4-diphenylmethane diisocyanate(MDI) and 1-4, butanediol. They found that with increase in OMMT loading level, tensile strength and tear strength were increased as compare to neat polyurethane(PU) and PU/ pure MMT nanocomposites. Even the tensile strength and tear strength of PU/ pure MMT nanocomposites were lower than pure PU due to poor dispersion of pure MMT platelets in PU matrix. [Jeong *et al.* (2008)]. reported the synthesis of MMT/ poly(ϵ -caprolactone)- based polyurethane cationomer named as MMT/ PCL- PUC nanocomposites based on biodegradable polyurethane via solution blending technique using DMF(dimethyl formamide) solvent. They reported that better exfoliation of MMT up to 7wt.% was achieved by introducing quaternary ammonium groups in the main PCL-PUC chain. They also studied mechanical properties, thermal stability and biodegradability of prepared nanocomposites. They found that with increase in loading level of MMT, the Young's modulus of MMT/PCL-PUC nanocomposites were increased because of good interfacial interaction between filler and the polymer matrix. However, the elongation at break and maximum stress were decreased with increase in loading level of MMT

beyond 1wt %. At 1wt % these properties were closely matching to pure PCL-PUC . They also reported the increase in biodegradability of prepared nanocomposites with increase in loading level of MMT because of good dispersion of MMT in the matrix and less phase separated morphology was formed in the prepared nanocomposites. In another study reported by [Ni et al (2004)]. the polyurethane(PU)/OMMT nanocomposites were prepared by incorporating highly functionalized OMMT sheets into polyurethane matrix. The functionalization of OMMT was achieved by reacting them with diamine which acted as a chain extender for the synthesis of PU nanocomposites. They reported the increase in tensile strength and elongation at break with increase in loading level of OMMT and these properties were maximum at a nanofiller loading level of 5 wt%. Similarly many other research group have reported the synthesis of clay nanocomposites based on a variety of polymers such as polystyrene(PS) [Liu et al (2004)], polypropylene(PP), epoxy resin, poly (methyl methacrylate) PMMA and polyolefins etc. Many conducting Polymers like polyaniline(PANI), poly (ethylene oxide)(PEO), polypropylene(PPR) and polythiophene(PTP) have been studied for a long time by reinforcing them with clay particles

2.6 Ternary Nanocomposites

Conductive polymer nanocomposites have become the object of numerous studies because of scientific challenges in their synthesis and potential applications in many fields. Their proposed uses ranges from antistatic coating, electromagnetic interference shielding in electronic devices, sensors and electrochemical display etc [Wang et al (2006)]. Various carbon based conductive fillers like carbon nanotubes(CNTs), GNPs, graphene, carbon fibers, carbon black(CB) are used to enhance the conductivity of a polymer matrix. The percolation threshold of various polymer nanocomposites has been found to be less than 0.1 % with CNT prepared by emulsion or solution blending technique. On the other hand, a very high percolation threshold of 7.5 wt.% was found to be for PE/MWNTs nanocomposites prepared by melt blending. This high reported value of percolation threshold was due to re-aggregation of CNTs during compounding process [McNally *et al.* (2005)]. Similarly, the graphite nanoplatelets have also the drawback of reaggregation during synthesis of various nanocomposites. Due to agglomeration of these carbon based nanofillers, the continuous conductive network is formed at high loding level of carbon fillers in the nanocomposites, which leads to high value of percolation threshold. Similarly, the

conventionally filled macroscopic composites also have high values of percolation threshold due to addition of microscale fillers in the polymers, so a large quantity of filler is required to reach the percolation threshold.

As the quantity of filler is further increased beyond percolation threshold, it leads to difficulty in processing of composites, high density and mechanical properties also starts to deteriorate [Wycisk *et al.* (2005)]. A lot of efforts are being in progress to lower down the population threshold as much as possible to obtain a nanocomposite material with good electrical conductivity alongwith retaining its mechanical properties also. Recently the new innovative studies are reported in Literature where the use of two and even the three combined nanofillers have been reinforced in the polymer matrices to improve their electrical properties by lowering down the percolation threshold, thermal conductivity, and mechanical properties [Zhang *et al.* (2010)]. The purpose of using two nanofillers in the polymer matrices is to combine the synergistic effects of two nanofillers in one polymeric matrix for example report are available in Literature where the combinations of two conductive nanofillers like GNPs/CNTs, CNTs/CB etc. have been added to the polymers to improve their electrical properties, thermal conductivity and lower down the percolation threshold of prepared nanocomposites by providing a better dispersion of fillers. [Jiang *et al.* (2010)] reported a study where the synergistic effects of multiwall carbon nanotubes(MWCNTs) and graphene nanoplatelets (GNPs) on mechanical properties and thermal conductivity of an epoxy resin was observed. However, the electrical conductivity was not the part of their investigation. [Chatterjee *et al.* (2012)] reported the synergistic effects of hybrid nanofillers namely graphene nanoplatelets (GNPs) and carbon nanotube (CNTs) on mechanical properties of epoxy polymer nanocomposites. The modulus and toughness were improved at a ratio of highest CNT content (9:1). The homogeneous dispersion of both the fillers was achieved by high shear calendaring method. An interconnected strong nanofiller network was formed in the matrix due to alignment of CNTs on GNPs flakes as indicated by TEM. [Nuruddin *et al.* (2015)] reported the synergistic effects of two nanofillers namely graphene nanoplatelets and nanoclays in epoxy polymer. They reported that good dispersion of two nanofillers was achieved by ultrasonication, calendaring and magnetic stirring. The mechanical properties of prepared nanocomposites were studied and it was concluded that highest flexural strength was achieved at 3 wt.% MMT and 0.1 wt.% GNPs and highest modulus was obtained at 3 wt.% percent MMT and 0.2 wt.% percent GNPs. The viscoelastic properties like storage modulus was achieved at 3 wt.%

MMT and 0.1 wt.% GNPs with no any change in glass transition temperature(T_g). In the epoxy nanocomposites, the synergistic effects of GNPs and carbon black(CB) and carbon nanotube (CNT) can lead to formation of excellent conductive networks which accounts for the highest electrical conductivity of epoxy/ GNP- CB- CNT hybrid filler nanocomposites. In another study reported by [Safdari *et al.* (2013)] of epoxy polymer were investigated. In this study the new developed computational models and geometric model were applied to explain both of these properties by making a comparison between predicted percolation threshold value and experimentally measured value of percolation threshold. The predicted percolation threshold and experimentally find out percolation threshold for CNT/ GNP/ epoxy hybrid nanocomposites were 0.8 wt.% and 0.9 wt.% , which were in good agreement with each other. In another study reported by [Liu *et al.* (2011)], hybrid nanofillers namely oxidized multi-walled carbon nanotubes (MWCNTs) and chemically modified graphene(CMG) from G0 were co-ordinated by copper ions (Cu^{2+}). These Cu^{2+} coordinated hybrid fillers were reinforced in Poly (styrene- co- butadiene-co-styrene) (SBS) and its electrical and mechanical properties were investigated. The percolation threshold of prepared nanocomposites were found to be 0.25 % which was much lower than SBS/ MWCNT (Pc 0.75wt%) and SBS/CMG (0.5wt.%) binary nanocomposites. Similarly, the mechanical properties like young's modulus were also enhanced due to efficient bridging between MWCNT and CMG in the SBS matrix.

In conclusion, the studies of ternary nanocomposite synthesized by combined effects of two nanofillers have shown many exciting results but still a lot of work is needed to be carried out in this area. Most of the reports available are focusing on improving the electrical conductivity and mechanical properties by using two combined conductive nanofillers in a polymer matrix. A very few studies have been published on the improvement of mechanical properties along with electrical properties by the addition of combined clay nanofiller and conductive nanofiller. Due to lack of limited studies on improvement of mechanical properties, we were motivated to prepare ternary nanocomposites based on PU by reinforcing it with OMMT and GNPs as combined fillers with the aim of investigating and comparing the electrical and mechanical properties of prepared ternary nanocomposites with respect to their binary nanocomposites, which has been explained in the successive chapter no.5

CHAPTER 3

SYNTHESIS OF CONDUCTIVE POLYURETHANE/GRAPHITE COMPOSITES FOR ELECTROMAGNETIC INTERFERENCE SHIELDING

3.1 *Introduction*

The modern technological world demands a variety of multifunctional materials with desirable mechanical, thermal, electrical and chemical properties for specialized applications. Composites are a class of materials which present rich possibilities for the development of such multifunctional novel materials desired for the new technological advancements [Qin *et al.* (2013); Allaer *et al.* (2014)]. Nanocomposites are the composite materials in which at least one dimension of the dispersed phase is in the nanometer range [Ajayan *et al.* (2003)]. The development of polymer nanocomposites is rapidly emerging as a multidisciplinary research activity whose results can broaden the applications of polymers to the great benefit of many different industries [Panupakorn *et al.* (2013)].

Recently, interest in carbon-based nanomaterials has revolutionized the field of polymer composites due to their ability to impart conductivity to the insulating matrix, along with providing excellent structural properties. A number of carbon-based fillers are being used as nanofillers, including carbon black (CB), carbon nanofiber (CNF), carbon nanotubes (CNTs), graphene, nano-graphite sheets, fullerene, etc. [Yan *et al.* (2011); Verdejo *et al.* (2008); Harikrishnan *et al.* (2009); Harikrishnan *et al.* (2010)]. A lot of work has been reported in the literature on graphene based nanofillers [as expanded graphite (EG), graphite nanoplatelets (GNPs), graphite oxides (GO), etc.] to fully exploit their potential in polymer nanocomposites. [McAllister *et al.* (2007); Bhaviripudi *et al.* (2010)]. Among the various graphene based fillers,

GNPs are of high current interest due to their superior mechanical, thermal, electrical properties, and ease of synthesis.

GNPs consist of small stacks of graphene layers which can further be intercalated by the matrix material. The incorporation of GNPs into polymers has resulted in the fabrication of nanocomposites with significantly enhanced electrical conductivities (several thousands of S/cm) and mechanical moduli (208–650 GPa), and their compatibility with the host polymer can be readily achieved due to their adaptable functionalization [Novoselov *et al.* (2005); Cho *et al.* (2005); Pal *et al.* (2009)].

The source material for GNPs is a natural and abundant graphite mineral and can be produced by convenient methods. GNPs with excellent mechanical, thermal and electrical properties of graphene as well as low cost have attracted considerable attention as a viable, inexpensive and good alternative filler to other carbon-based nanofillers. [Kim *et al.* (2009)] have compared GNPs and CNTs for reinforcement of ethylene vinyl acetate (EVA) nanocomposites and have recommended that GNPs are more suitable additive material for polymer composites. It was reported by [Ramanathan *et al.* (2008)] that using graphene sheets as a filler in polymer nanocomposites yielded outstanding thermal, mechanical, and electrical properties, incorporating in one material the best features of both nanoclay and carbon nanotube based nanocomposites. Innumerable applications of these polymer nanocomposites in nanoelectronic devices, optoelectrical devices, sensors, ion-selective electrodes have been extensively reported [Thomassin *et al.* (2013); Yerawar *et al.* (2012); Kondawar *et al.* (2012)].

In the present work, GNPs have been used as nanofiller in polyurethane matrix to prepare polyurethane composites, which have been evaluated for electromagnetic interference (EMI) shielding applications. In the recent past, the conventional electrical conductive fillers have been used to enhance the electrical conductivity of various polymers with limited applications. When the size of the filler is at a micrometre scale, a large quantity of filler is required to reach the percolation threshold (minimum quantity of filler which must be added to the composite so that it starts to show conduction from its insulating behaviour) [Jiang *et al.* (2005)]. Moreover, as the quantity of conductive filler increases, it leads to deterioration of the mechanical properties of the composites. Thus, attempts are in progress to minimize the quantity of filler as much as possible. Further, when there is a transition of GNPs thickness from micro- to nanoscale, a dramatic increase in surface/volume ratio occurs which results in GNPs of high

aspect ratio, which favours the good dispersion of GNPs in a polymer matrix and also minimizes the filler concentration [Lau *et al.* (2010)].

Among the various polymers, polyurethane has attracted attention due to its myriad applications in industry as well as in daily life. The wide range of polyurethanes available from flexible or rigid lightweight foams to tough, sticky elastomers allows them to be used in a wide diversity of consumer and industrial applications. Polyurethane (PU) has high abrasion resistance, tear strength, excellent shock absorption, flexibility and elasticity. By blending with inorganic nanofillers, its performance has been dramatically improved [Yu *et al.* (2008)]. There are numerous studies on dispersion and mechanical properties of polyurethane composites with clay particles [Ajayan *et al.* (2003); Harikrishnan *et al.* (2010)], but rare reports are available on study of electrical properties of polyurethane with carbon nanofillers.

The polyurethane composites with graphite nanoparticles have been prepared by using an in situ polymerization technique and the percolation threshold of the resulting composites have been studied and validated with the analytical results. It is known that in situ polymerization is an efficient method to improve the dispersion of graphite nanoparticles in the polymer matrix [Zheng *et al.* (2004)], in which the monomers are polymerized in the presence of filler, and consequently this technique would confer a strong interaction between the reinforcing filler and the polymeric phase [Chen *et al.* (2003)]. The resulting composites were characterized by x-ray diffraction (XRD), transmission electron microscope (TEM), and scanning electron microscope (SEM), and their conductive properties for EMI shielding were studied by a four-point probe method.

3.2. *Experimental Section*

3.2.1 *Materials*

The graphite used for preparing GNPs was graphite intercalation compound (GIC), acidified with concentrated H_2SO_4 and HNO_3 . The monomers for PU polymerization, Toluene, 2,4-diisocyanate (TDI) with molecular weight 174.16 and polypropylene glycol (PPG) with a molecular weight of 2000, were supplied by MP Biomedicals Fine Chemicals Division, India. The monomers were of analytical grade and were used as received. The chain extender 1,4-

butanediol (BDO) was supplied by the same company, while 95% (v/v) alcohol and distilled water were used as solvents for the preparation of the GNPs.

3.2.2 *Preparation of Expanded Graphite and Graphite Nanoplatelets*

EG was prepared by adopting the procedure reported by [Chen *et al.* (2004); Yasmin *et al.* (2006)]. The GIC (powder form) was given a thermal shock at 1050°C for 15 s in a muffle furnace to obtain EG particles, having about several hundred times thickness in the original c direction dimension [Lau *et al.* (2010)]. The gallery space of EG expands due to evaporation of intercalants trapped between the layers. The EG thus obtained was mixed and saturated with 400 ml alcohol (ethyl alcohol) and distilled water in a ratio of 70:30 by volume for 8 h. This mixture was subjected to sonication using a horn-type sonicator for various time intervals: 5 h, 8 h, 10 h, and 12 h. After sonication, EG particles were effectively fragmented into foliated graphite (the layers are still interlocked with each other in the nm thickness range). The GNPs dispersion was then dried at 80°C to remove the residual solvents. In this way, the GNPs were obtained to be used as nanofiller in PU composites. The TEM image of prepared GNPs with particle size estimation and particles distribution is shown in Figure 3.1.

3.2.3 *Preparation of Polyurethane Graphite Composites by In-situ Polymerization*

The PU/Graphite composites were prepared by using TDI:PPG:BDO in the mole ratio 3:1:2. PPG and prepared GNPs were mixed and stirred for 12 h at 50°C to obtain a dehydrated PPG–GNPs suspension. This suspension was subjected to sonication for 1 h to avoid the agglomeration of the graphite nanoparticles. The low viscosity of PPG facilitates maintaining a uniform dispersion of particles in the solution. TDI was poured into this suspension with continuous stirring. During the mixing of the TDI, the temperature was maintained at 70°C as it was an exothermic reaction. After mixing of the TDI, the resultant solution was heated at 85°C (the best temperature for polymerization) for 4 h with stirring. Subsequently, after cooling the reaction mixture to 40°C, BDO was added with vigorous stirring for 1 min. Immediately after this, a small portion of the solution was mixed with dimethylformamide (DMF) for spin-

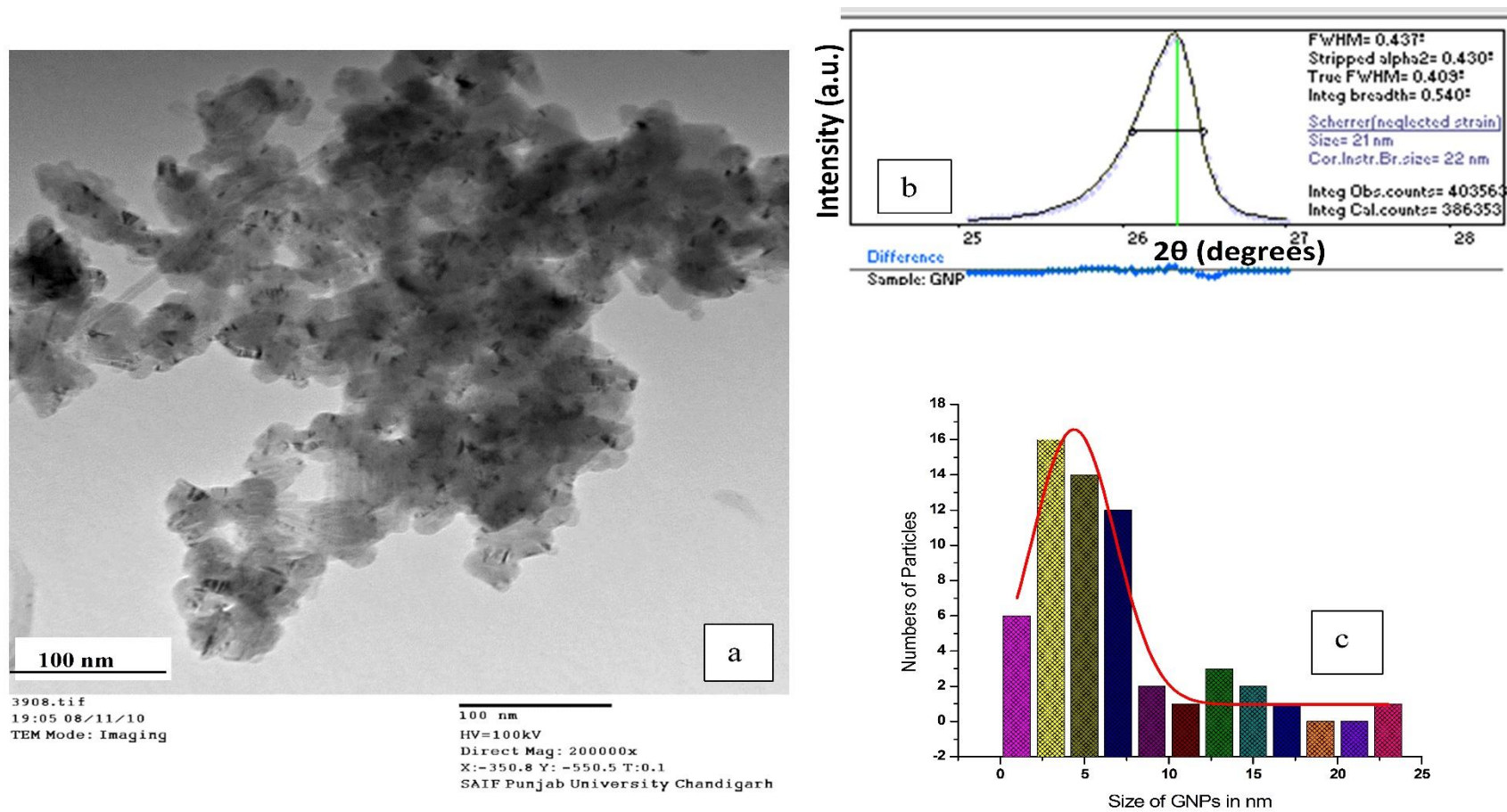


Figure 3.1: Graphite nanoparticles: (a) TEM, (b) particle size estimation from XRD, (c) particle size distribution in the TEM image (a).

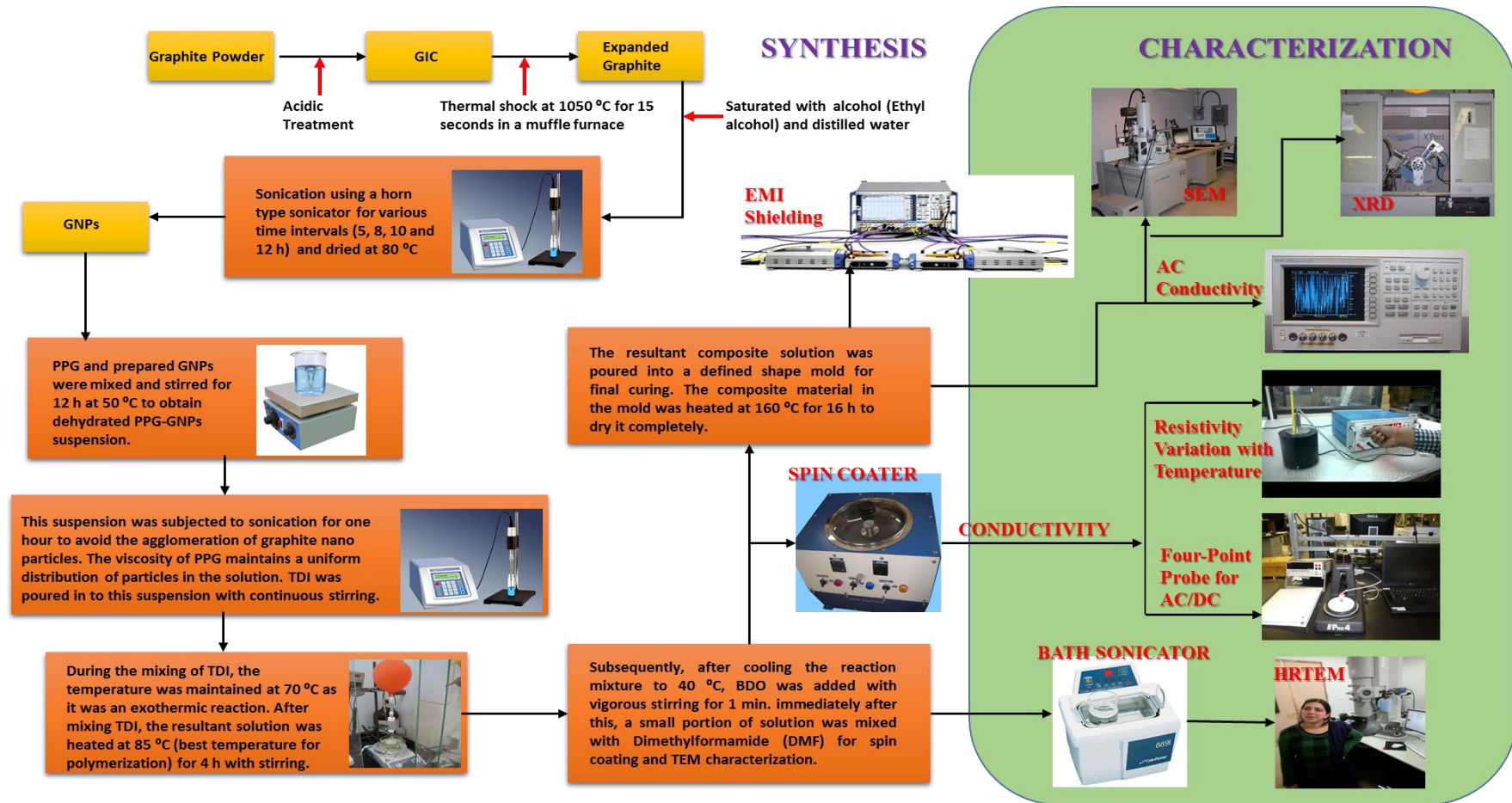


Figure 3.2: Schematic diagram of whole synthesis process of polyurethane/graphite composites

coating and, for TEM characterization using drop casting on TEM grid. The resultant composite solution was poured into a defined shaped mold for final curing. The composite material in the mold was heated at 160 °C for 16 h to be completely dried as shown in Figure 3.1.

3.2.4 Characterization

The XRD patterns of the processed materials were recorded on a PANalytical's XPERT-PRO Diffractometer system with Cu K-Alpha1 [\AA]: 1.54060 and $2\theta(10^\circ - 40^\circ)$. SEM was employed to study the surface morphology of the prepared composites material. The dispersion states of the prepared composite samples were studied by TEM. The nanofiller prepared for these composites was also studied by TEM. The observed size of the GNPs was 2–22 nm. The samples were prepared by dispersing the film on glass/silicon substrates by spin-coating. The electrical conductivities of the prepared composites samples were studied by a four-point probe method and the percolation threshold of the samples was also studied. The electrical conductivity under DC condition was measured by the four-point probe method. In this method, the four probes are placed on the surface of the spin-coated sample film with four-point probe heads on a Pro-4 stand. The four-point probe heads are controlled through a computer for easy use. The computer automatically controls the Keithley 2400 source meter. The current is supplied through the outer probes and the voltage was measured through the inner probes. The conductivity measurement setup was interfaced with the computer loaded with tracing software, a four-point probe head with 0.0625 inches (1.5875 mm) spacing between the tips at a pressure of 180 g, and Labview to validate the analytically calculated results. The variation of the electrical resistivity with temperature was measured with an Instrument which consisted of a source with a constant current generator with a multi-range voltmeter and an oven with a sample holder fitted with a resistance temperature detector (RTD) and temperature gauge. The relationship between resistivity and temperature was measured from room temperature to 200°C by putting the samples into the oven. The electrical conductivity under alternating current (AC) condition was measured with a 4294A Precision Impedance Analyzer from 40 Hz to 110 MHz. All the electrical conductivity measurements were carried out on rectangular samples with dimensions of $\sim 10 \times 10 \times 1 \text{ mm}^3$ of spin-coated films. The electromagnetic shielding of the prepared nanocomposite was measured using an Agilent 8753ES-H39 (30 kHz to 3 GHz or 6 GHz) Vector Network Analyzer. The dimensions of the specimens were of

annular shape with an outer diameter 115 mm, inner diameter 10 mm and thickness of about 1 mm.

3.3 Results and Discussion

3.3.1 XRD Analysis

The XRD is an important tool to investigate the dispersion of filler into the matrix by considering the shifting of the major peaks of filler towards a lower diffraction angle 2θ (increased d spacing), reduction in intensity of peaks, and the disappearance of the major diffraction peak of filler (indicating exfoliation) [Chen *et al.* (2008)]. By taking into consideration the above assumptions, the results of XRD for various samples were analysed [Wakabayashi *et al.* (2008)]. These results are shown in Figure 3.3, in the form of diffraction peaks for EG, graphite nanoparticles and prepared samples of composites with different loadings of filler. The EG displayed one major peak at $2\theta = 26.388^\circ$. After ultrasonication for 10 h, the EG was converted into GNPs. The XRD of these prepared GNPs displayed the same sharp diffraction peak as found for EG.

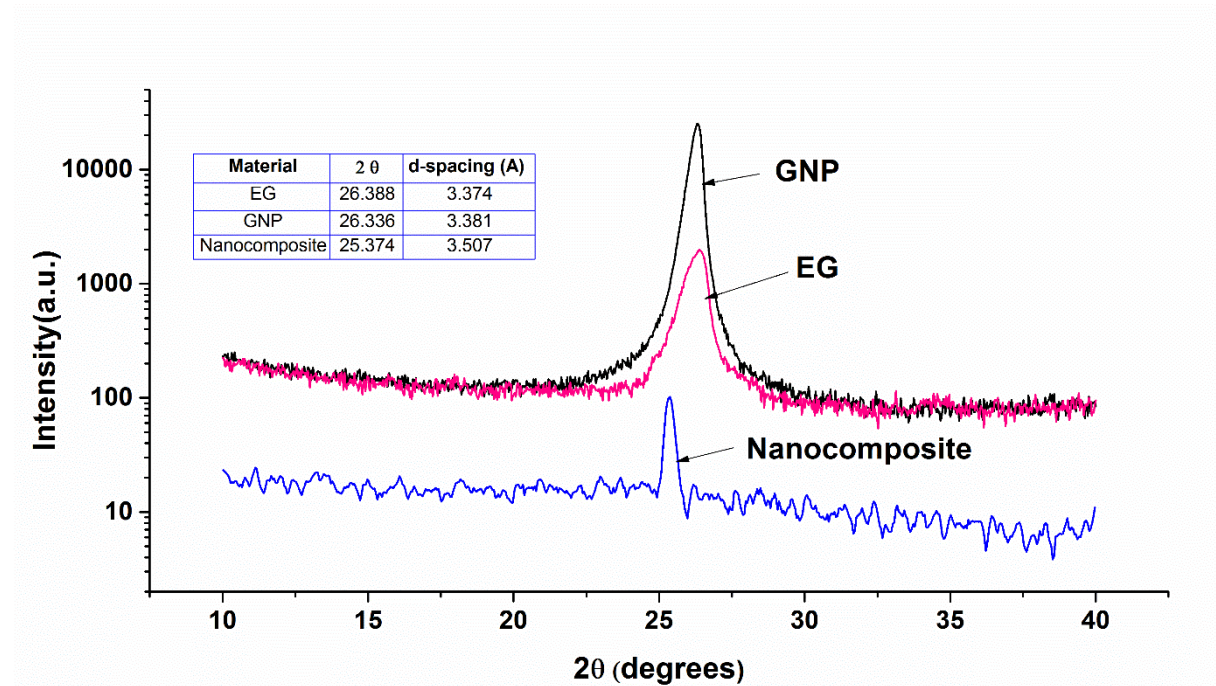


Figure 3.3: X-ray diffraction of expanded graphite, graphite nanoparticles and prepared samples of composites.

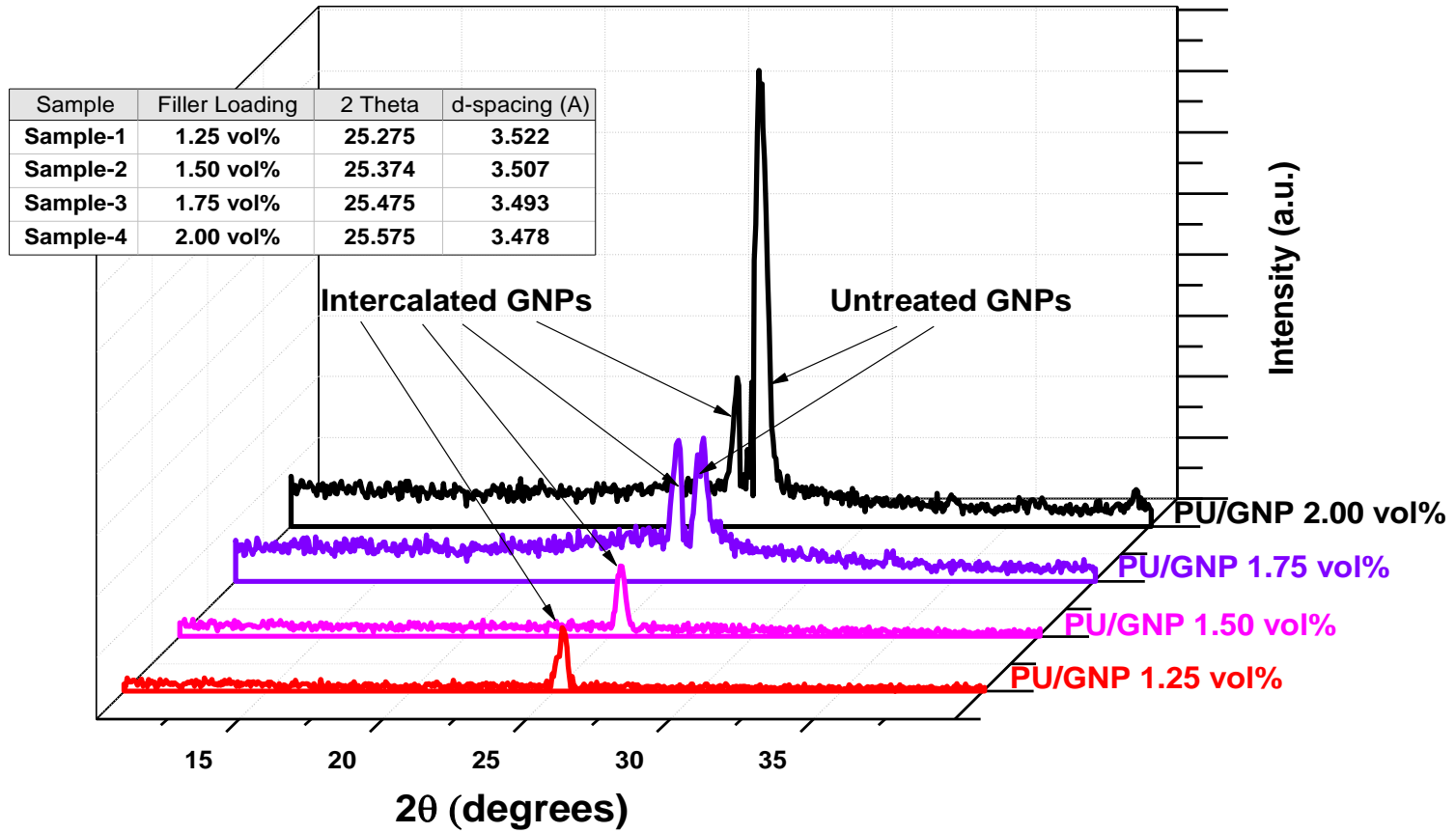


Figure 3.4: X-ray diffraction of prepared samples of composites with different loadings.

This indicates that ultrasonic treatment had no effect on inter-planar spacing but just separated the graphite layers and reduced the numbers of layers in each graphite sheet. In EG, a large number of delaminated graphite sheets are firmly interlocked with each other so it is not easy to disperse these interlocked layers directly into the matrix. To overcome this, ultrasonication was carried out to separate these interlocked graphite sheets to improve the dispersion of these platelets into the matrix. The TEM of these prepared GNPs revealed that these particles had sizes of 2–20 nm. The XRD of the prepared composites samples with different filler loadings is shown in Figure 3.4. All the three samples show the shifting of the major diffraction peak (002) towards a lower angle with reduced intensity which indicates intercalation, further verified by TEM. With the 1.25 vol.% loading, the polyurethane enters into the GNPs layers and the d-spacing of the layers increases, which results in the intercalation type of dispersion indicated by the left shift of the XRD peak. A further increase in the loading of GNPs decreases the available vol.% of polymer to enter into the layers of the GNPs. So, at the high loadings, the XRD peak shift towards the left is less as compared to the 1.25 vol.%. At a high percentage of GNPs loading, the available polyurethane enters only into some portion of the GNPs and due to this the XRD at high vol.% loading gives two peaks, one corresponding to the intercalated GNPs and the other to the untreated GNPs. Earlier work [Chen *et al.* (2001); Chen *et al.* (2001); Paul *et al.* (2008); Afanasov *et al.* (2009)] has shown that, as the concentration of GNPs is increased as filler in the matrix, these nanoparticles have a tendency to agglomerate which make them hard to get to disperse in the polymer matrix. Thus, the in situ polymerization technique and use of sonication during the processing method has reduced the agglomeration tendency of GNPs to some extent, and resulted in an intercalation-type of dispersion as also verified by SEM and TEM.

3.3.2 SEM and TEM Analysis

Figure 3.5 shows SEM images (a to f) at different magnifications. These images clearly indicate the formation of GNPs from loose and porous worm-like EG using ultrasonication. The nanoplatelets formed are well dispersed in the PU matrix. Individual GNP can be seen in Figure 3.5 c and d. High-resolution transmission electron microscopy (HRTEM) images (Figure 3.6) show that, when the loading level is 0.5 vol.%, the GNPs are well dispersed in the matrix in an intercalated manner (where GNPs are still regularly stacked layers, but with increased gallery size). In these images, the edges of the graphene layers are clearly seen as dark straight lines;

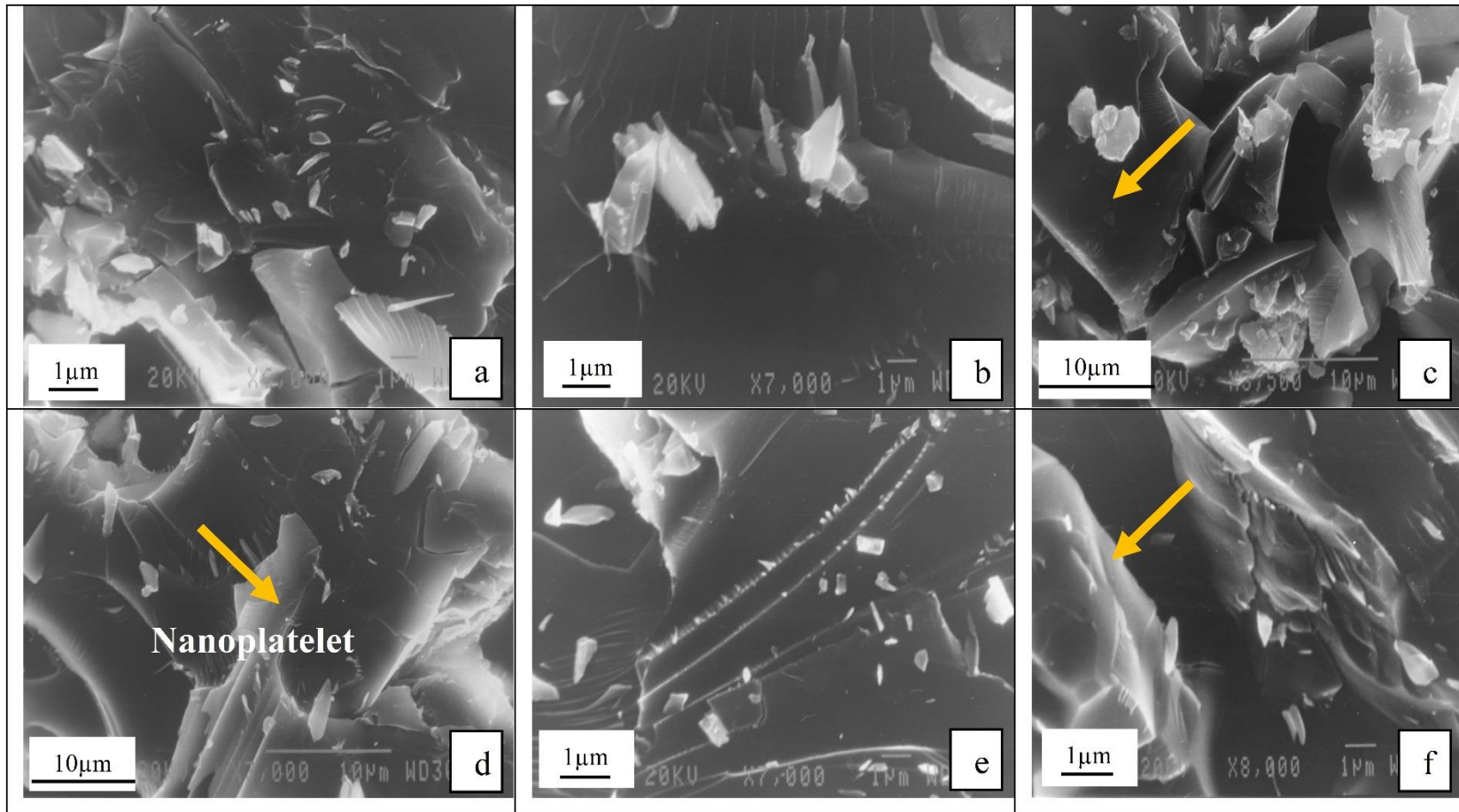


Figure 3.5: SEM images of prepared PU/GNPs 1.5 vol.% composites with (a, b, e) low magnification at 1 μm, (f) high magnification at 1 μm, (c) low magnification at 10 μm, (d) high magnification at 10 μm.

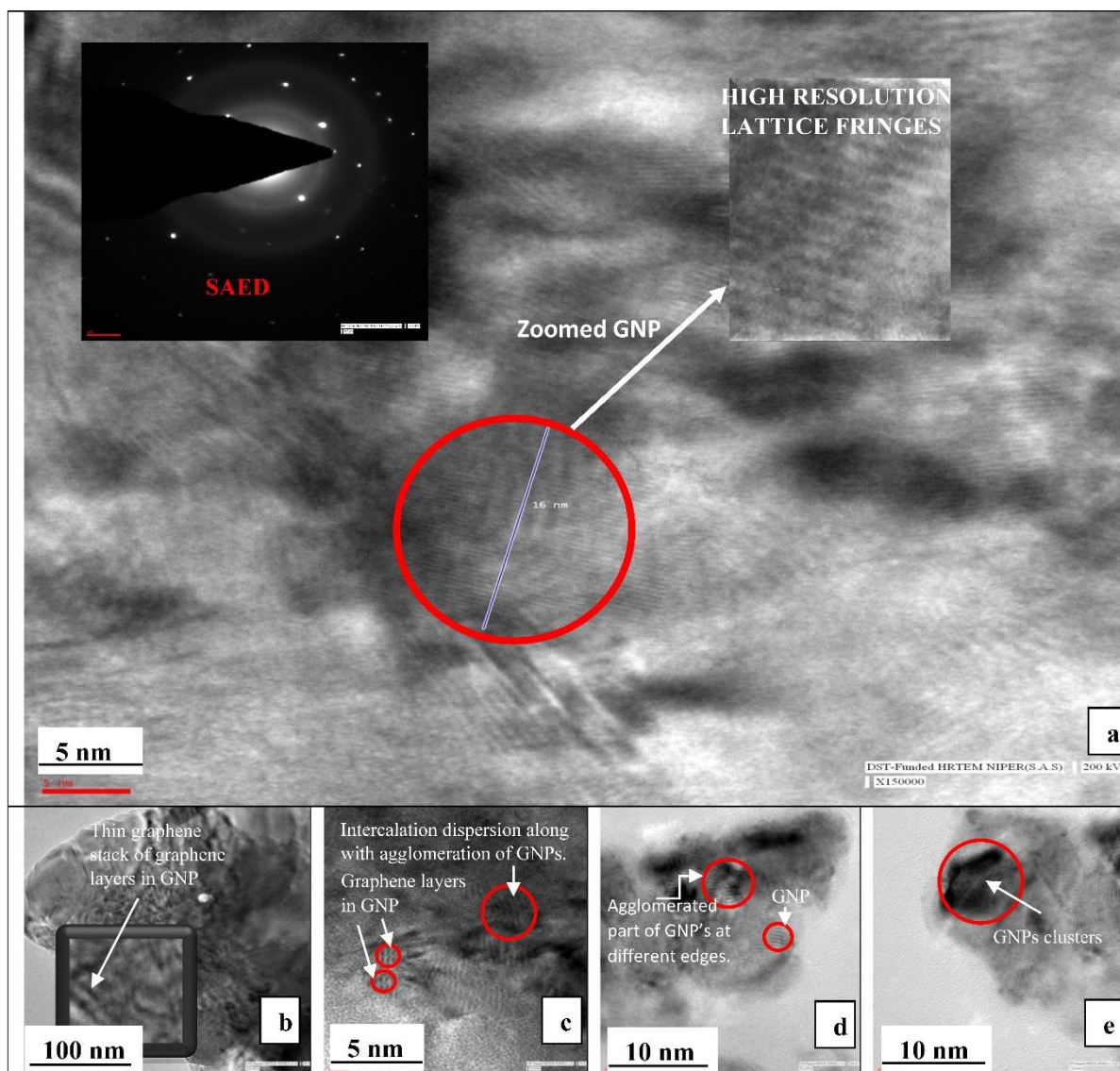


Figure 3.6: HRTEM images of prepared PU/GNPs 0.5 vol.% composites with (a) SAED pattern of composite and lattice fringes of dispersed GNP, (b) number of graphene layers forming a thin graphene stack, (c) graphene layers in GNP and intercalation dispersion along with agglomeration of GNPs, (d) agglomerated part of GNP's at different edges, (e) GNPs clusters.

similar results are reported in [Li *et al.* (2007)]. The high resolution lattice fringes fingerprints, shown in Figures 3.6a, b and 3.7a, d, represent the GNPs consisting of a few graphene layer bundles. The clusters of GNPs can also be seen in Figures 3.6c–e and 3.7b, c, which are due to the aggregation behavior of the graphite nanosheets. This confirms that ultrasonication has not torn up the EG into individual carbon layers, i.e. they are not completely exfoliated (complete layer separation). Selected area electron diffraction (SAED), shown in the inset of Figure 3.6a, reveals the crystalline behavior of the formed composite. The profile of the fringes in Figure 3.8 is used to calculate the d-spacing in the layers. The live fast Fourier transform (FFT) of the

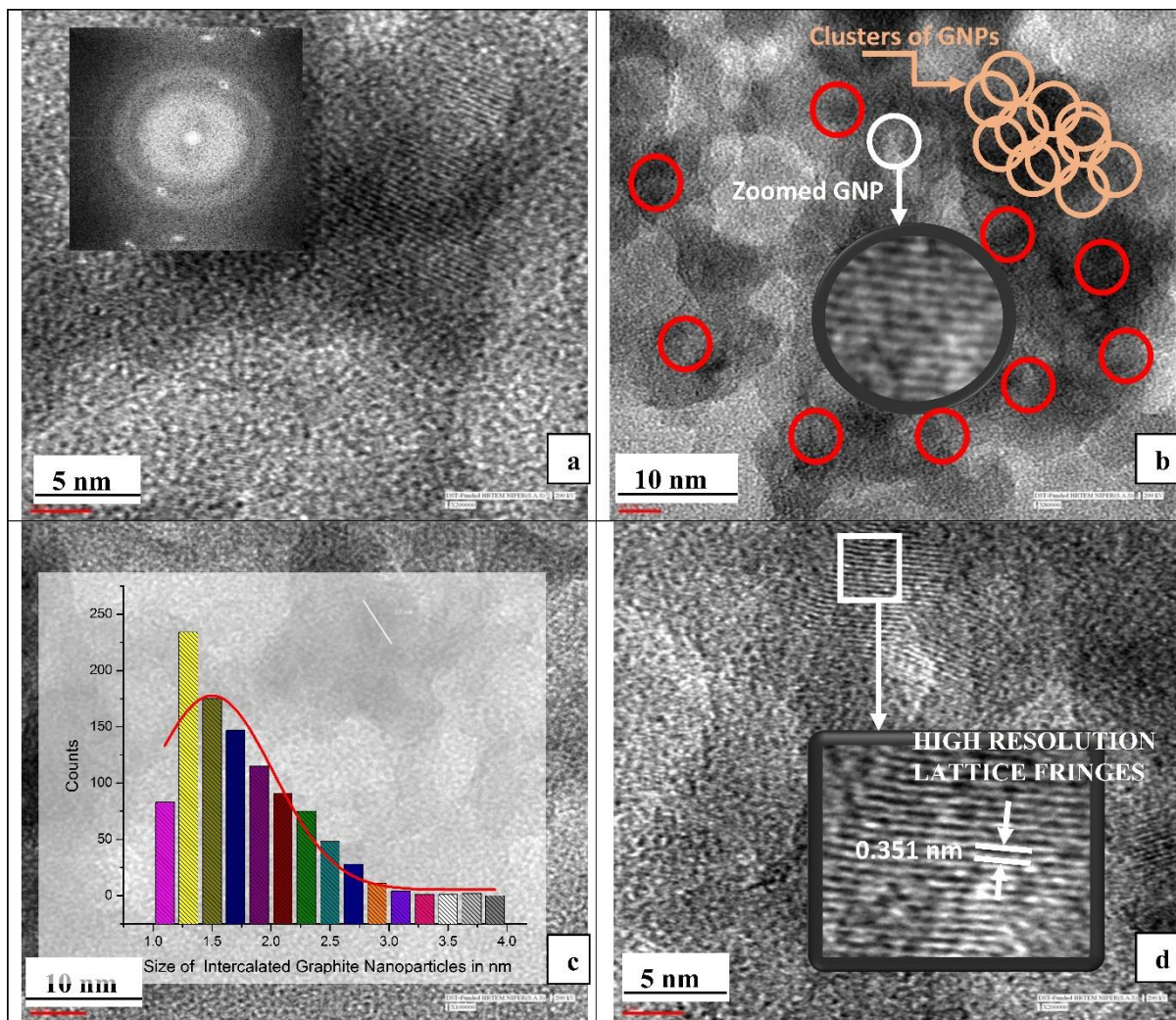


Figure 3.7: HRTEM images of prepared PU/GNPs 1.5 vol.% composites with (a) live FFT, (b) clusters of GNPs, (c) graphite nanoparticles size distribution in composite material, (d) high-resolution lattice fringes.

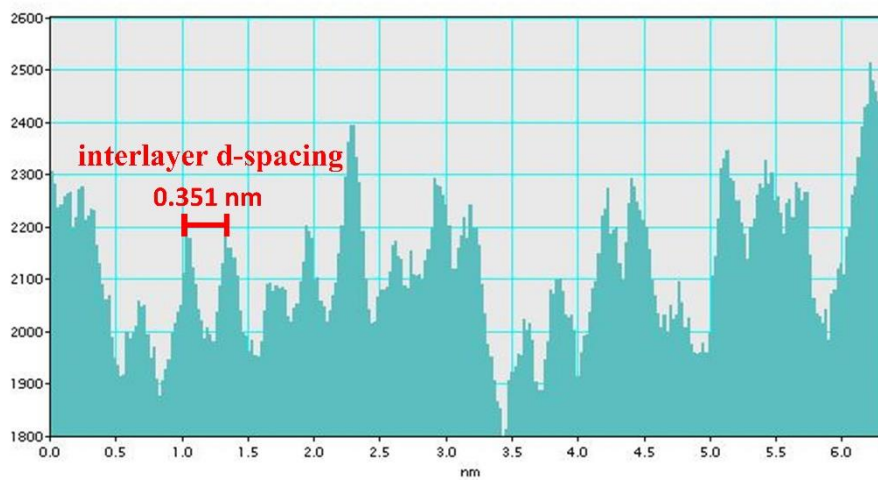


Figure 3.8: Fringes profile of Figure 3.7d.

composite material is shown in the inset of Figure 3.7a. From Figure 3.7d, the dark lines correspond to intersection sheet layers with the distance of two adjacent layers being about 0.351 nm. Individual layers of graphite are clearly visible as regions of alternating narrow, dark and light bands within the particles (fringes) as shown in Figure 3.7b and d. The intercalated particle size distribution in the resultant nanocomposite is shown in Figure 3.7c in which the solid line represents a Gaussian fit to the data.

3.3.3 *Electrical Conductivity and Percolation Threshold*

Measurement

The prepared polymer composites are conducting in nature as they contain conducting filler and insulating matrix. These composites are capable of dissipating electrostatic charges and shielding devices from electromagnetic radiation [Sarto *et al.* (2012)]. Due to the good adhesive properties of polyurethane, these composites can be used as interconnection wires in integrated devices. In general, there is a rapid increase in the electrical conductivity of the prepared composites when a conductive network is formed by the conductive fillers [Wang *et al.* (2010)]. It causes a transition in composite material from insulator to conductor [Du *et al.* (2004); Li *et al.* (2007)]. The fraction of filler material at which there is an establishment of multiple, continuous electron path or continuous electrical network, called the percolation threshold. In order to maintain the electrical conductivity of the composite containing insulating matrix, the concentration of the conducting filler must be equal or greater than the percolation threshold. The electrical behaviour of the composite is explained on the basis of percolation theory.^{36,37} According to this theory, near the percolation threshold, the electrical conductivity of the composite follows the following power law relationship:

$$\sigma = \sigma_0 (V_f - V_c)^s, \quad (3.1)$$

where σ is the electrical conductivity of the composite, σ_0 is the electrical conductivity of the filler, V_f is the filler volume fraction, V_c is the percolation threshold and s is a conductivity exponent. According to the tunnelling mechanism, conduction can take place via tunnelling between thin polymer layers surrounding the filler particles. The percolation threshold of GNP-

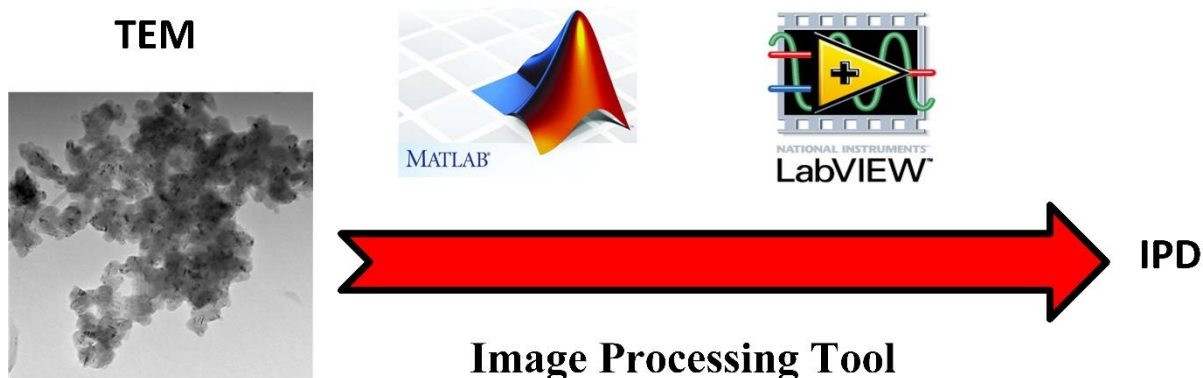


Figure 3.9: Interparticle distance (IPD) model for PU/graphite composite.

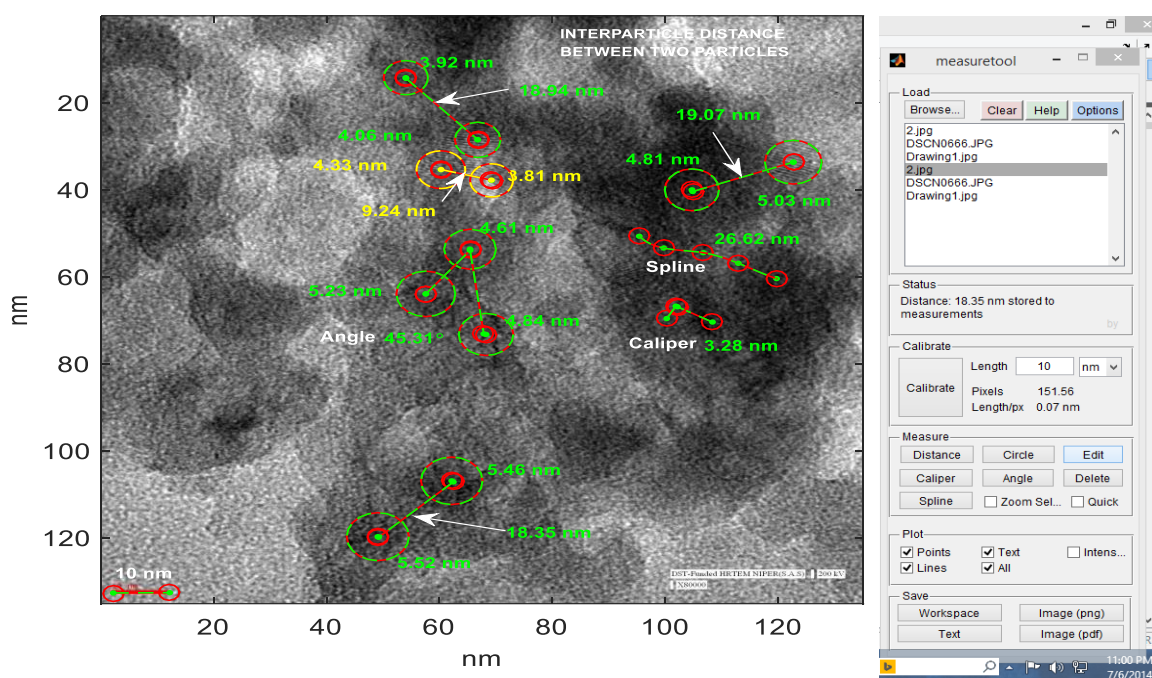


Figure 3.10: Geometrical orientations measurement for IPD using Matlab.

reinforced polymer is much lower than other carbon fillers like carbon fibers and CB, due to extremely large surface area and high aspect ratio of GNPs. [Kalaitzidou *et al.* (2007)], has proposed an analytical model to predict the percolation threshold using interparticle distance (*IPD*) with certain assumptions. To calculate the *IPD* between adjacent conductive particles, it is assumed that the particles are homogeneously distributed in the polymer matrix and are perfectly bonded with the polymer during in situ polymerization. *IPD* of the particles can be measured using image processing software like Matlab, Labview, and Image J as shown in Figures 3.9 and 3.10.

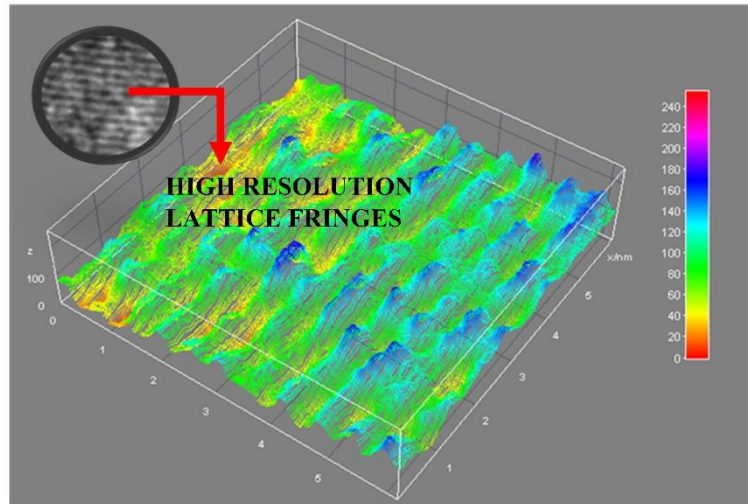


Figure 3.11: Surface morphology of composite material using image J.

The GNP is assumed with thickness t and diameter D , dispersed individually in the matrix (Figure 3.10). The volume fraction, P , of GNP is given by [Li *et al.* (2007)]:

$$P = \frac{V_{filler}}{V_{total}} = \frac{V_p}{L^3} = \frac{\frac{\pi D^2 t}{4}}{[\langle \cos^2 \theta \rangle \cdot (D + IPD)]^3} , \quad (3.2)$$

where IPD is the interparticle distance between adjacent conductive particles, L is the length of each cubic element, in which the composite is divided, is the angle between the GNP and the direction of preferred orientation. For 3D random distribution, the average orientation is [Li *et al.* (2007)]:

$$\langle \cos^2 \theta \rangle = \frac{1}{3} . \quad (3.3)$$

Combining Equations (3.2) and (3.3), percolation threshold P_c is:

$$P_c = \frac{27\pi D^2 t}{4(D + IPD)^3} . \quad (3.4)$$

To create an electrical network in composite, filler particles must be overlapped in the thin polymer layers as shown in the surface morphology of composite in Figure 3.11. For overlapped particles $D \gg IPD$, is measured by matlab tool. Equation (3.4) then reduces to:

$$P_c = \frac{27\pi t}{4D} = \frac{21.195}{\alpha}, \quad (3.5)$$

where α is the aspect ratio. The value α can be determined using Image J [Igathinathane *et al.* (2008)].

As per the power law in Equation (3.1), the plot of $\log \sigma$ versus $\log(V_f - V_c)$ is drawn and shown in the inset of Figure 3.12. The best linear fit is found for $V_c = 0.022$. Here, the power law for the conductivity values is well obeyed above the percolation threshold. In A.C. condition, shown in Figure 3.13, there is similar transition from insulator to semiconductor at the same percolation value. But this value of percolation threshold is not constant for all the frequencies under A.C. conditions. The same percolation threshold is found at frequency of 100 Hz. Summary of the percolation threshold and maximum conductivity of various GNPs/polymer nanocomposites is given in Table 3.1.

Table 3.1: Summary of the percolation threshold and maximum conductivity of various GNPs/polymer nanocomposites

Polymer matrix	Percolation threshold	Maximum conductivity (S/cm)	GNPs content at maximum conductivity	Reference
PS	0.1 vol%	10^{-3}	1.0 vol%	[Stankovich <i>et al.</i> (2006)]
PMMA	0.3 vol%	10^{-2}	4.0 vol%	[Chen <i>et al.</i> (2003)]
HDPE	2.0 wt%	10^{-5}	5.0 wt%	[Zheng <i>et al.</i> (2004)]
MA-PP	0.67 vol%	10^{-3}	3.9 vol%	[Shen <i>et al.</i> (2003)]
PA6	0.75 vol%	10^{-4}	2.0 vol%	[Weng <i>et al.</i> (2004)]
PAN+ GNP, CPAN + GNP, PAN+ Br-GNP and CPAN + Br-GNP	---	2×10^{-3}	6wt.%	[Green <i>et al.</i> (2008)]
SAN	1.5 vol%	10^{-2}	3.0 vol%	[Panwar <i>et al.</i> (2008)]
PVDF	1.0 vol%	10^{-2}	3.0 vol%	[He <i>et al.</i> (2009)]
PPS	1 wt%	10^{-1}	10 wt%	[Zhao <i>et al.</i> (2007)]
Phenolic resin	3.2 wt%	10^{-1}	11 wt%	[Zhang <i>et al.</i> (2008)]
CMPVA	0.8 wt%	10^{-5}	1.0 wt%	[Yu <i>et al.</i> (2008)]
PANI	1.3 wt%	22	1.3 wt%	[Mo <i>et al.</i> (2009)]

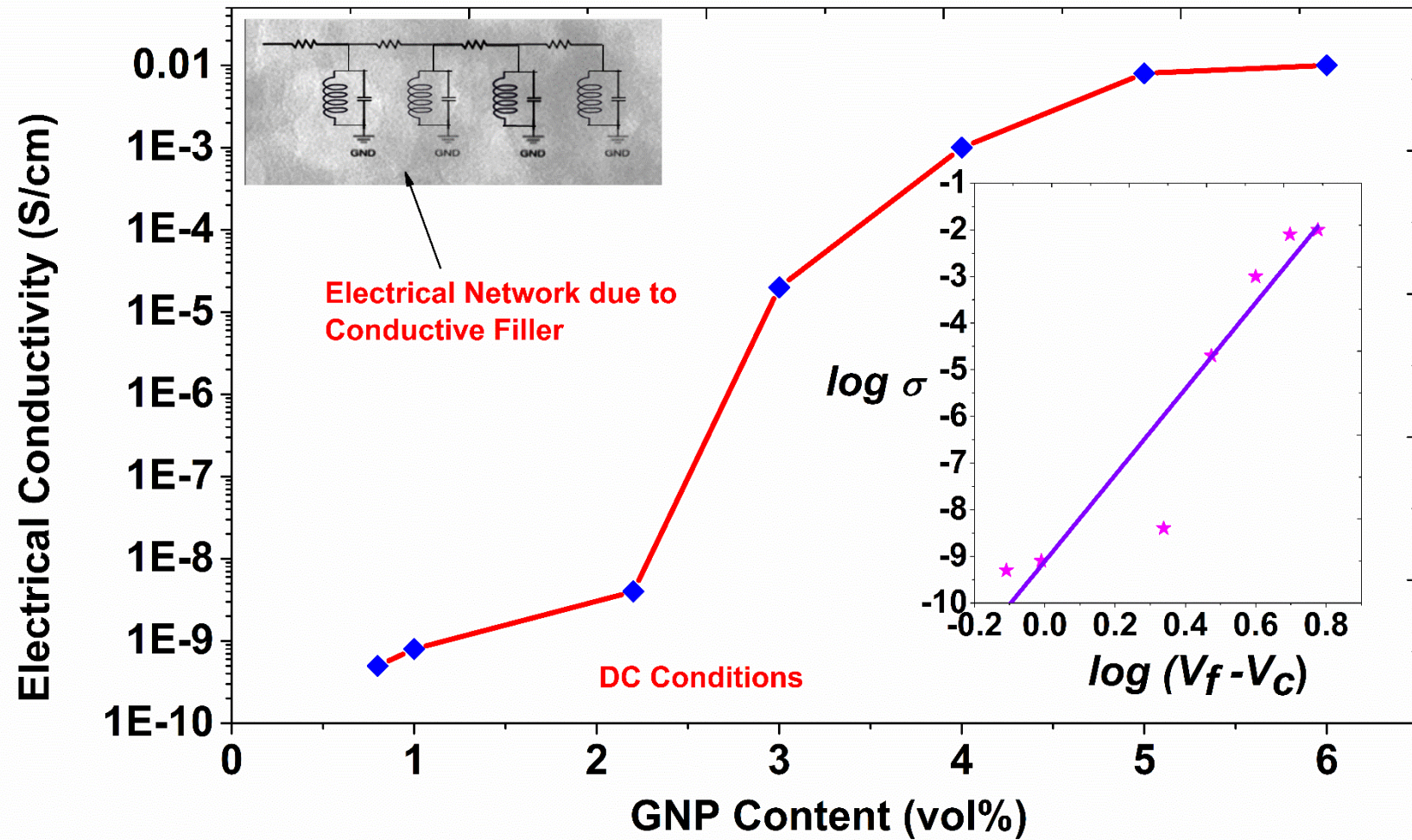


Figure 3.12: Electrical conductivity of PU/graphite composites as a function of GNP content under DC conditions.

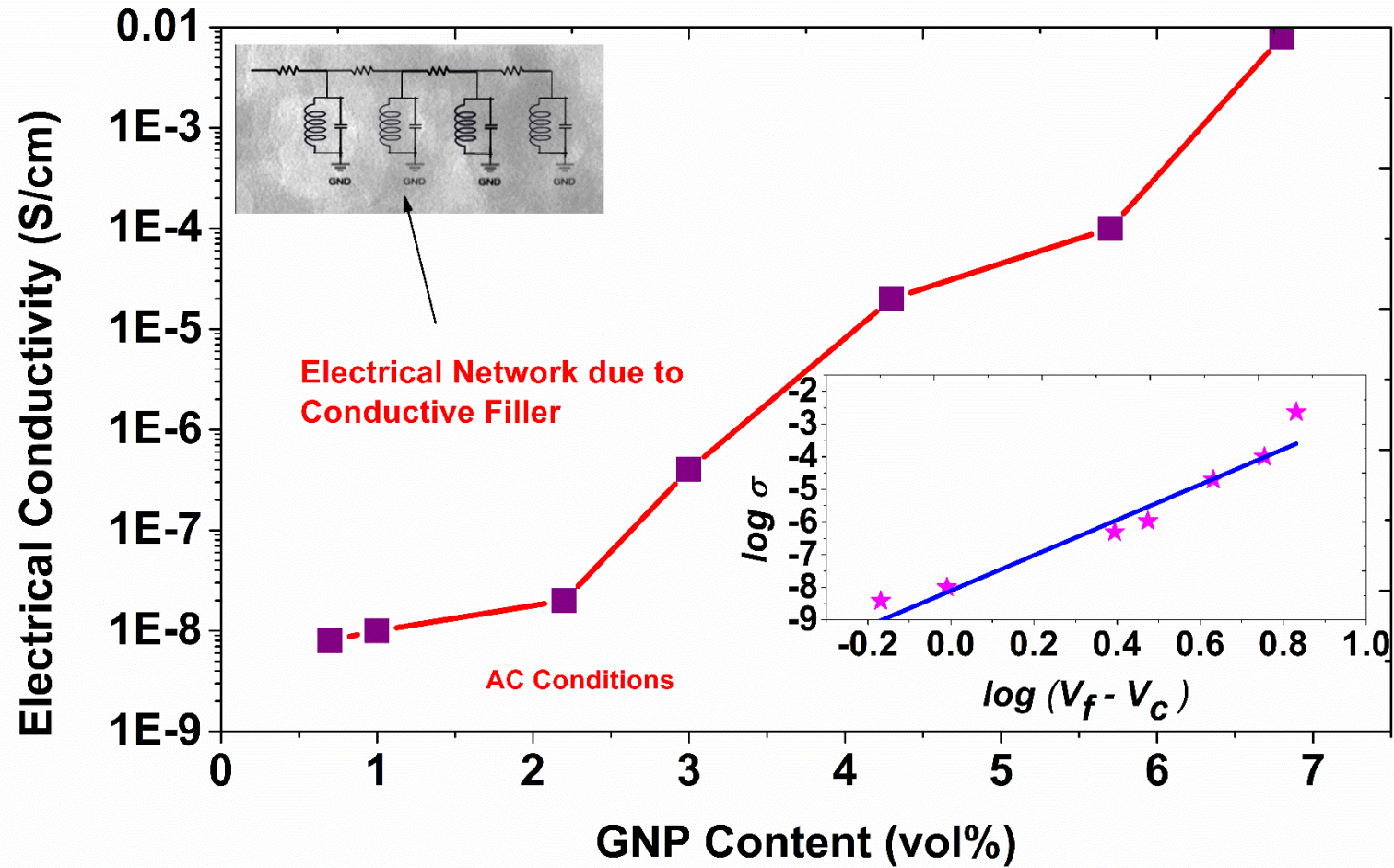


Figure 3.13: Electrical conductivity of PU/graphite composites as a function of GNP content under AC conditions.

Composites with filler loading close to percolation threshold give a rapid change in resistivity with increase in temperature as shown in Figure 3.14. The resistivity initially increases significantly and then decreases with an increase in temperature. This variation in the resistivity is with positive temperature coefficient (PTC) up to transition temperature, near about 130°C. The variation in the resistivity is with negative temperature coefficient (NTC) as the temperature increases above the transition temperature. The PTC effect is due to the breakage of conducting networks and increase in tunnelling resistance, caused by expansion of polymer matrix at low filler contents. The NTC effect is due to dominance of interplatelet contact resistance over the tunnelling resistance [Potts *et al.* (2011); Kim *et al.* (2008)].

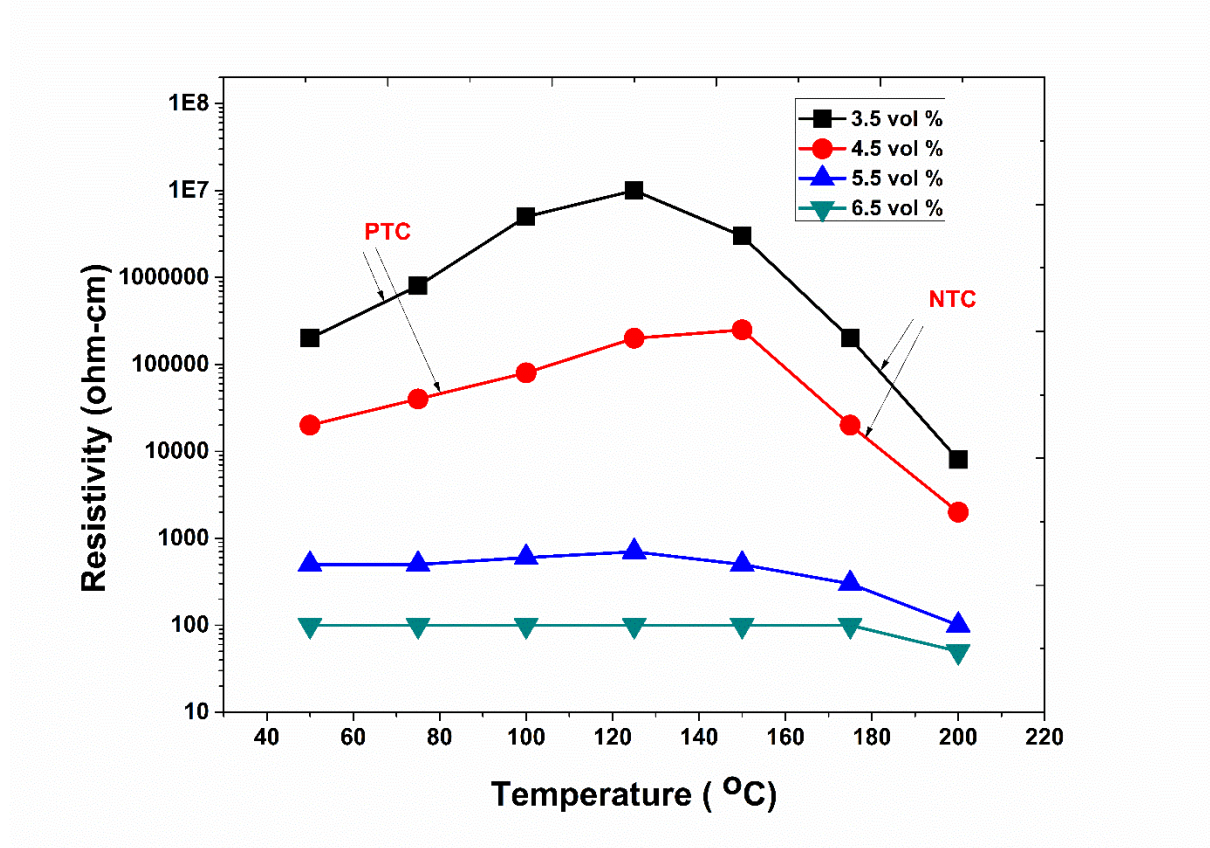


Figure 3.14: Resistivity variations with temperature on different loadings of filler in composites.

The relationship between voltage and current is given by Ohm's law:

$$V = R(I)^{\frac{1}{n}}, \quad (3.6)$$

where V is the applied voltage, I is applied current, R is resistance and n is an exponent. The Equation (3.6) can be rewritten as:

$$I = KV^n, \quad (3.7)$$

where K represent the electrical conductivity of nanocomposites. This Equation is nonlinear, which implies that the composite material is semiconductor in nature. Further, this Equation can be used with power law to obtained the values of n and K from the slope and the intercept in the $\log I \sim \log V$ plot. The current and voltage curves shown in Figure 3.15, are plotted for composite material at percolation threshold loading (2.2 vol%). The values of the n obtained by the linear fit (inset of Figure 3.15) is found greater than unity (~ 1.7). The current and voltage curves shown in Figure 3.16, are plotted for composite material above percolation threshold loading (6.0 vol%). The value of n was decreased with increase in loading % of filler contents above percolation threshold. As n approaches to unity (inset of Figure 3.16), this indicates that a continuous conducting network of GNPs has formed in the polymer matrix.

The VI graph will become linear and there will be perfect curve fitting for $\log V$ verses $\log I$ plot. For $n = 1$ composite material will be a conductor in nature. The transition of the conduction mechanism from nonlinear to linear can be generally understood by the tunnelling-hopping model. Below V_c , the filler particles are far apart and consequently there are very small current flows in the nanocomposite, thus the I - V characteristics below V_c is non-ohmic in nature; when the filler content approaches V_c , the conductivity suddenly increases because the fillers becoming close together, and the conduction mechanism is hopping up of the electrons; above V_c , filler particles either come in close contact or with very small gaps from one another, thus the conduction mechanism is tunnelling up of the electrons. The measured electrical conductivity is validated via VI characteristics as shown in Figure 3.17.

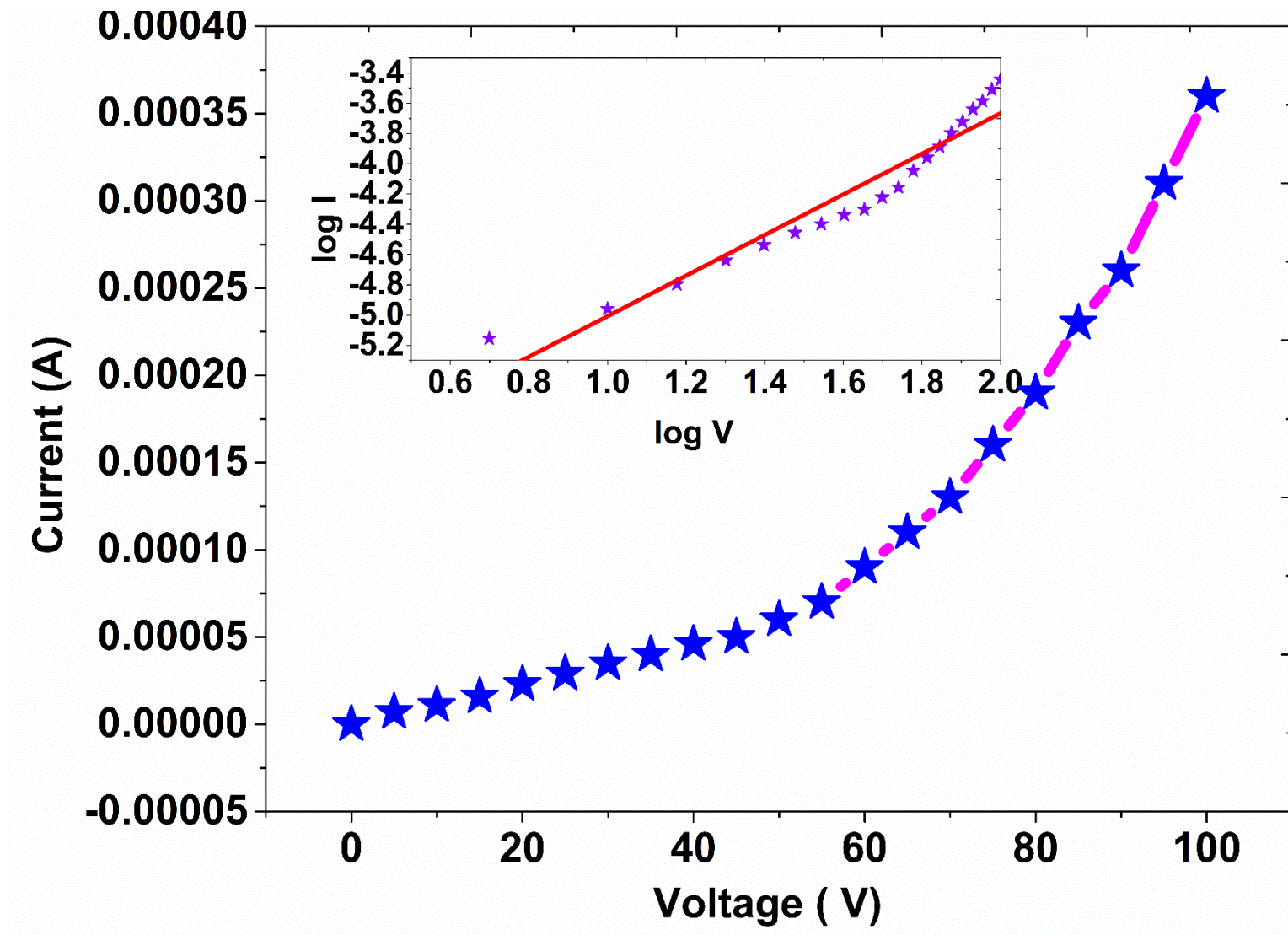


Figure 3.15: Voltage, current characteristics of composite at percolation threshold.

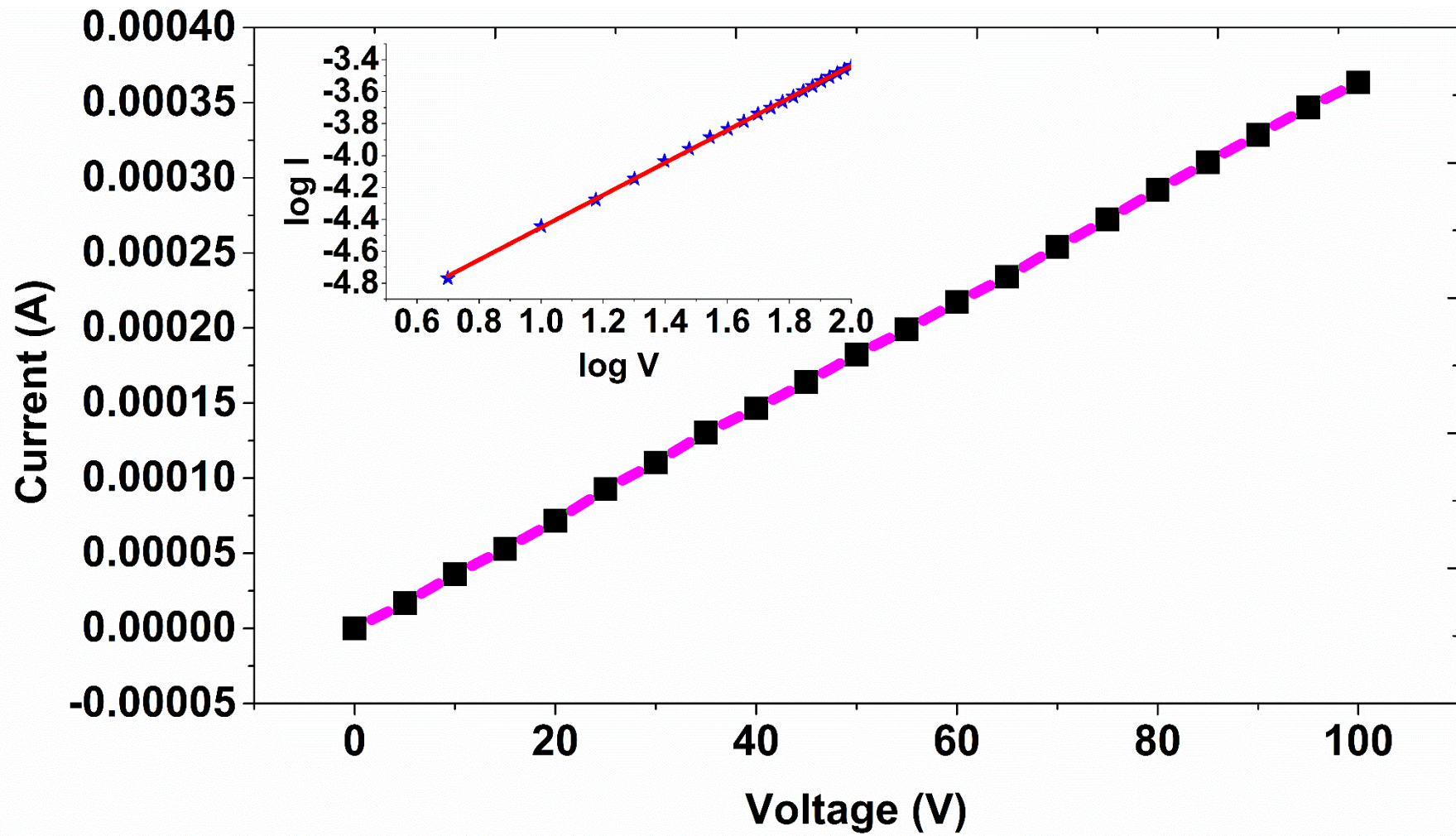


Figure 3.16: Voltage, current characteristics of composite above percolation threshold.

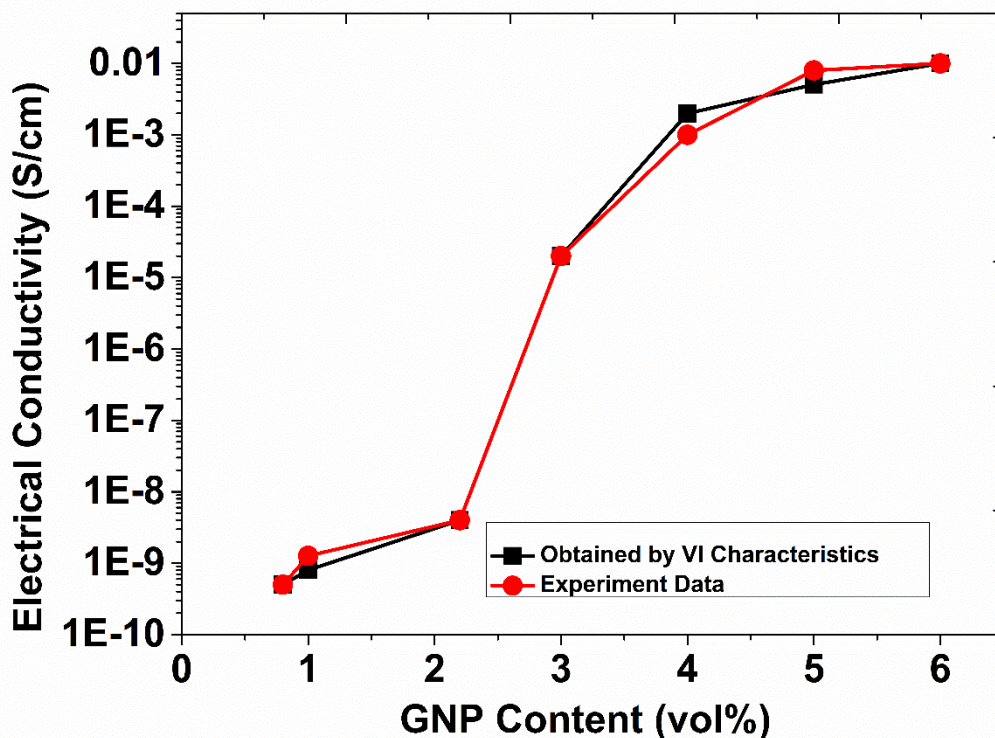


Figure 3.17: Electrical conductivity of PU/graphite composites calculated from V I characteristics compared with experimental data.

3.4 EMI Shielding of Polyurethane Graphite Composites

Carbon based polymer composites are well suitable for EMI shielding due to their easy processing, flexibility and low density. The CNT based composites are highly conductive with low percolation threshold, but still CNT based composites are not used due to certain drawbacks such as its difficulty in dispersion, high probability of breakage during the processing, alignment in the matrix, poor compatibility with polymer, and high cost. So in the present study, instead of CNT based composites, EMI Shielding Effectiveness (SE) is studied for prepared PU/graphite composites. There are two basic mechanisms of EMI shielding, one is reflection and other is absorption. For reflection of radiations by the shield, the shield must have free charge carriers, which makes it conductive with the incident electromagnetic radiations on shielding. Therefore, for a composite material which contains the conductive filler, must have the filler fraction above the percolation threshold. In the second mechanism, the incident electromagnetic radiations absorbed in the composite material or other shielding

material due to the interaction of these radiations with electrical or magnetic dipoles in the shield.

The absorption loss is a function of the product $\sigma_r \mu_r$, whereas the reflection loss is a function of the ratio σ_r / μ_r , where σ_r is the electrical conductivity relative to copper and μ_r is the relative magnetic permeability [Chung *et al.* (2001)]. The materials with excellent conductivity are good for reflection, whereas the materials with high magnetic permeability are good for absorption. These both losses are frequency dependent, the reflection loss decreases with increase in frequency, whereas absorption loss increases with increase in frequency. The absorption loss also depends upon the thickness of shielding material. Apart from these two mechanisms, there is one more mechanism which causes the electromagnetic shielding due to multiple internal reflection losses. These losses are due to fillers with large surface area in the composite material. In these losses, the distance between the surfaces causes internal reflection should not exceed the skin depth. Phenomenon in which high frequency electromagnetic radiation interacts with only the near surface region of an electrical conductor is called skin effect.

$$\text{Skin depth } (\delta) = \frac{1}{\sqrt{\pi f \mu \sigma}}, \quad (3.8)$$

where f is frequency, μ is magnetic permeability = $\mu_0 \mu_r$, μ_r is relative magnetic permeability, $\mu_0 = 4\pi \times 10^{-7} \text{ H/m}$, and σ is electrical conductivity in $\Omega^{-1} \text{ m}^{-1}$. The variation of skin depth with frequency is explained by Equation (3.8).

According to Schelkunoff shielding effect theory [Schelkunoff *et al.* (1934); Lai *et al.* (1993)], the total shielding effectiveness is the sum of reflection, absorption, and multiple reflection losses described by the following set of Equations:

$$SE = R + A + B \text{ (dB)}, \quad (3.9)$$

where R is reflection loss, A is absorption loss, and B is multiple reflection loss

$$R = 168.1 + 10 \log \left[\frac{\sigma_r}{(\mu_r f)} \right] \text{ (dB)}, \quad (3.10)$$

$$A = 1.31t(\sigma_r\mu_rf)(dB), \quad (3.11)$$

and

$$B = 20\log(1 - 10^{-0.1A})(dB). \quad (3.12)$$

For Equations (3.10) to (3.12):

σ_r is electrical conductivity relative to copper, μ_r is relative magnetic permeability f is frequency of radiations in MHz, and t is thickness of shielding material in cm. The value of third part B is very small and it is related to A . Other analytical approach to calculate the effective shielding is given by [Zhang *et al.* (2007)]:

$$R = 50 + 10\log\left(\frac{\sigma_c}{f}\right) (dB), \quad (3.13)$$

and

$$A = 1.7t(\sigma_cf)^{1/2}(dB). \quad (3.14)$$

For Equations (3.13) to (3.14):

σ_c is electrical conductivity of shielding material in $\Omega^{-1}m^{-1}$, f is frequency of radiations in MHz, and t is thickness of shielding material in cm. Above stated analytical methods can be further validated through Shielding Effectiveness Calculator by Clemson University.

Inner Diameter = 10mm
Outer diameter = 115 mm



Figure 3.18: Experimental setup for electromagnetic shielding effectiveness measurement.

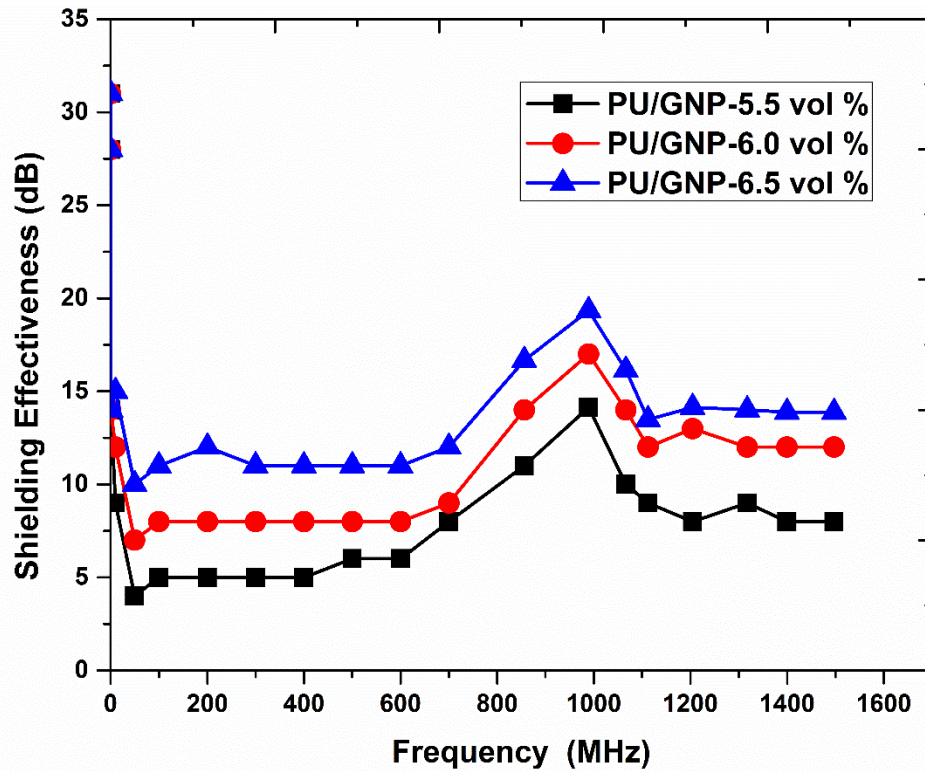


Figure 3.19: SE of PU/graphite composites with different loadings of GNPs.

The electromagnetic shielding effectiveness can be measured through analytical as well as experimentally as explained in Figure 3.18. The electromagnetic testing of composite was performed using the coaxial cable line method which is designed according to ASTM D4935 Standard [Steffan *et al.* (2010)]. Where, electromagnetic shielding effectiveness is defined as the ratio of transmitted power to the incident power as given by following Equation:

$$SE = 10 \log \frac{P_t}{P_i} (dB). \quad (3.15)$$

The experimental setup is consisting of an Agilent 8753ES-H39 30 KHz to 3 or 6 GHz Vector Network Analyzer, coaxial cable lines with flange holders, attenuator (10 dB). The sample of composite material for electromagnetic shielding is kept on low filler concentration. This is because the mechanical strength and ductility of PU/graphite composite tend to decrease with increasing GNPs filler content when the filler-matrix bonding is poor. Lower filler contents also desirable due to the greater process ability, low cost, and low weight. The primary mechanism of electromagnetic shielding in the prepared PU/GNPs composites is reflection and multiple reflections due to the large surface area of GNPs. Due to reflection the shielding

effectiveness decreases with increase in frequency. The prepared PU/GNPs composites are highly effective EMI shielding materials at 0.9-1 GHz. In order to increase the absorbing effectiveness, this composite must also some highly permeable matrix like nickel nanoparticles with GNPs. Due to the amorphous nature of PU it is more effective for EMI shielding than any other crystalline polymer. The experimental results are shown in Figure 3.19.

3.5 Interconnect Track at Nanoscale in Integrated Circuits

The proposed material is easy to fabricate as the interconnect track at nanoscale in integrated circuits due to good adhesive nature as illustrated the RLC model of a transmission line of PU/GNPs in Figure 3.20(a). Interconnects made of N Parallel PU/GNP tracks of the same lengths L and widths W . R_C represent the equivalent resistances introduced by the imperfect contacts, R_Q is the resistances introduced by quantum effect, and R_S represent the equivalent resistances introduced by the carriers' scatterings. PU/GNPs interconnect, is driven by a repeater of output resistance R_{out} and output parasitic capacitance C_{out} . It is driving an identical repeater with an input capacitance of $C_L=C_{out}$. In order to calculate the input output transfer function for the configuration, shown in Figure 3.20(b), one can use the $ABCD$ transmission parameter matrix for a uniform RLC transmission line:

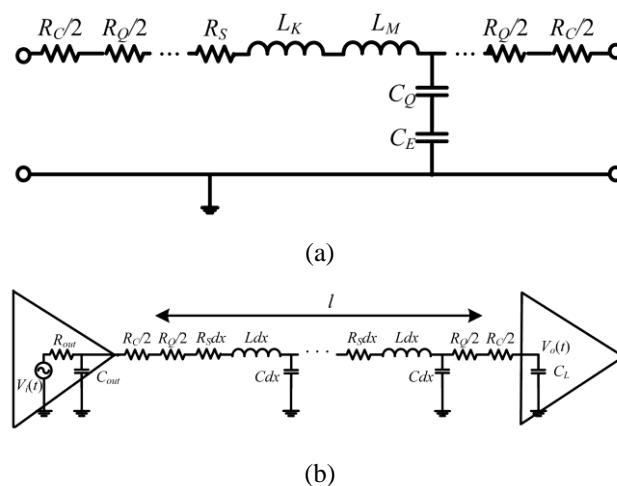


Figure 3.20: Schematic of (a) A typical RLC model for nano scaled interconnects, and (b) A transmission line circuit model for a driver-PU/GNPs interconnect-load configuration.

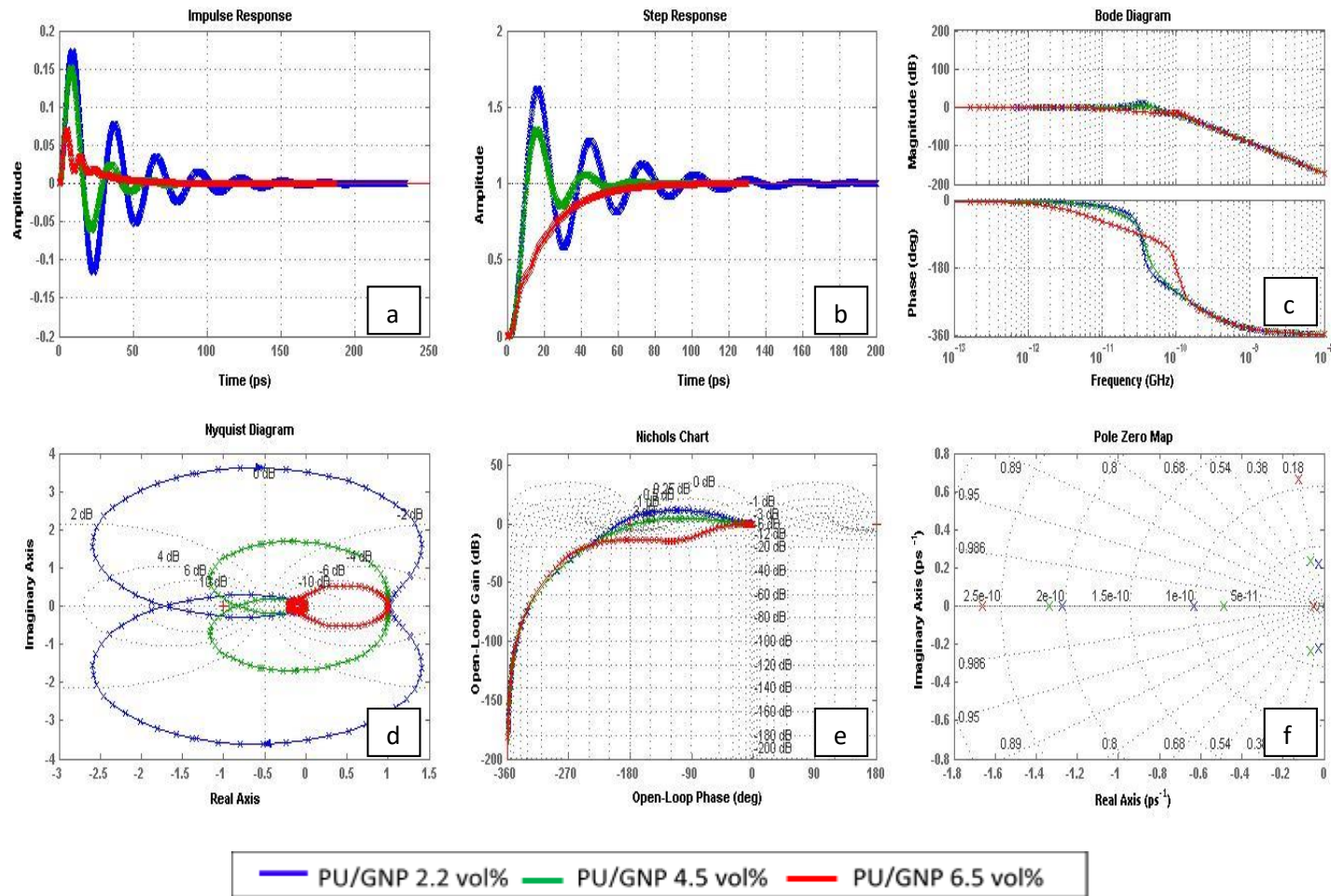


Figure 3.21: Time and frequency responses of PU/GNP composites based interconnects using (a) Impulse response, (b) Step response, (c) Bode plot, (d) Nyquist plot, (e) Nichols chart, (f) Pole zero map.

$$T_{total} = \begin{bmatrix} A_T & B_T \\ C_T & D_T \end{bmatrix} \equiv \begin{bmatrix} 1 & R_{out} \\ 0 & 1 \end{bmatrix} \begin{bmatrix} 1 & 0 \\ sC_{out} & 1 \end{bmatrix} \begin{bmatrix} 1 & R_{ex} \\ 0 & 1 \end{bmatrix} X \begin{bmatrix} \cosh(\gamma^T l) & Z_0^T \sinh(\gamma^T l) \\ Z_0^{-T} \sinh(\gamma^T l) & \cosh(\gamma^T l) \end{bmatrix} \begin{bmatrix} 1 & R_{ex} \\ 0 & 1 \end{bmatrix}, \quad (3.16)$$

where complex frequency is ($s = j\omega$), $R_{ex} = (R_C + R_Q)/2$, $Z_0^T = \sqrt{(R_s + sL)/sC}$,
 $\gamma^T = \sqrt{(R_s + sL)sC}$.

The elements of T_{total} are given by [Nasiri *et al.* (2012)].

The time and frequency responses are shown in Figure 3.21. The tracks for integrated circuits interconnects are studied at different loading levels of GNPs. These tracks are found stable in both time and frequency domain, however there is oscillatory response due low loading of GNPs. The oscillatory behaviour in transient response is due to the energy storage elements in the interconnects. Due to the partial establishment of electrical networks at a lower loading level the factitious capacitance of interconnect is act as energy storage element.

This material can be used in 3D integrated circuits to prevent the crosstalk among the interconnects at nanoscale fabrication. This material can also be used in the MEMS industries for efficient energy harvesting devices. Furthermore, this nanocomposite can be used to reduce the productivity gap between the integrated devices and interconnect speed defined by the International Technology Roadmap for Semiconductors (ITRS).

3.6 Conclusion

Polyurethane /Graphite composites were prepared by *in-situ* polymerization technique. Better dispersion of nanoparticles was achieved as indicated by X-ray diffraction, SEM and TEM. PU/graphite composites have shown an intercalated composite structure. The layered structure of graphite nanoparticles has been clearly seen by HRTEM, which reveal the intercalation of GNPs in nanocomposite. The sonication during *in-situ* polymerization had played a key role to prevent the aggregation of GNPs to a significant extent. The electrically conductive films of PU/graphite composites were made by spin coating process. The percolation threshold of the prepared films was studied and found experimentally to be 2.2 vol%, which was validated with

IPD based theoretical predictions. Due to enhanced electrical conductivity and EMI shielding, the potential utility of prepared nanocomposite is in adsorbents for gas chromatography, electrical brushes and contact strips in MEMS based wafer motor.

CHAPTER 4

SYNTHESIS AND MECHANICAL PROPERTIES OF POLYURETHANE/CLAY NANOCOMPOSITES

4.1. *Introduction*

Polymer nanocomposites are developing a great deal of interest due to their unusual properties and some new novel properties developed in to them, which are not present in the neat polymers or the conventional composites. These unusual and new properties are derived by the addition of some nanoscale fillers into the matrix. The nanoscale filler means that the filler has at least one dimension in the nanometer range (<100 nm). Nanocomposite technology has been described as the next great new frontier of materials science because it involves the use of a small quantity of nanofiller (< 5 wt%) and enhances the mechanical, thermal, optical, electrical, and barrier performance properties significantly [Song *et al.* (2003)]. Various polymers have been studied to prepare polymer nanocomposites by using different types of nanofillers. This chapter presents the study of polyurethane (PU)/clay nanocomposite. The inorganic layered nonofillers like graphite, clay minerals, transition metal dichalcogenides, metal phosphates, and layered doubly hydroxides are widely used in preparation of nanocomposites [Thirumal *et al.* (2009)]. Among these the clay nanoplatelets belonging to semantic family are attracting attention due to their high aspect ratio (100-1500), high surface area to volume ratio (750 m²/gm), abundantly present in nature, high cation exchange capacity and low cost [Solarski *et al.* (2005)]. Moreover, in the structure of clay the atoms in the layers are held together by chemical bonds while the successive layers are held together by weak Vander wall forces. These weak physical forces can easily be broken when the large organic polymer molecules enter into the gallery. Therefore, the layered structure of clay provides a great potential for the large organic molecules to be intercalated/exfoliated into them. The clays are consisting of units called sheets or platelets. One platelet is made up of two silica tetrahedral layers and one central alumina or magnesia octahedral layers. The octahedral layer is sandwiched in between the two silicon tetrahedral layers. The inorganic cations like Na⁺, K⁺, Li⁺ are naturally present in gallery

which can be exchanged with some organic ammonium cations e.g. alkylammonium cations in order to modify the clay platelets so that they become hydrophobic to be compatible with most of the polymers. Naturally the clay platelets are not present in nanometer range but they can be easily delaminated or exfoliated into nanometer platelets with a thickness of about one nm [Hu *et al.* (2001); Capek *et al.* (2000)].

The clay nanoplatelets are generally supposed to enhance the mechanical performance of various polymers which find their applications in transport industries (automotive and aerospace). The research of polymer nanocomposites got a boost up after the pioneer work from Toyota motors in 1987 [Rehav *et al.* (2005)]. Toyota prepared Nylon-6/Clay (OMMT) nanocomposites and first commercial product of clay based polymer nanocomposites was the timing-belt cover in 1990. These Nylon-6/clay based nanocomposites prepared by Toyota had significant improvement in strength and modulus namely 40% in tensile strength, 60% in flexural strength, 68% in tensile modulus, 126% in flexural modulus, and heat distortion temperature was increased by 80°C as compare to pure Nylon [Cao *et al.* (2005)]. There are numerous studies on dispersion and mechanical properties of PU nanocomposites with clay particles. The present work addresses the enhancement in mechanical properties of PU with nanoclay. The PU nanocomposites with OMMT have been prepared by using *in-situ* polymerization technique and mechanical properties of resulting nanocomposites were studied. It is known that *in-situ* polymerization is an efficient method to improve the dispersion of OMMT in the polymer matrix [Askari *et al.* (2015)]. Here the monomers are polymerized in the presence of filler and consequently the *in-situ* technique would confer strong interaction between the reinforcing filler and polymeric phase [Yu *et al.* (2008)]. The resulting nanocomposites were characterized by XRD and TEM and their mechanical properties were also studied by universal testing machine.

4.2. Experimental Section

4.2.1 Materials

Cloisite[®] 30B is supplied by Connell Bros. Company (India) Pvt. Ltd. The monomers Toluene, 2,4-Diisocyanate (TDI) with molecular weight 174.16 and Polypropylene glycol (PPG) with molecular weight 2000 were supplied by MP Biomedicals Fine Chemicals Division, India. The

monomers were of analytical grade purity and were used as received. The chain extender 1,4-Butanediol (BDO) was supplied by same company.

4.2.2 Preparation of Polyurethane OMMT Nanocomposites by In-situ Polymerization

The PU/OMMT nanocomposites were prepared by using TDI:PPG:BDO in the mole ratio of 3:1:2. PPG and nanoclay were mixed and stirred for 12 h at 50°C to obtain PPG-OMMT suspension. This suspension was subjected to sonication for one hour to avoid the agglomeration of nanoclay particles. The low viscosity of PPG helps in maintaining a uniform distribution of clay particles in the solution. TDI was poured in to this suspension with continuous stirring. During the mixing of TDI, the temperature was maintained at 70°C as it was an exothermic reaction. After mixing TDI, the resultant solution was heated at 85°C for 4 h with stirring. Subsequently, after cooling the reaction mixture to 40°C, BDO was added with vigorous stirring for 1 min. Immediately after this, a small portion of solution was mixed with DMF for spin coating and, for TEM characterization using drop casting on TEM grid. The resultant nanocomposite solution was poured into a defined shape mold for final curing. The nanocomposite material in the mold was heated at 160°C for 16 h to dry it completely.

4.2.3 Characterization

The X-ray diffraction (XRD) patterns of processed materials were recorded on PANalytical's XPERT-PRO Diffractometer system with Cu K-Alpha1 [\AA]: 1.54060 and 2θ (2° - 30°). The dispersion state of prepared nanocomposites samples were studied by Transmission Electron Microscope (TEM). The samples were prepared by dispersing the film on glass/silicon substrates by spin coater. The mechanical properties of prepared nanocomposites samples were studied by universal testing machine. The whole schematic diagram of synthesis process of polyurethane/OMMT composites is shown in Figure 4.1.

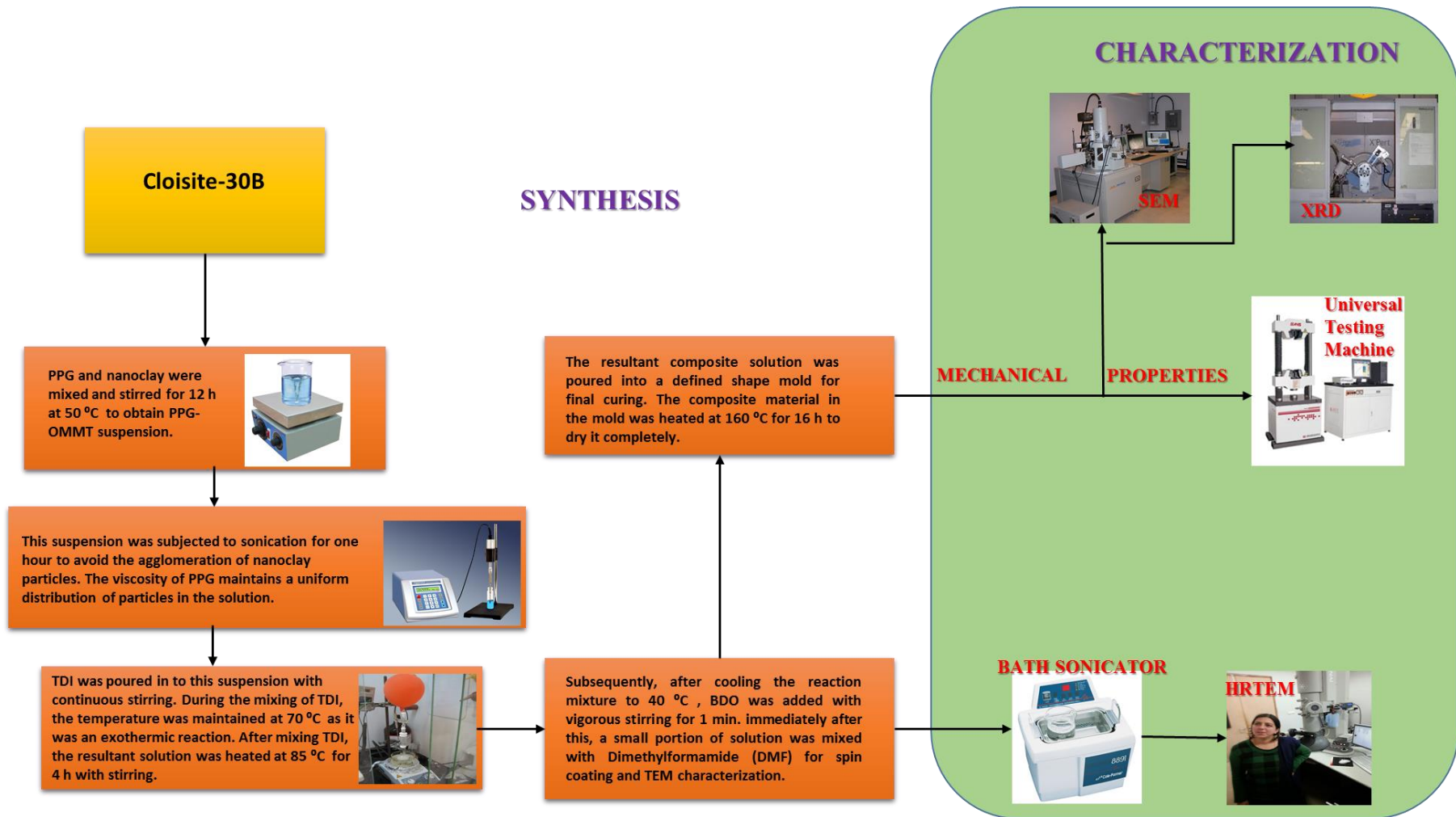


Figure 4.1: Schematic diagram of whole synthesis process of polyurethane/OMMT composites

4.3. Results and Discussion

4.3.1 XRD and TEM Analysis

The results of X ray diffraction are shown in Figure 4.2 in the form of diffraction peaks for the Cloisite[®]30B and nanocomposite samples containing 0.5 and 1.5 wt% loading levels of clay Cloisite[®]30B displayed the major diffraction peaks at 4.81° corresponding to d-spacing (d_{001})

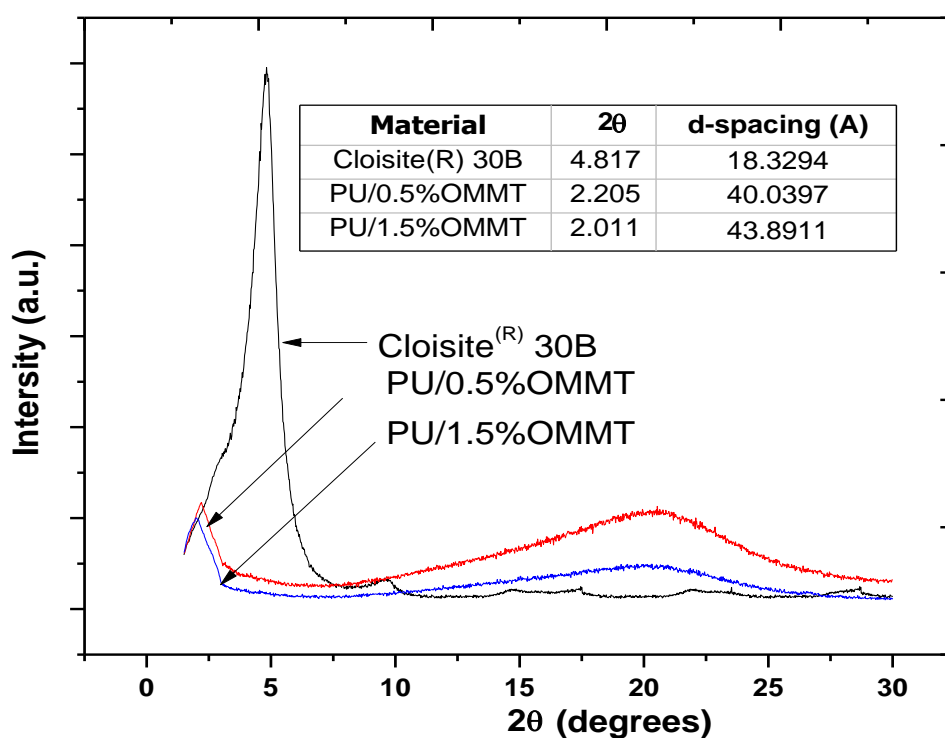


Figure 4.2: X-ray Diffraction of pure Cloisite[®] 30B, and prepared samples of polyurethane/clay nanocomposites.

of 1.8329 nm. The nanocomposite containing 0.5 wt% of clay nanoparticles showed the shifting of diffraction peak towards the lower angle (2.205°) indicating the d spacing of 4.0039 nm. Similarly, the nanocomposite containing 1.5 wt% of OMMT displayed the major deflection peak at lower angle of 2.011° indicating the d spacing of 4.389 nm. so, this can be concluded that increase in d-spacing means that the polymer chains have diffused inside the gallery and intercalated type of nanocomposites are formed. The *in-situ* polymerization technique confers the strong interaction between clay platelets and the monomers, as polymerization takes place inside the galleries and hence expands it significantly.

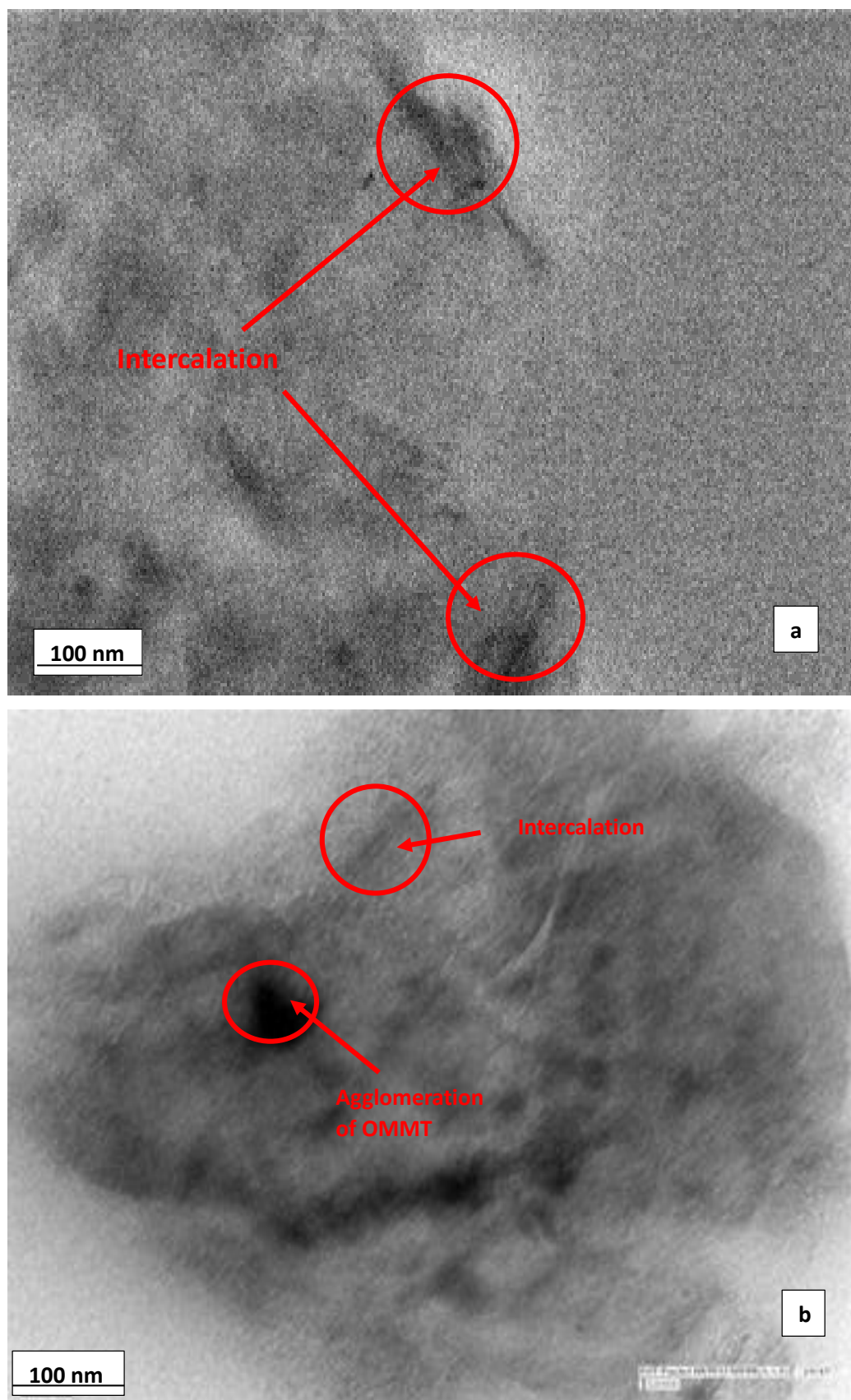


Figure 4.3: TEM images of prepared samples of polyurethane/clay nanocomposites showing intercalation and agglomeration in (a) and (b).

The morphology of prepared nanocomposites was further confirmed by TEM. The TEM images shown in Figure 4.3 are clearly indicating the presence of clay platelets in the form of stacks or tactoids marked by arrows. Simultaneously the small quantity of clay platelets was agglomerated as the loading level was increased (Figure 4.3 b).

4.3.2 Mechanical Properties

The mechanical properties of prepared nanocomposites were studied with a universal testing machine with dumbbell sample specifications shown in Figure 4.4.

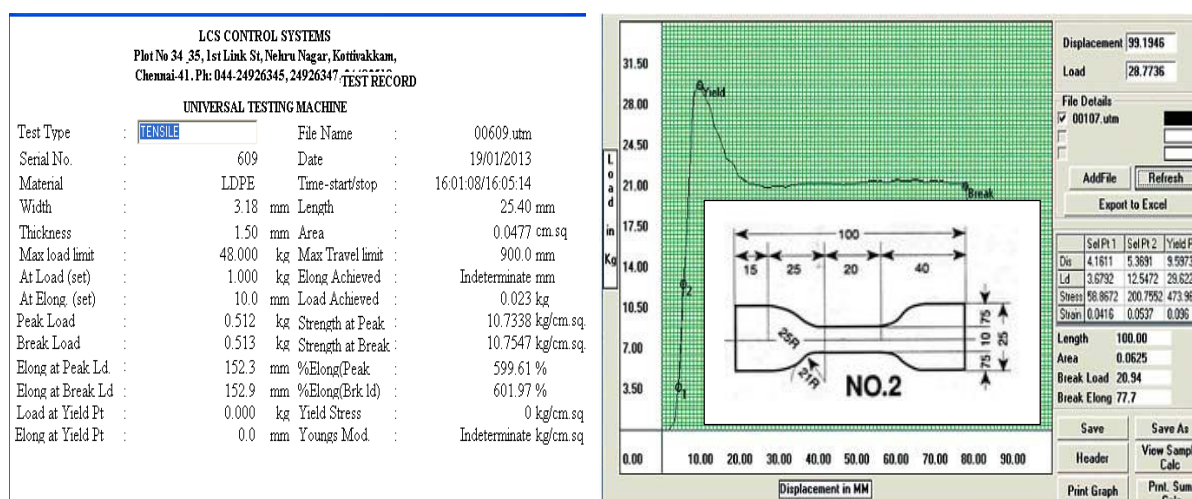
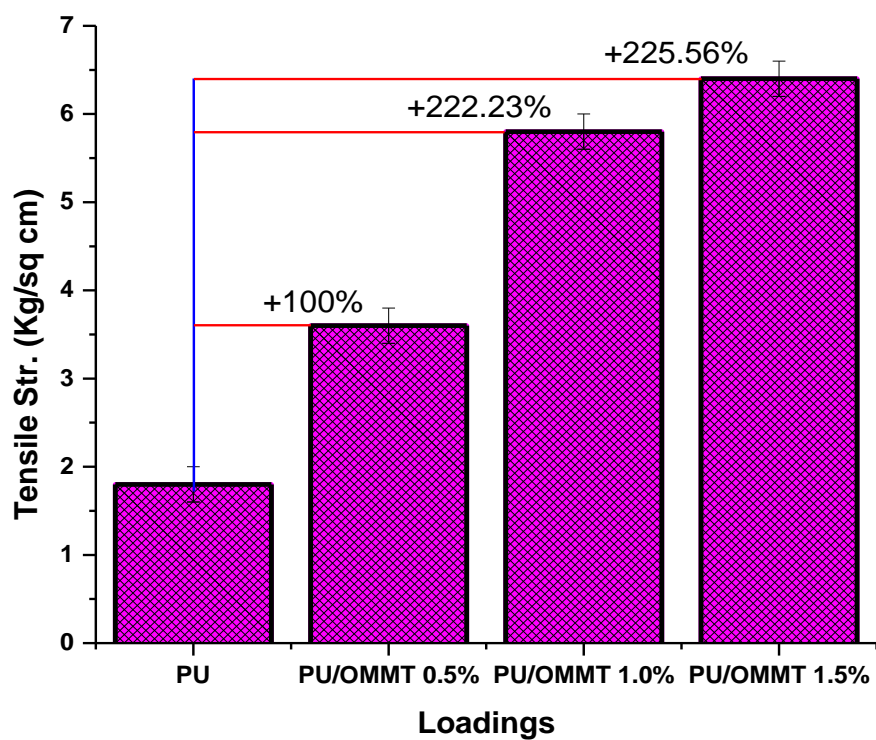
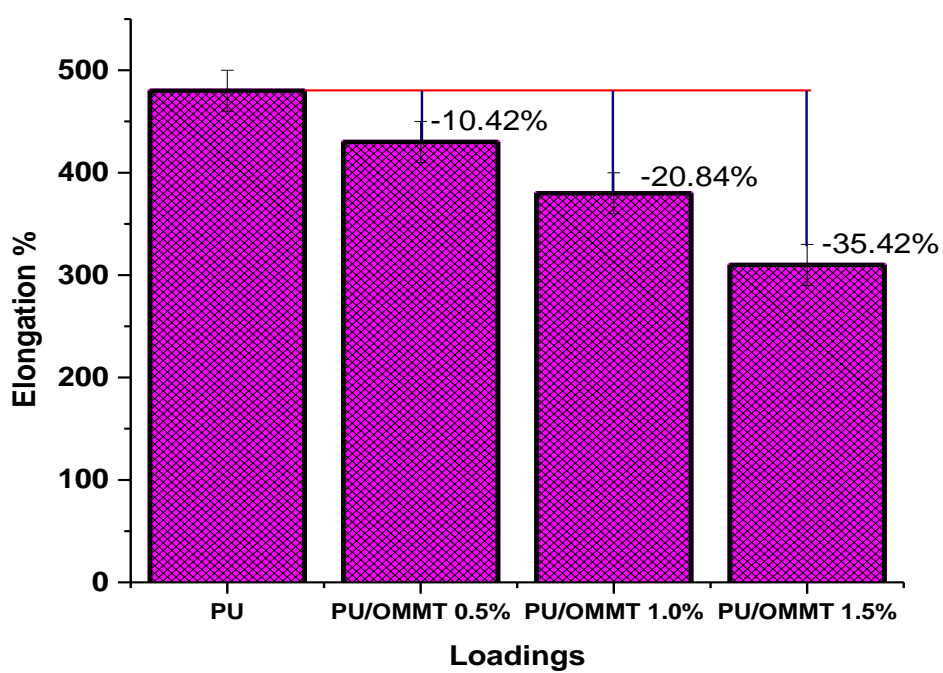


Figure 4.4: Characterization of nanocomposite with universal testing machine.

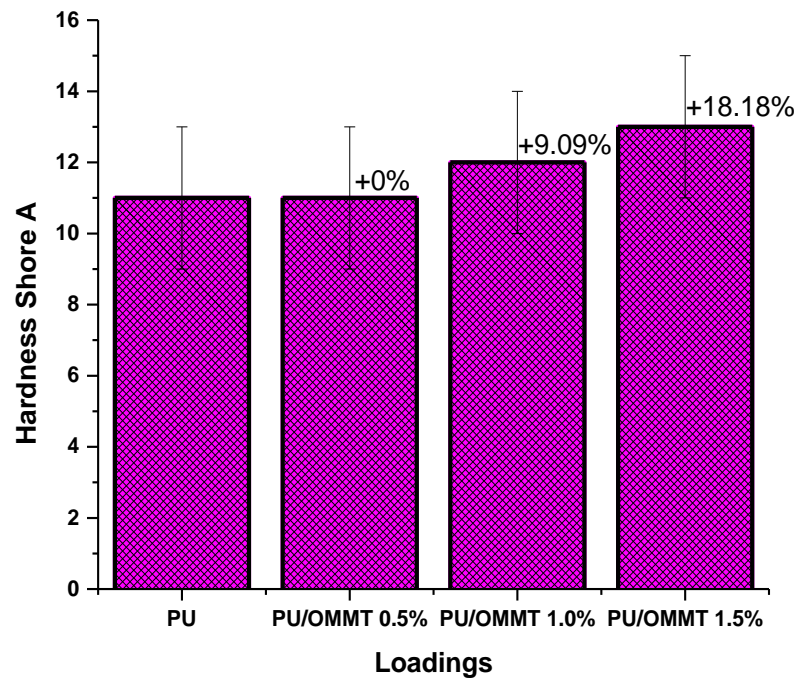
The mechanical properties of pristine PU and PU/OMMT nanocomposite, cut in dumbbell-type samples are shown in Figure 4.5. The tensile strength of composite samples is increased with the increase in % loading levels as compare to pristine PU (Figure 4.5 a), because of good interfacial interaction between the OMMT layers and polymer matrix [Deng *et al.* (2008); Xiong *et al.* (2004); Chun *et al.* (2007)]. Due to high aspect ratio of layered silicate fillers similar to fibers within a fiber reinforced plastic, the tensile strength of PU enhanced. The elongation % is decreased with the different loading levels, however this downfall is very less as compare to pure PU (Figure 4.5 b) and was maintained at a level close to that of pure PU [Goettler *et al.* (2007)]. Shore hardness is a measure of the resistance of a material to the penetration of a needle under a define spring force. The letter A is used for flexible type. The hardness shore A is also increased with the increase in % loading levels as compare to pristine PU (Figure 4.5 c) [Ray *et al.* (2014)]. At 0.5 wt%.



(a)

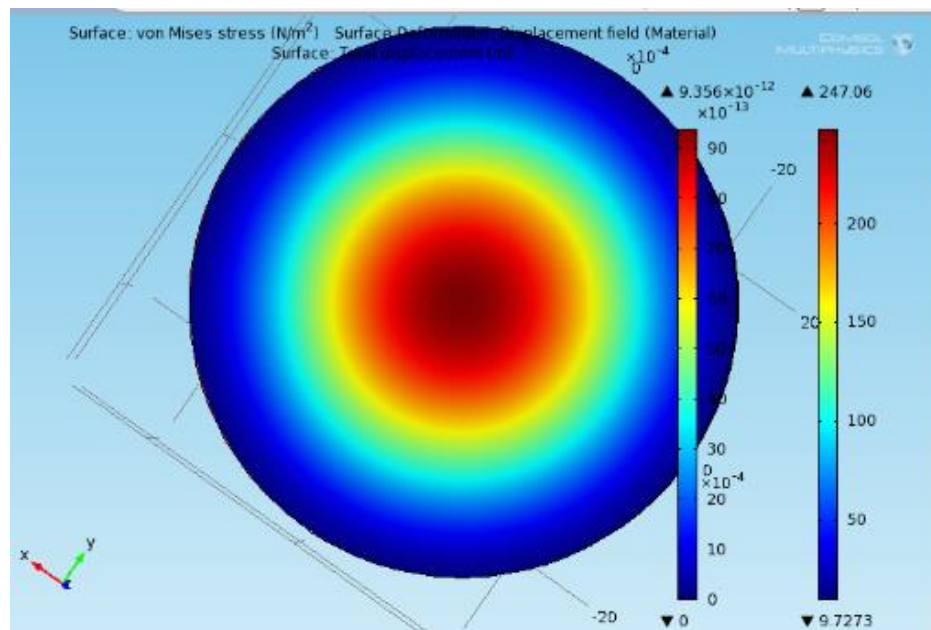


(b)

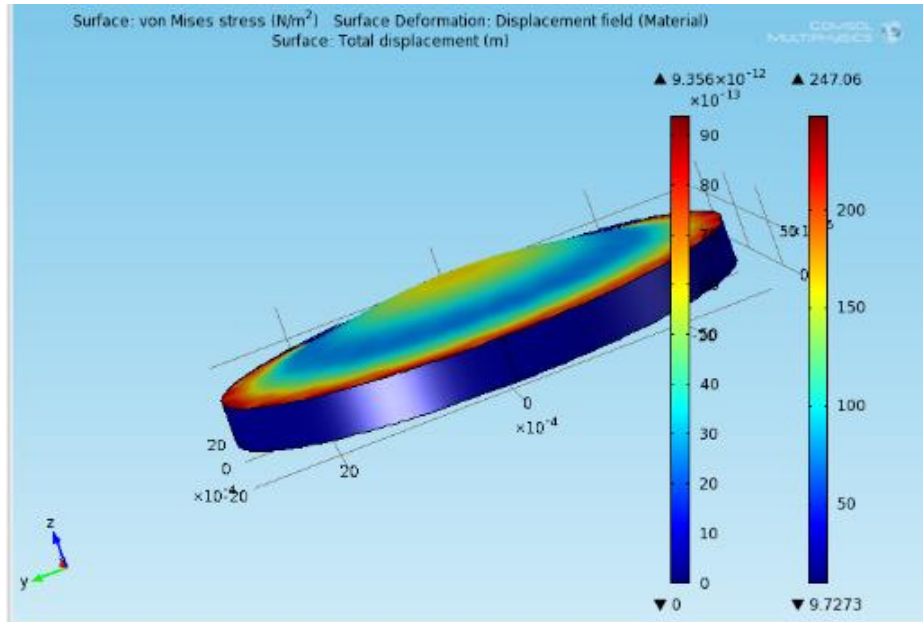


(c)

Figure: 4.5. Mechanical properties of PU/OMMT nanocomposites (a) tensile strength (b) elongation % (c) hardness shore A.

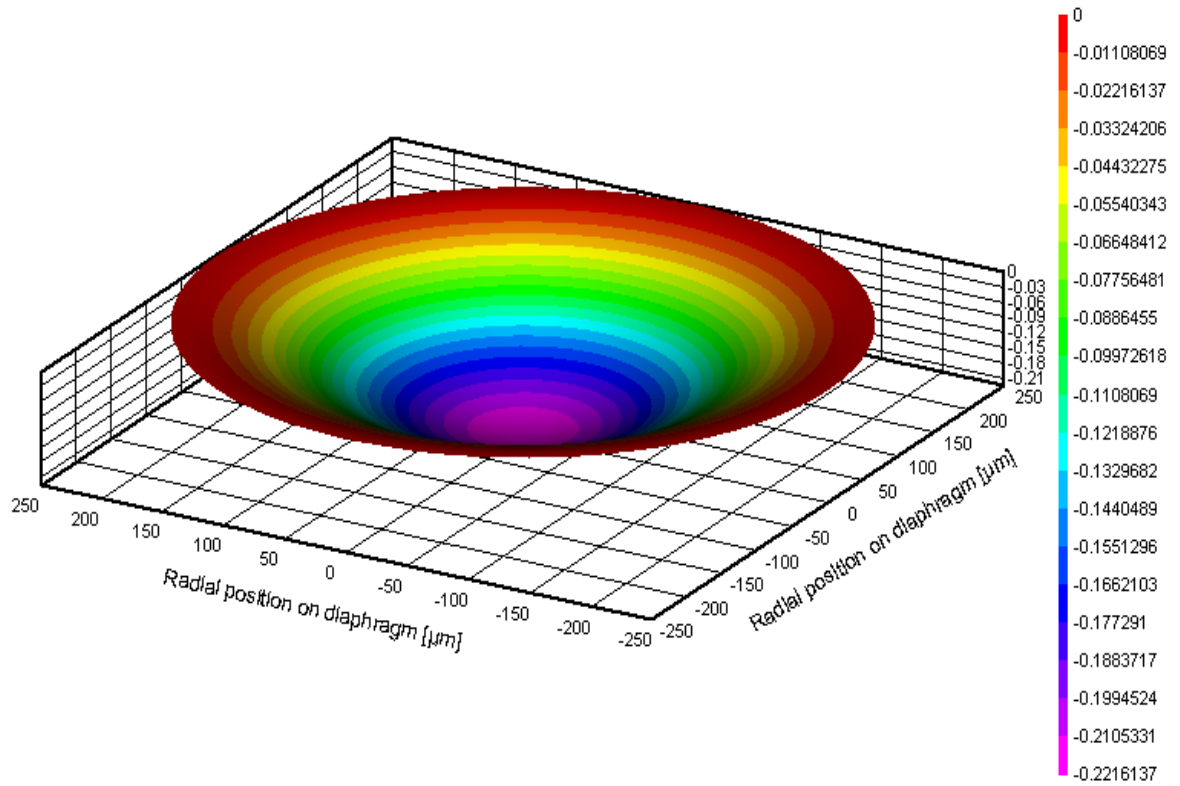


(a)

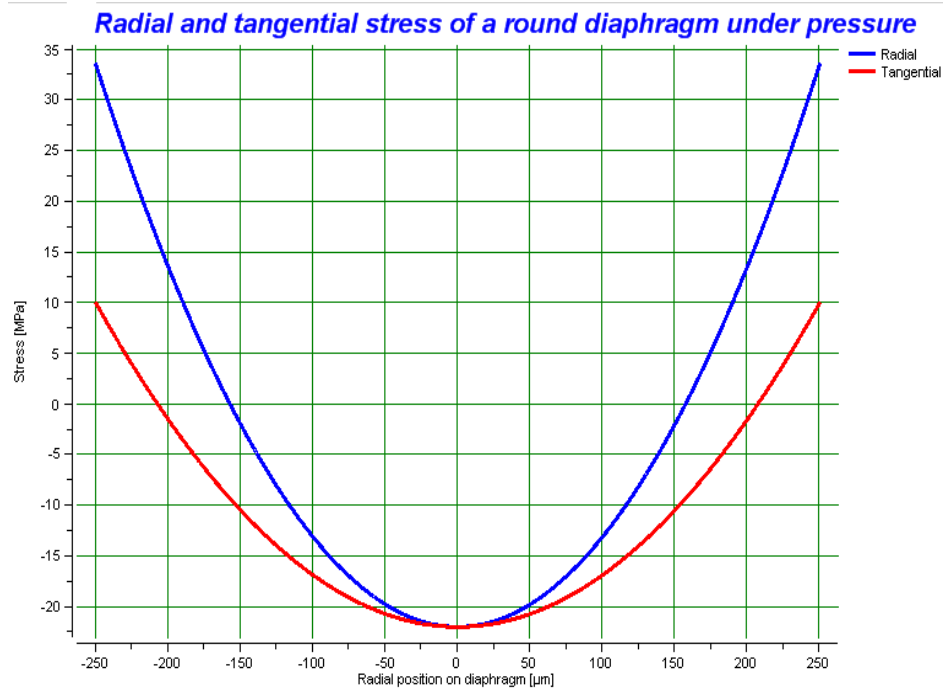


(a)

Deflection of a round diaphragm under pressure



(b)



(c)

Figure: 4.6. PU/OMMT as pressure MEMS (a) comsol simulation snapshots (b) deflection of round diaphragm (c) radial and tangential characteristics.

loading level of OMMT, the harness shore A was maintained at a level closed to that of pure PU. At 1.0 and 1.5 wt % of OMMT, a slight increase in hardness has been observed. Importing the obtained mechanical properties, the PU/OMMT for pressure MEMS application have been simulated and shown in Figure 4.6a and b. In addition, the prepared diaphragm has been simulated on platform [Gall *et al.* (2004)]. The maximum possible deflection of this diaphragm is 30% of its thickness. The deflection y at radial distance r of a round diaphragm rigidly clamped, under a uniform pressure P , is given by:

$$y = \frac{3(1-\nu^2)P}{16Eh^3} (a^2 - r^2)^2 \quad (4.1)$$

where h is thickness of diaphragm, E is the Yong's modules, ν is the Poisson's ratio, a is the radius of diaphragm. The maximum deflection in Figure 4.6b, will occurs at the center of diaphragm where $r = 0$. The Poisson's ratio of nanocomposite is ≈ 0.5 , the maximum deflection is given by:

$$y_o = \frac{0.14063Pa^4}{Eh^3} \quad (4.2)$$

Radial and tangential characteristics with respect to radial position of diaphragm are shown in Figure 4.6 c.

4.4. Conclusion

Finally, it can be seen that the PU/OMMT nanocomposites were prepared by using *in-situ* polymerization. The structure and morphology of prepared nanocomposites were studied by XRD and TEM. Both techniques revealed the formation of an intercalated type of nanocomposites and some agglomerated clay platelets were also observed by TEM. The tensile strength of nanocomposite was increased as compare to pristine PU on increasing the loading level of clay. However, the elongation % was decrease as compare to pure PU. The hardness shore A of these nanocomposites was also increased on increasing the loading level of clay but it was a fractional increase as compare to tensile strength. A pressure diaphragm is also simulated by using these properties as simulation parameters. In these MEMS the sensitivity of diaphragms is improved.

CHAPTER 5

SYNERGISTIC EFFECTS OF CLAY AND GNPS ON ELECTRICAL AND MECHANICAL PROPERTIES OF PU/GNP/OMMT TERNARY COMPOSITE

5.1. *Introduction*

In the recent year a lot of research has been done to study the synergistic effects of two nanofillers in one system. The two key factors associated with nanofillers are their proper dispersion in the matrix and strong interfacial interaction with the matrix. According to previous studies, PU/nanofiller binary nanocomposites drew attention because of their interesting and fine-tuned properties. [Khudyakov *et al.* (2009)]. However, the PU based ternary nanocomposites are less studied. Ternary nanocomposites are anticipated to show more versatile properties and higher potential in applications.

Carbon nanotubes, carbon black, graphite nano particles are considered excellent fillers because of their conducting properties [Sandler *et al.* (2003)]. However, being inert, these conductive fillers are not properly dispersed in the matrix and get agglomerate at higher loading level (beyond percolation threshold). Further, as the concentration of conductive filler increases above percolation threshold, the mechanical properties of prepared nanocomposites also start to deteriorate because the agglomerated part of conductive filler acts as the stress concentration area leading to poor mechanical properties like decrease in strength and modulus of the nanocomposites [Han *et al.* (2005)]. The poor interface interaction with matrix along with poor dispersion leads to poor mechanical as well as electrical properties. The preparation of multifunctional, high performance nanocomposite which having well electrical (low percolation threshold) as well as mechanical properties can overcome these limitations. Various methods are available in literature to lower down the percolation threshold of CNTs in polymers like use of additives, the optimization of processing conditions and managing the size distribution [Han *et al.* (2005)] and the use of multiphase polymer blends [Dasari *et al.* (2005)].

Recently Seung Bin [Park *et al.* (2014)] attempted to lower down the percolation threshold of CNTs by using an immiscible polymer blending approach and mechanofusion technique. Synergistic effects of CNTs and layered double hydroxide (LDH) nanoplatelets in nylon matrix with improved mechanical properties were studied in [Peng *et al.* (2014)]. A similar approach of using a second filler/nanofiller working in a synergy with CNT has been proposed by [Huang *et al.* (2010)], and is defined as mixed (nano) filler system.

Recently, utmost attention is being directed to the use of CNTs with clay as binary filler. Polymer nanocomposites using clay/silica nanoparticles [Q.Fu *et al.* (2010)], clay/carbon black nanoparticles [Peeterbroeck *et al.* (2004)], and CNTs/titanium [Xu *et al.* (2010)], have been prepared. Adding clay into the nanotube/EVA composite has shown to enhance the formation of graphitic carbon. [Tang *et al.* (2008)]. Poly (methyl methacrylate)/silica/titania ternary nanocomposites with greatly improved thermal and ultraviolet-shielding properties were prepared by [Wang *et al.* (2006)]. A ternary cobalt ferrite/graphene/ polyaniline nanocomposite is synthesized for high-performance supercapacitors [Xiong *et al.* (2014)].

In this thesis, the preparation and characterization of PU/OMMT/GNPs ternary nanocomposites by using in situ polymerization technique have been reported. The synergistic effects of both the fillers were studied on electrical (percolation threshold) and mechanical properties of prepared nanocomposites. An effort has been made to retain the mechanical properties by lowering down the percolation threshold. The results were compared with the corresponding binary systems, i.e., PU having GNP as the only filler and significant improvement of the electrical and mechanical properties has been observed in ternary nanocomposites. A plausible explanation has been given to explain the observed improvements.

5.2 Experimental Section

5.2.1 Materials

Cloisite-30B was supplied by Connell Bros. Company (India) Pvt. Ltd. The graphite used for preparing GNPs was GIC, acidified with concentrated H₂SO₄ and HNO₃. The monomers Toluene, 2,4-Diisocyanate (TDI) with molecular weight 174.16 and Polypropylene glycol (PPG) with molecular weight 2000 were supplied by MP Biomedicals Fine Chemicals

Division, India. The monomers were of analytical grade purity and were used as received. The chain extender 1,4-Butanediol (BDO) was supplied by same company. 95% (v/v) alcohol and distilled water were used as solvents for preparation of GNPs.

5.2.2 Preparation of Expanded Graphite and Graphite Nano Sheets

Expanded graphite was prepared by adopting the procedure reported by [Chen *et al.* (2004); Yasmin *et al.* (2006)]. The GIC (powder form) was given a thermal shock at 1050 °C for 15 seconds in a muffle furnace to obtain expanded graphite particles along c direction or thickness direction about several hundred times that of original c direction dimension [Ganster *et al.* (2010)]. The gallery space of expanded graphite expands due to evaporation of intercalants trapped between the layers. The expanded graphite so obtained was mixed and saturated with 400 ml alcohol and distilled water in a ratio of 70:30 for 8 h. This mixture was subjected to sonication using a horn type sonicator for various time intervals (5, 8, 10 and 12 h). After sonication, expanded graphite particles were effectively fragmented in to foliated graphite. The graphite nano sheets dispersion was then dried at 80 °C to remove the residual solvents. In this way, the graphite nano sheets were obtained to be used as nanofiller in proposed nanocomposites.

5.2.3 Preparation of Polyurethane Graphite Clay Composites by In-Situ Polymerization

The PU/GNPs/OMMT composites were prepared by using TDI:PPG:BDO in the mole ratio of 3:1:2. PPG and prepared GNPs were mixed with Cloisite-30B and stirred for 12 h at 50° C to obtain PPG-GNPs-OMMT suspension. This suspension was subjected to sonication for one hour to avoid the agglomeration of graphite nano particles. The viscosity of PPG maintains a uniform distribution of particles in the solution. TDI was poured in to this suspension with continuous stirring. During the mixing of TDI, the temperature was maintained at 70o C as it was an exothermic reaction. After mixing TDI, the resultant solution was heated at 85° C for 4 h with stirring. Subsequently, after cooling the reaction mixture to 40° C, BDO was added with vigorous stirring for 1 min. immediately after this, a small portion of solution was mixed with DMF for spin coating and TEM characterization. The resultant composite solution was poured into a defined shape mold for final curing. The composite material in the mold was heated at

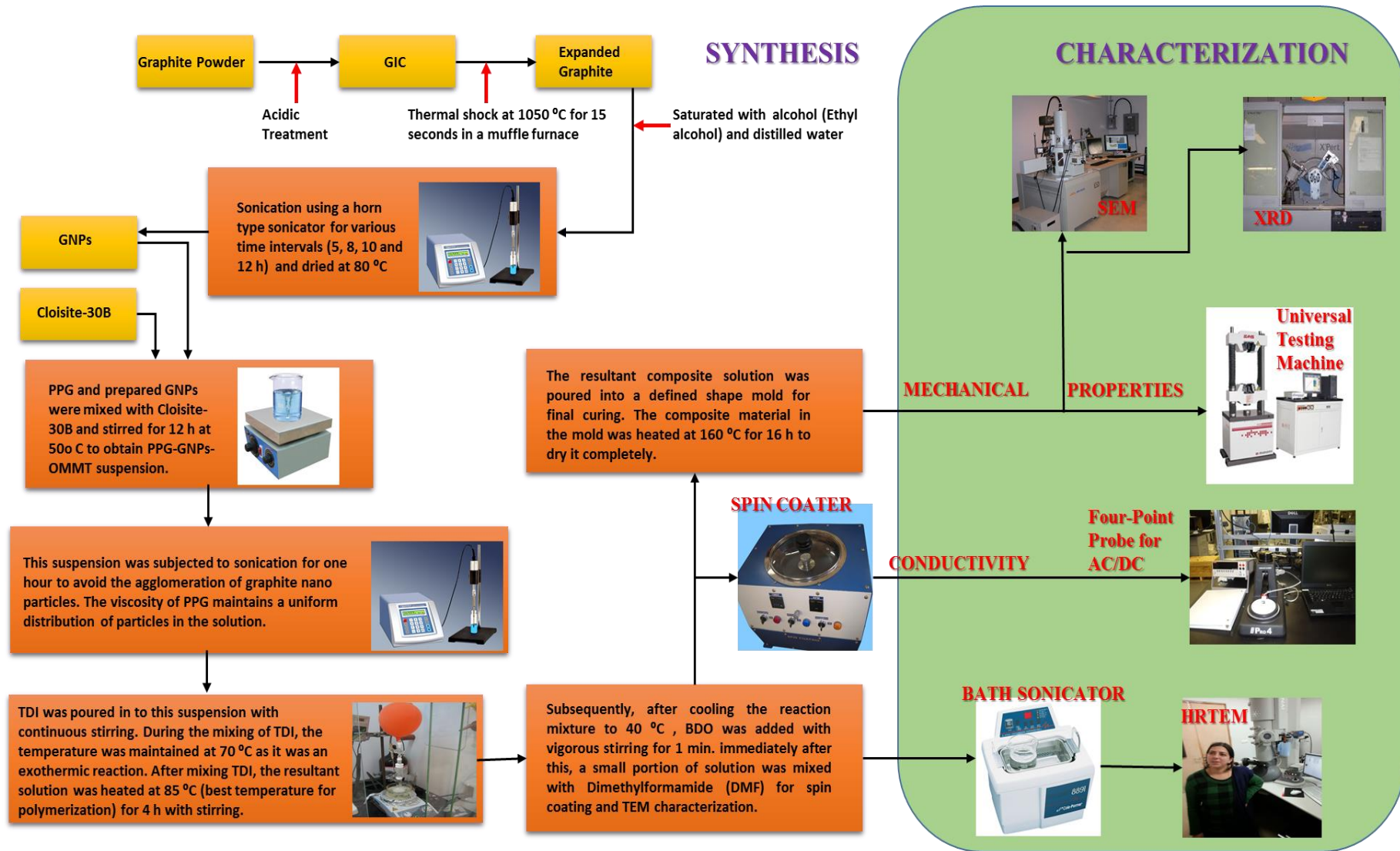


Figure 5.1: Schematic diagram of whole synthesis process of ternary PU/GNP/OMMT composites

160° C for 16 h to dry it completely. To do the comparative studies of properties on equal dimensions, the dimensions of prepared samples are maintained by use of equal sized molds. Similarly, all spin coated films are made using the same dimensions of glass/silicon substrates. The dispersion state of prepared nanocomposites samples was studied by Transmission Electron Microscope (TEM) using drop casting method. The samples were prepared by dispersing the film on glass/silicon substrates by spin coater. The mechanical properties of prepared nanocomposites samples were studied by universal testing machine as shown in the Figure 5.1.

5.2.4 Characterization

To have an idea about the dispersion of both the fillers in the matrix X ray diffraction (XRD) patterns of prepared nanocomposites were recorded on PANalytical's XPERT-PRO Diffractometer system with Cu K-Alpha1 [\AA]: 1.54060 and 2θ (3° - 40°). The dispersion of both the fillers, was further confirmed by TEM images. The surface morphology of the nanocomposites was studied by SEM. The electrical properties of prepared samples were studied by four-point method and effect of addition of clay on percolation threshold was observed. The mechanical properties of these prepared samples using binary fillers were studied by universal testing machine, and were compared to nanocomposites of PU/GNPs and PU/OMMT.

5.3 Results and Discussion

5.3.1 XRD Analysis

The results of XRD are shown in Figure 5.2, in the form of diffraction peaks of GNP, Cloisite 30B, and ternary nanocomposites containing GNP and Cloisite-30B as binary fillers. The pure GNP and pure Cloisite-30B has displayed the sharp intended peaks at 26.3° and 4.81° indicating D- spacing of 3.38 \AA and 18.32 \AA respectively. As disappearance of major diffraction peak of filler indicates the exfoliation morphology and shifting of diffraction peak

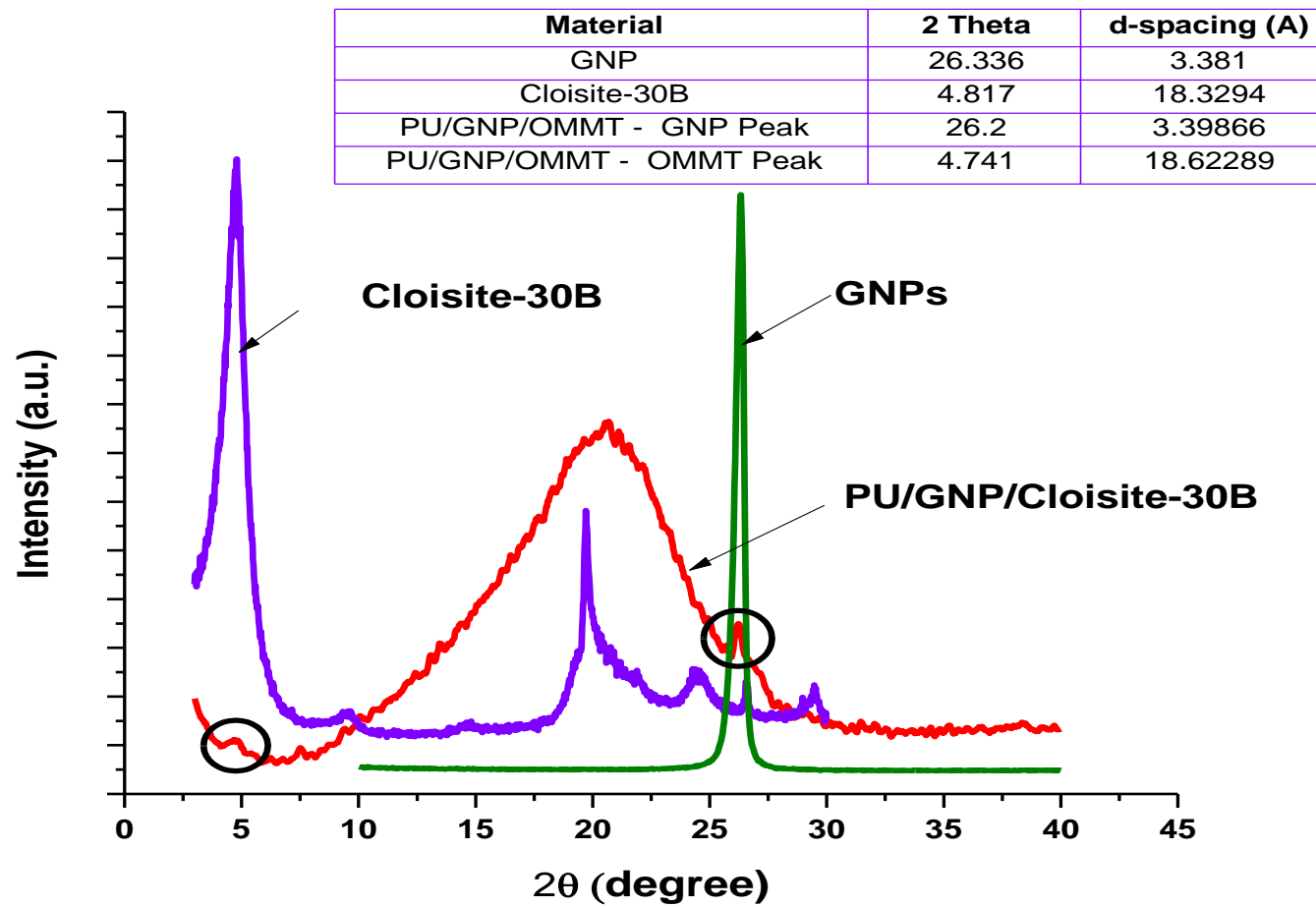


Figure5.2. X-ray Diffraction of GNPs, Cloisite 30B, and Prepared Samples of Ternary Composites

towards lower angle with reduced intensity indicates the intercalated morphology of nanocomposites. Based on these facts our prepared ternary nanocomposites revealed an intercalated type of morphology as the major diffraction peaks of both the fillers have shifted towards lower angle with much reduced intensity. A broaden peak in nanocomposite sample near 20° indicates the peak of PU, means the crystallinity of matrix has not been effected by dispersion of these two fillers. The dispersion was further confirmed by TEM images of nanocomposites.

5.3.2 SEM and TEM Analysis

The surface morphology of prepared PU/GNPs/OMMT ternary nanocomposites was absorbed by SEM at different magnifications as shown in Figure 5.3. At low magnification the GNP and clay particles are well dispersed in the matrix. It can be seen that clay particles are anchored on the surface of GNPs, making a continuous conductive network in the matrix, which helped to lower down the percolation of nanocomposite (Figure 5.3(a) and Figure 5.3(b). At high magnifications, the roughness of surface can also be seen due to presence of GNPs of different sizes. The bundles of GNPs can also be seen at high magnification and are well connected to each other which again helped to lower down the percolation threshold of nanocomposite. At the same time pulled out graphene bundle can also be seen at some places showing not a good adhesion between GNPs and matrix at those points (Figure 5.3(c) and Figure 5.3(d)). The intercalated GNP particles are shown in Figure 5.4(a) TEM image. The intercalated clay is shown in Figure 5.4(b). The stack of graphene layer can be easily seen in the Figure 5.4(c). The d-spacing can also be calculated from the profile of fringes is shown in the Figure 5.5. Individual layers of graphite are clearly visible as regions of alternating narrow, dark and light bands within the particles (fringes) as shown in Figure 5.4(d) along with the live FFT the inset of Figure 5.4(d).

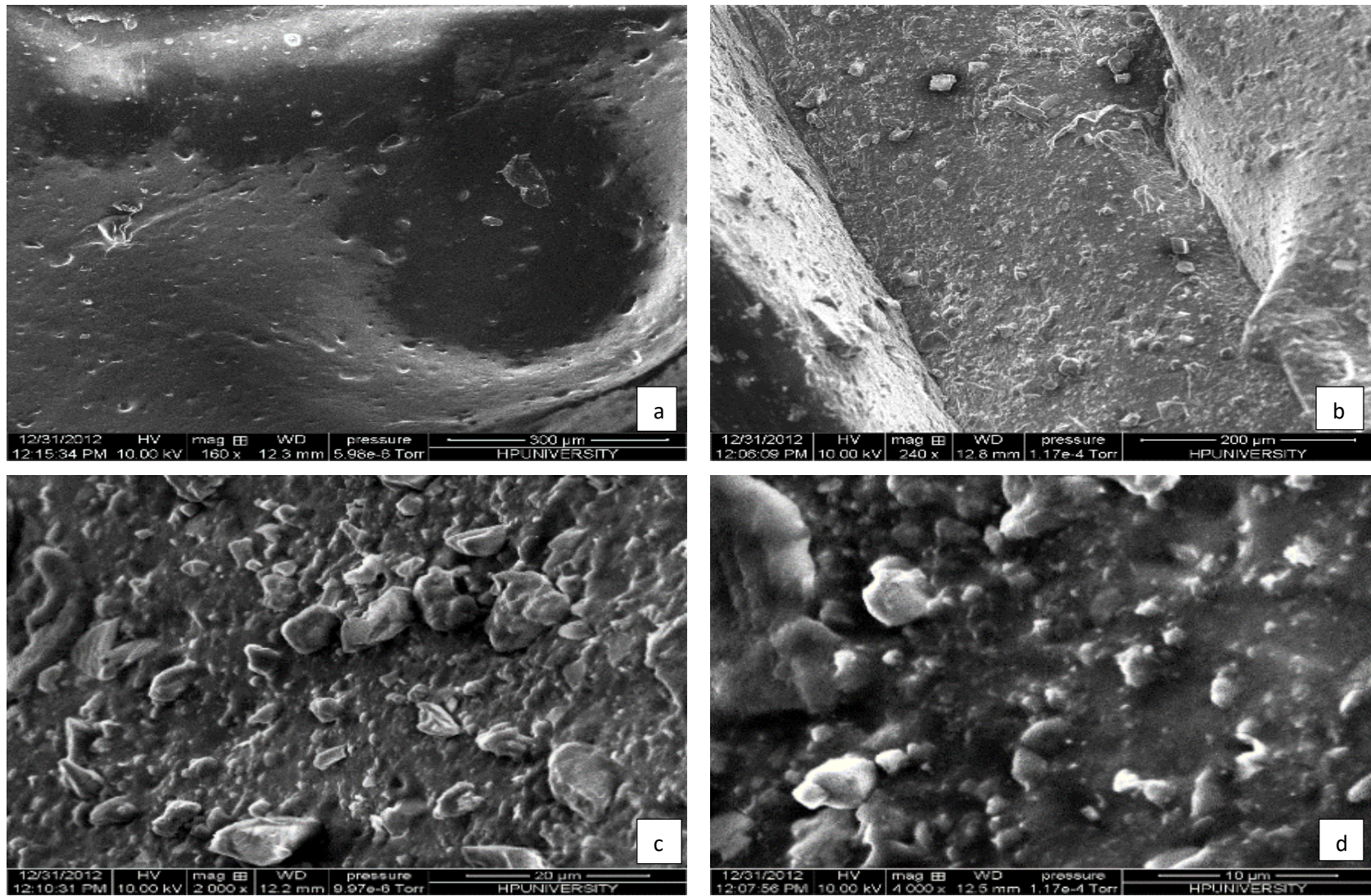


Figure 5.3. SEM images of prepared PU/GNPs/Cloisite-30B composites: (a, b) Clay particles are anchored on the surface of GNPs, (c, d) The bundles of GNPs at high magnification

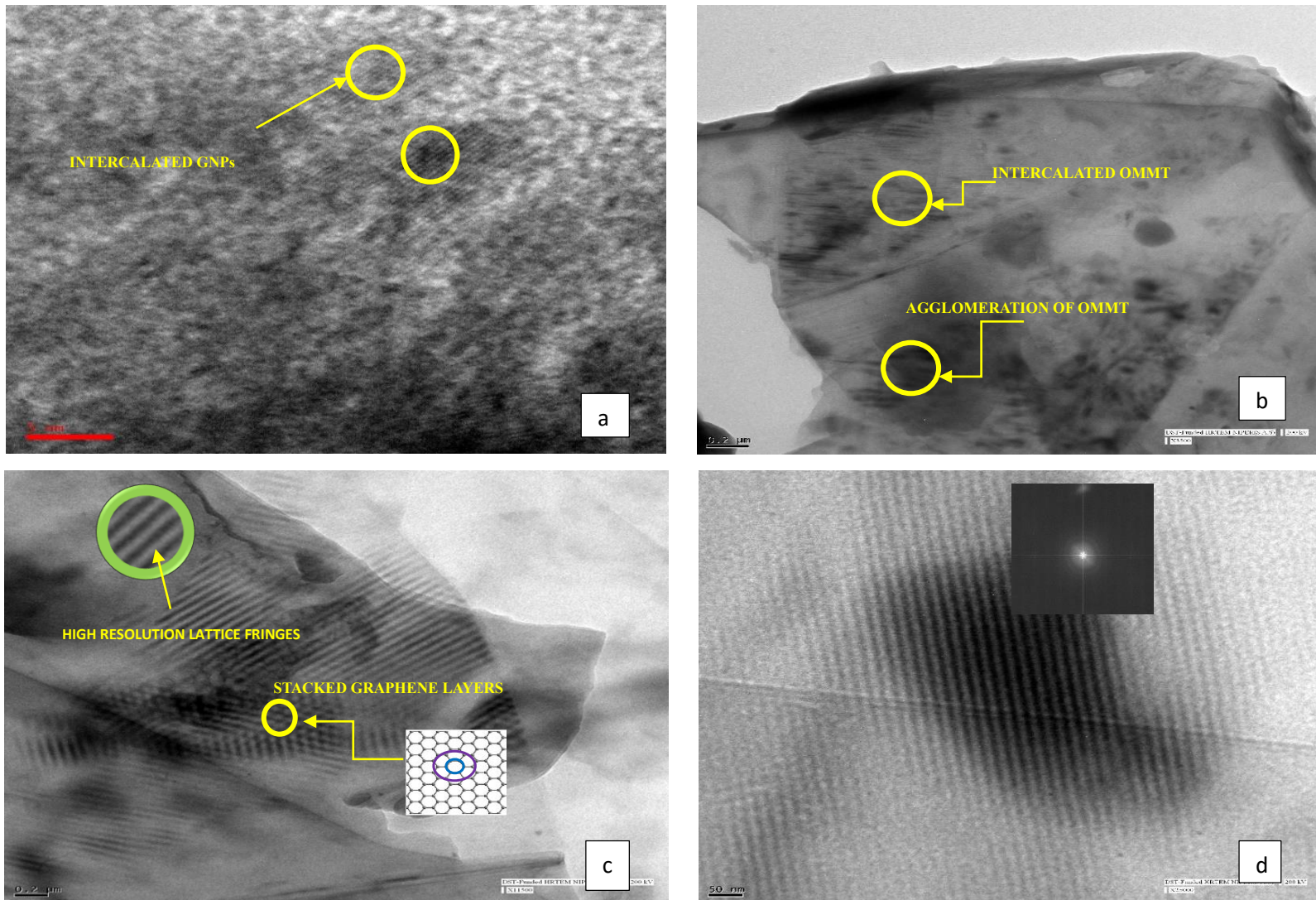


Figure 5.4. TEM images of prepared PU/GNPs/Cloisite-30B composites, (a) Intercalated GNPs, (b) Intercalated OMMT, (c) Stacked graphene layers with high resolution lattice fringes, (d) Live FFT.

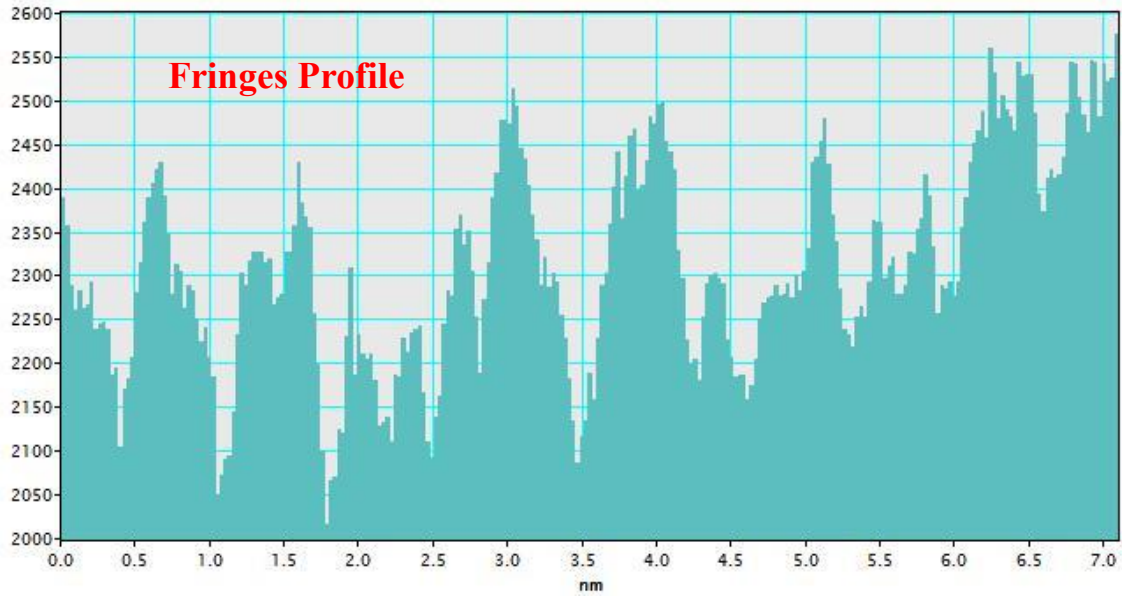


Figure 5.5. Profile of fringes to calculate d spacing

5.3.3 Electrical Conductivity and Percolation Threshold Measurement

The prepared polymer composites are conducting in nature as they contain conducting filler and insulating matrix. These composites are capable of dissipating electrostatic charges and shielding devices from electromagnetic radiation. Due to good adhesive properties of polyurethane, these composites can be used as interconnection wires in integrated devices. In general, there is a rapid increase in the electrical conductivity of prepared composite when a conductive network is formed by the conductive fillers. It causes a transition in composite material from insulator to conductor [Du *et al.* (2004)]. The fraction of filler material at which there is an establishment of multiple, continuous electron path or continuous electrical network, is called percolation threshold. In order to maintain the electrical conductivity of composite containing insulating matrix, the concentration of conducting filler must be equal or greater than the percolation threshold. However, this percolation threshold is lower down in case of ternary nanocomposites as shown in Figure 5.6. In this thesis an effort has been made to lower down the percolation threshold by addition of OMMT along with GNPs as binary fillers. It was found out that with the addition of 2wt% of clay (calculated from the vol% of clay using its density), the percolation threshold is reduced to 0.6 vol% from 2.2 vol%. With this reduction in percolation the electrical conductivity is also increased at different loadings of GNP with constant fraction of OMMT. This improvement in electrical conductivity as well reduction in percolation threshold may be due to presence of clay increases the melt viscosity of the matrix

polymer, and thus shear force during mixing, which helps to better dispersion of the GNP [Khudyakov *et al.* (2009)]. The electrical behavior of the composite is explained on the basis of percolation theory [Potts *et al.* (2011)]. According to this theory, near the percolation threshold, the electrical conductivity of the composite follows the following power law relationship.

$$\sigma = \sigma_0 (V_f - V_c)^s \quad (5.1)$$

Where σ the electrical conductivity of the composite, σ_0 is the electrical conductivity of the filler, V_f is the filler volume fraction, V_c is the percolation threshold and s is a conductivity exponent. According to the tunneling mechanism, conduction can take place via tunneling between thin polymer layers surrounding the filler particles. Percolation threshold of GNP reinforced polymer is much lower than other carbon fillers like carbon fibers and carbon black, due to extremely large surface area and high aspect ratio of GNPs. As per the power law in Equation 5.1, the plot of $\log \sigma$ versus $\log (V_f - V_c)$ is drawn and shown in the inset of Figure 5.6. The best linear fit is found for $V_c = 0.022$ without clay and $V_c = 0.006$ with clay. Here the power law for the conductivity values is well obeyed above the percolation threshold. The improvement in electrical properties along with the reduction in percolation threshold shown in Figure 5.6 is maximum with 2wt% fraction of clay as shown in Figure 5.8. Further increase in clay loading reduces the electrical conductivity gradually. May be, above this loading of clay, which is non-conducting in nature, the insulating clay platelets plays an important role, formation of hybrid network path of GNP and insulating clay silicates.

The percolation threshold is further validated analytically by measuring the inter particle distance (IPD) using Matlab. The volume fraction, P , of GNP is given by [Li *et al.* (2007)]:

$$P_c = \frac{27\pi D^2 t}{4(D+IPD)^3} \quad (5.2)$$

Where D and t are the diameter and thickness of GNP with clay dispersed individually in the matrix. To create an electrical network in nanocomposite, filler particles must be overlapped in the thin polymer layers as shown in the TEM images of composite in Figure 5.7. For overlapped particles $D \gg IPD$, is measured by matlab tool. Equation 5.2 then reduces to:

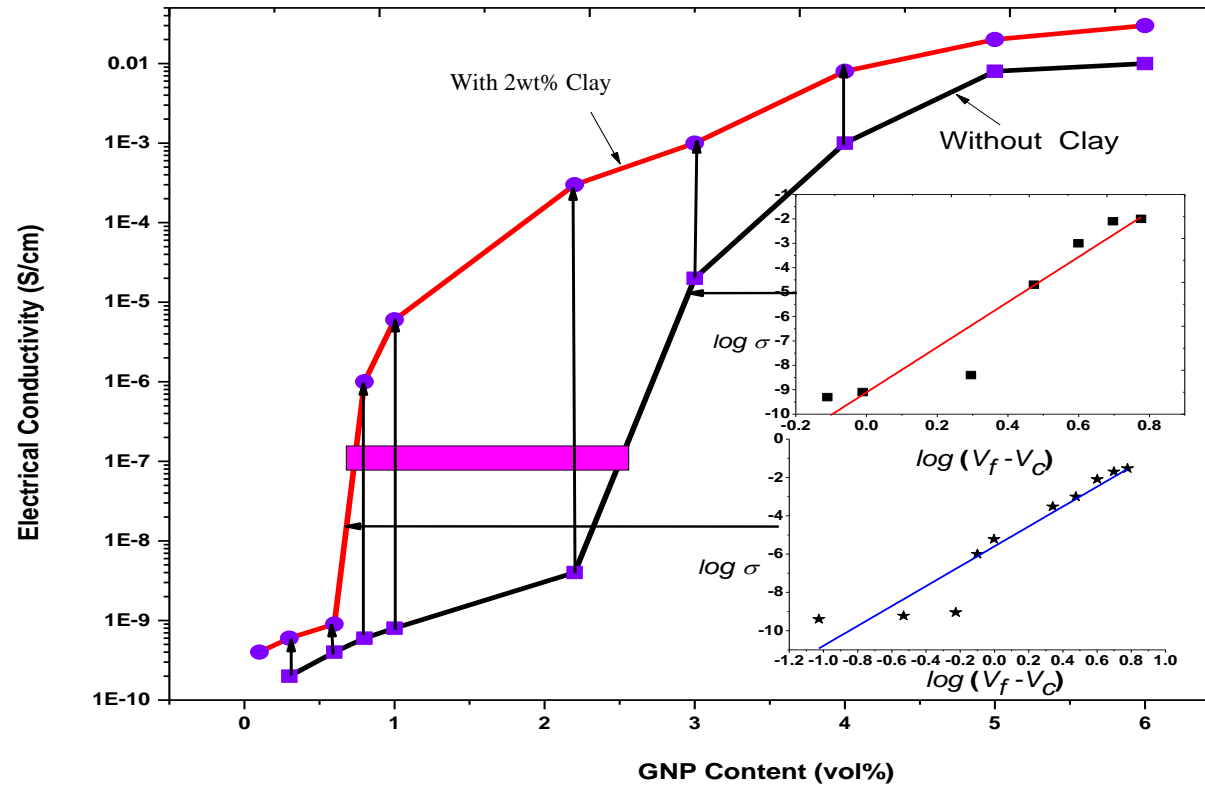


Figure 5.6. Electrical conductivity of PU/GNPs and PU/GNPs/Cloisite-30B composites as a function of GNP content

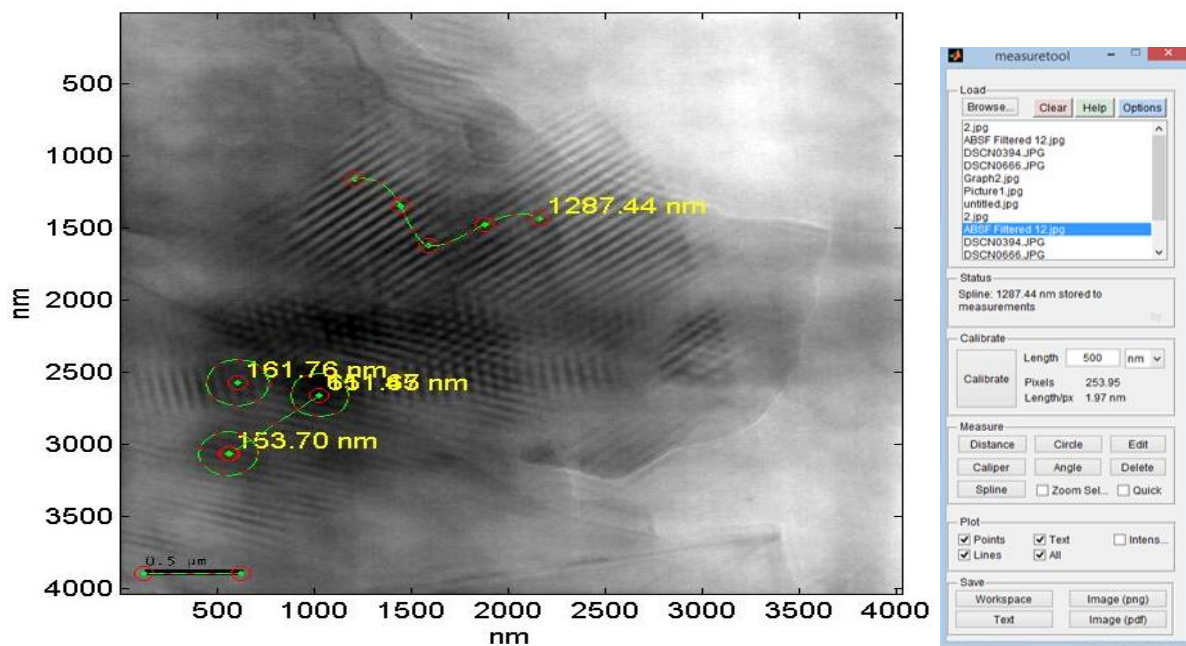


Figure 5.7. Geometrical orientations measurement for IPD using Matlab

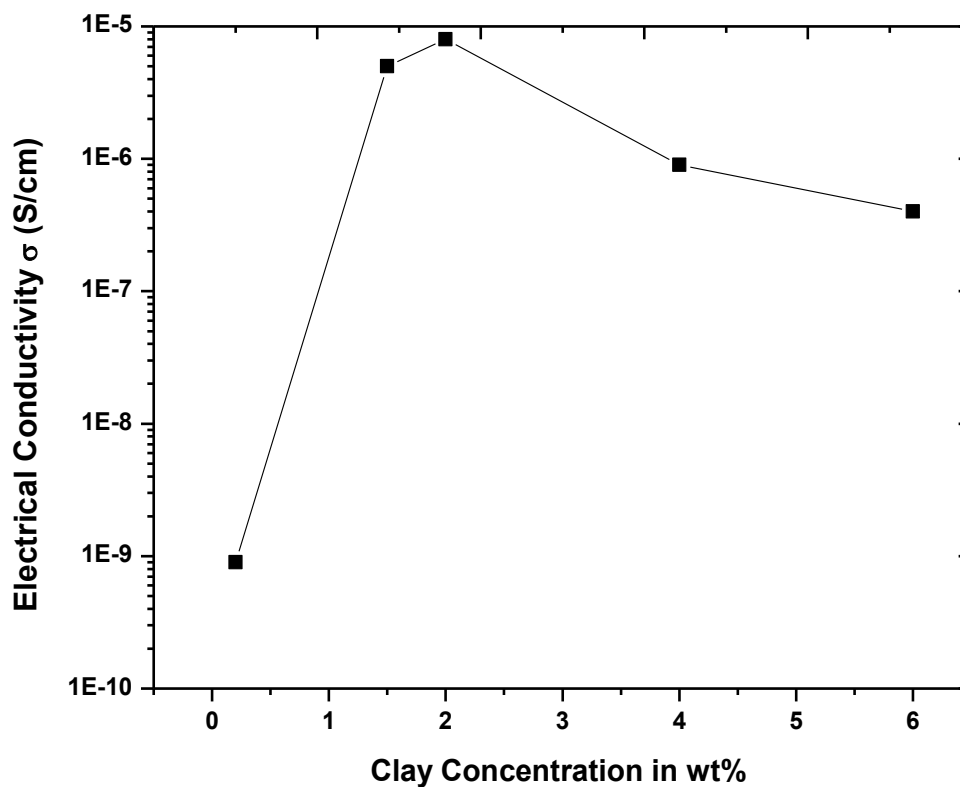


Figure 5.8. Effect of clay concentration on electrical conductivity of ternary nanocomposite

$$P_c = \frac{27\pi t}{4D} = \frac{21.195}{\alpha} \quad (5.3)$$

Where α is the aspect ratio. The value α can be determined using Image J [Igathinathane *et al.* (2008)].

5.4 Mechanical Properties

The mechanical properties of ternary nanocomposites were studied, and compared to binary nanocomposites PU/GNPs, PU/Cloisite-30B, and pure PU respectively. All samples were in dumbbell shape with equal dimensions $100 \times 25 \times 1 \text{ mm}^3$. It was observed at fraction of GNPs (0.5 wt%) the tensile strength gets decreased as compare to pure PU. In order to get good tensile strength at this fraction of GNP along with the improved electrical properties, the OMMT was added with different loading levels by keeping this GNP fraction constant at 0.5 wt%. It was observed that upon addition of clay the tensile strength was increased upon increasing the loading level of OMMT. But this increase in tensile strength was very less as compare to PU/OMMT binary nanocomposite as shown in Figure 5.9. In ternary nanocomposite at 2.0 wt% of clay, the tensile strength was found almost equal to pure PU. The addition of clay at different loading in ternary nanocomposite may leads to uniform stress distribution from matrix to filler due to their uniform dispersion. It can be said that there must be formation of interconnected hybrid network of GNP-clay-GNP or clay-GNP-clay which helped to reduce the agglomeration of GNPs and improve the uniform distribution of stress. An opposite trend was observed for elongation % as compare to tensile strength. The elongation % decreases with increase in loading level OMMT at constant fraction of GNPs as shown in Figure 5.10, and was less than pure PU at all loading levels of clay. Shore hardness is a measure of the resistance of a material to the penetration of a needle under a define spring force. The letter A is used for flexible type. The hardness shore A is also increased with the increase in % loading levels as compare to pristine PU [Xu *et al.* (2007)]. At 0.5 wt% loading level of OMMT, the harness shore A was maintained at a level closed to that of pure PU. At 1.0 and 1.5 wt % of OMMT, a slight increase in hardness has been observed. The hardness shore A also increases with increase in loading level of OMMT at constant fraction of GNPs, and was equal to that of pure PU at 2.0 wt% loading level of clay as shown in Figure 5.11.

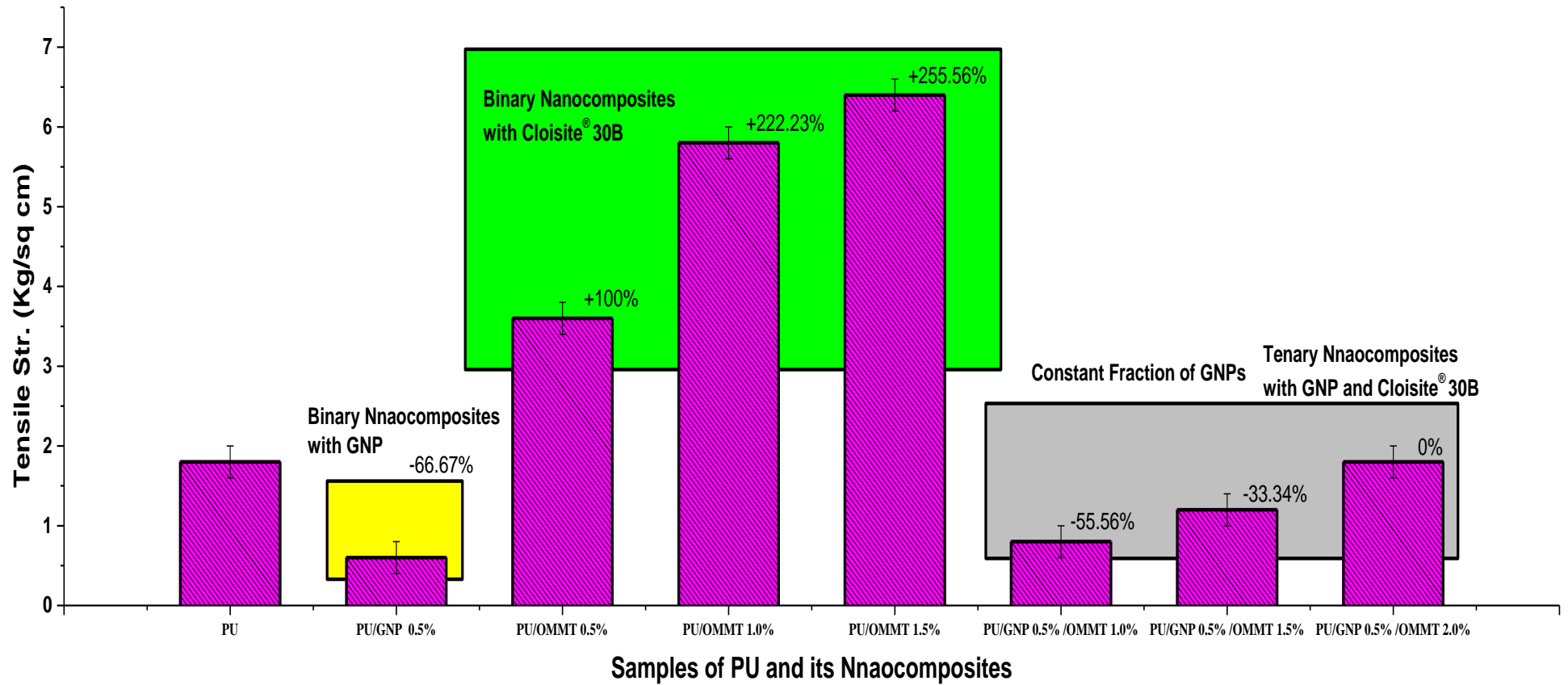


Figure 5.9. Tensile strength of pure PU, PU/GNPs, and PU/Cloisite-30B.

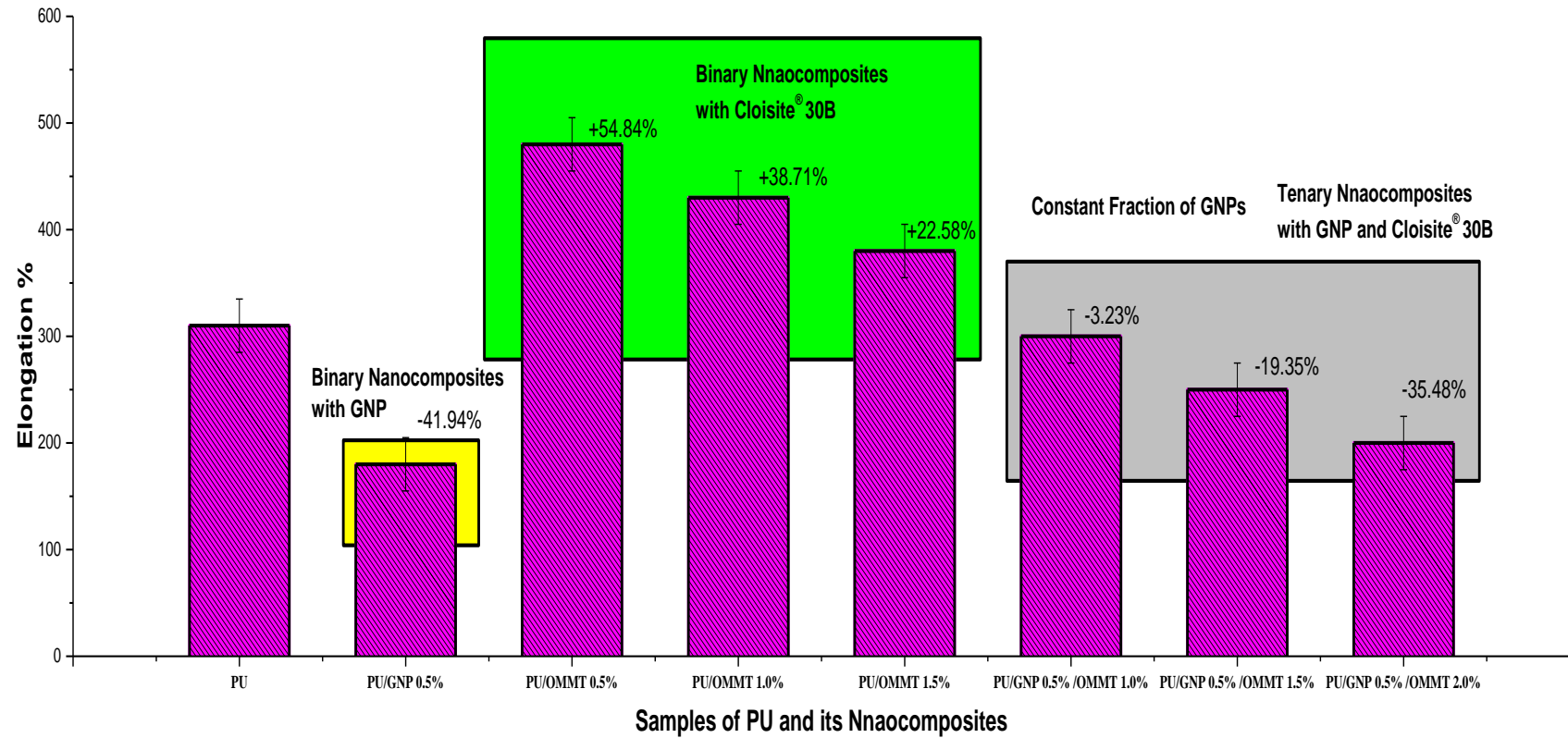


Figure 5.10. Elongation % of pure PU, PU/GNPs, and PU/Cloisite-30B.

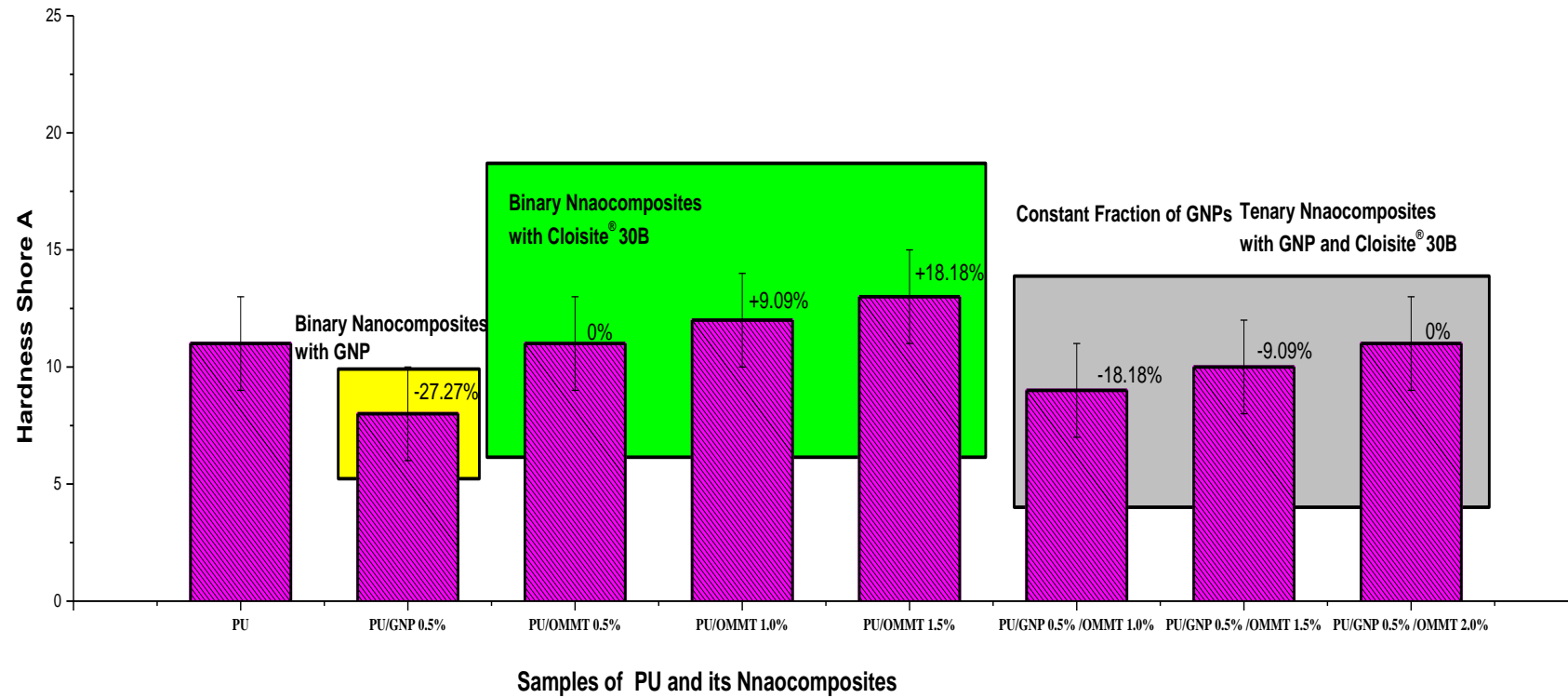


Figure 5.11. Hardness Shore A of pure PU, PU/GNPs, and PU/Cloisite-30B.

5.5 Conclusion

Finally, Ternary nanocomposites reinforced with OMMT and GNPs as binary fillers were prepared by in-situ technique to observe the effect of addition of OMMT on percolation threshold and mechanical properties as compare to composite containing GNPs alone. SEM indicated a satisfactory dispersion of OMMT and GNPs with the matrix revealing a good interfacial bonding between fillers and the matrix. The TEM and XRD revealed the formation of intercalated type of ternary nanocomposites. The percolation threshold was lowered to 0.6 vol% with addition of 2 wt% of OMMT. Wt % is calculated using

$$vol\%filler = wt\%filler / \left[wt\%filler + wt\%matrix \left(\frac{\rho_{filler}}{\rho_{matrix}} \right) \right]. \quad (5.3)$$

This was much lower as compare to percolation threshold of nanocomposite containing only GNPs as filler (2.2 vol%) with this improvement in percolation threshold, the electrical conductivity was also increased. The optimized electrical properties were found at 2 wt% loading of clay, further increase in clay concentration lead to decay in electrical conductivity. Along with electrical properties, the effect of addition of OMMT was also studied for mechanical properties. It was observed that tensile strength and hardness shore A were increased as compare to PU/GNP nanocomposites but were lower than PU/OMMT nanocomposites. An opposite trend was found for elongation %. The elongation % decrease with the increase in loading levels of clay at constant fraction of GNPs (0.5wt %) in ternary nanocomposites. The aim of this work was to prepare a ternary nanocomposite with lower percolation threshold with good mechanical properties as compare to composite containing GNPs alone, which was satisfactory achieved. The possible application of such ternary nanocomposites packaging in integrated circuits, micro sensors, and MEMS, where both electrical and mechanical properties are required.

CHAPTER 6

CONCLUSION AND FUTURE SCOPE

6.1 *Conclusion*

PU/OMMT, PU/GNPs, and PU/OMMT/GNPs nanocomposites were successfully prepared by *in situ* polymerization technique. The nano dispersion of both the fillers was achieved by sonication which helped to reduce the agglomeration of these fillers to a significant extent. The tensile strength and hardness shore A was increased on addition of clay as compared to the pure polyurethane. Hence by combining the attractive functionalities of both components, nanocomposites derived from polyurethane and OMMT are made to display synergistically improved properties. These nanocomposites have various potential applications e.g. automotive, aerospace, opto-electronics, *etc.*

Similarly, the introduction of GNPs as conductive filler transforms polyurethane from an insulator to a conductive polymer. Formation of conductive network improved the electrical properties but deteriorate the mechanical properties. The resulting composites were evaluated for electromagnetic interference (EMI) shielding at different filler loadings. The prepared PU/GNPs composites were found to be highly effective with shielding effectiveness of 19.34 dB, and with electromagnetic interference shielding materials at 0.9–1 GHz. Because of the improved electrical properties, the resultant nanocomposites can be widely used in the various fields such as military equipments, safety, automotive, electronics and optical devices. However, these application areas continuously demand additional properties and functions such as high mechanical properties, flame retardation, chemical resistance. Therefore, attempts were made to use a second filler with GNPs to enhance the mechanical properties of PU along with its electrical properties so that the synergetic enhancements should originate from the specific attribute of each component.

Clay was used as second filler which also contributed to lower the percolation threshold of ternary nanocomposites, which in turn helped to retain the mechanical properties of PU as well. It was observed that the addition of OMMT at a concentration of around 2 wt%, significantly enhances the electrical and mechanical properties of the nanocomposites with the percolation threshold at much lower concentration of the GNPs.

6.2 *Future Scope*

The advantages of nanoscale inorganic particle incorporation into polymer matrices can lead to a number of applications that the incorporation of the analogous larger scale particles do not allow due to an insufficient property profile for utilization. These areas include barrier properties, membrane separation, flame retardation, polymer blend compatibilization, electrical conductivity, impact modification, biomedical applications, *etc.* Hence, polymer-based inorganic nanoparticle nanocomposites emerging as new materials provide opportunities and rewards creating a new world of interest.

The conductive PU/GNP nanocomposite, showing good EMI shielding, have best application in integrated circuits interconnects. Similarly, PU/OMMT nanocomposites with improved mechanical properties can be used for pressure MEMS design. The optimized electrical and mechanical properties of PU/OMMT/GNPs nanocomposites may be utilized in microscale based strain gauge MEMS.

REFERENCES

- Afanasov, I. M., Morozov, V. A., Kepman, A. V., Ionov, S. G., Seleznev, A. N., Van Tendeloo, G., & Avdeev, V. V. (2009). Preparation, electrical and thermal properties of new exfoliated graphite-based composites. *Carbon*, 47(1), 263-270.
- Ahmad, S., Riaz, U., & Alam, J. (2009). Development of sustainable resource-based nanostructured polyaniline/castor oil polyurethane composites. *Advances in Polymer Technology*, 28(1), 26-31.
- Ahmadi, S. J., Huang, Y. D., & Li, W. (2004). Synthetic routes, properties and future applications of polymer-layered silicate nanocomposites. *Journal of materials science*, 39(6), 1919-1925.
- Ajayan, P. M., Schadler, L. S., & Braun, P. V. (2006). *Nanocomposite science and technology*. John Wiley & Sons.
- Allaer, K., De Baere, I., Lava, P., Van Paepegem, W., & Degrieck, J. (2014). On the in-plane mechanical properties of stainless steel fibre reinforced ductile composites. *Composites Science and Technology*, 100, 34-43.
- Amado, F. D. R., Rodrigues Jr, L. F., Forte, M. M. C., & Ferreira, C. A. (2006). Properties Evaluation of the Membranes Synthesized With Castor Oil Polyurethane and Polyaniline.
- Anadão, P. (2012). Polymer/clay nanocomposites: Concepts, researches, applications and trends for the future. *Nanocomposites: New Trends and Developments*, 1-16.
- AngeláRodríguez-Perez, M., de Saja, J., & AngeláLopez-Manchado, M. (2008). Functionalized graphene sheet filled silicone foam nanocomposites. *Journal of Materials Chemistry*, 18(19), 2221-2226.
- Askari, F., Barikani, M., Barmar, M., Shokrolahi, F., & Vafayan, M. (2015). Study of thermal stability and degradation kinetics of polyurethane–ureas by thermogravimetry. *Iranian Polymer Journal*, 1-7.
- Bhaviripudi, S., Jia, X., Dresselhaus, M. S., & Kong, J. (2010). Role of kinetic factors in chemical vapor deposition synthesis of uniform large area graphene using copper catalyst. *Nano letters*, 10(10), 4128-4133.

- Bhushan, R., & Tanwar, S. (2008). Synthesis of succinimidyl-(S)-naproxen ester and its application for indirect enantioresolution of penicillamine by reversed-phase high-performance liquid chromatography. *Journal of Chromatography A*, 1209(1), 174-178
- Bower, C. A. (1949). Studies on the form and availability of organic soil phosphorous. *IOWA Agriculture Experiment Station Research Bulletin*; , 362-39.
- Brady, S., Diamond, D., & Lau, K. T. (2005). Inherently conducting polymer modified polyurethane smart foam for pressure sensing. *Sensors and Actuators A: Physical*, 119(2), 398-404.
- Cai, W., Piner, R. D., Stadermann, F. J., Park, S., Shaibat, M. A., Ishii, Y., ... & Ruoff, R. S. (2008). Synthesis and solid-state NMR structural characterization of ¹³C-labeled graphite oxide. *Science*, 321(5897), 1815-1817.
- Cao, X., Lee, L. J., Widya, T., & Macosko, C. (2005). Polyurethane/clay nanocomposites foams: processing, structure and properties. *Polymer*, 46(3), 775-783.
- Capek, I., Nguyen, S. H., & Berek, D. (2000). Polystyrene-graft-poly (ethylene oxide) copolymers prepared by macromonomer technique in dispersion. 2. Mechanism of dispersion copolymerization. *Polymer*, 41(19), 7011-7016.
- Celzard, A., McRae, E., Mareche, J. F., Furdin, G., Dufort, M., & Deleuze, C. (1996). Composites based on micron-sized exfoliated graphite particles: electrical conduction, critical exponents and anisotropy. *Journal of Physics and Chemistry of Solids*, 57(6), 715-718.
- Chatterjee, S., Nafezarefi, F., Tai, N. H., Schlagenhauf, L., Nüesch, F. A., & Chu, B. T. T. (2012). Size and synergy effects of nanofiller hybrids including graphene nanoplatelets and carbon nanotubes in mechanical properties of epoxy composites. *Carbon*, 50(15), 5380-5386.
- Chen, B., Evans, J. R., Greenwell, H. C., Boulet, P., Coveney, P. V., Bowden, A. A., & Whiting, A. (2008). A critical appraisal of polymer–clay nanocomposites. *Chemical Society Reviews*, 37(3), 568-594.
- Chen, G. H., Wu, D. J., Weng, W. G., & Yan, W. L. (2001). Dispersion of graphite nanosheets in a polymer matrix and the conducting property of the nanocomposites. *Polymer Engineering & Science*, 41(12), 2148-2154.

- Chen, G. H., Wu, D. J., Weng, W. G., & Yan, W. L. (2001). Preparation of polymer/graphite conducting nanocomposite by intercalation polymerization. *Journal of Applied Polymer Science*, 82(10), 2506-2513.
- Chen, G. H., Wu, D. J., Weng, W. G., He, B., & Yan, W. L. (2001). Preparation of polystyrene-graphite conducting nanocomposites via intercalation polymerization. *Polymer International*, 50(9), 980-985.
- Chen, G., Weng, W., Wu, D., & Wu, C. (2003). PMMA/graphite nanosheets composite and its conducting properties. *European Polymer Journal*, 39(12), 2329-2335.
- Chen, G., Weng, W., Wu, D., Wu, C., Lu, J., Wang, P., & Chen, X. (2004). Preparation and characterization of graphite nanosheets from ultrasonic powdering technique. *Carbon*, 42(4), 753-759.
- Chen, G., Wu, C., Weng, W., Wu, D., & Yan, W. (2003). Preparation of polystyrene/graphite nanosheet composite. *Polymer*, 44(6), 1781-1784.
- Chen, S. G., Hu, J. W., Zhang, M. Q., Li, M. W., & Rong, M. Z. (2004). Gas sensitivity of carbon black/waterborne polyurethane composites. *Carbon*, 42(3), 645-651.
- Cheng, A., Wu, S., Jiang, D., Wu, F., & Shen, J. (2006). Study of elastomeric polyurethane nanocomposites prepared from grafted organic-montmorillonite. *Colloid and Polymer Science*, 284(9), 1057-1061.
- Cho, D., Lee, S., Yang, G., Fukushima, H., & Drzal, L. T. (2005). Dynamic Mechanical and Thermal Properties of Phenylethynyl-Terminated Polyimide Composites Reinforced With Expanded Graphite Nanoplatelets. *Macromolecular Materials and Engineering*, 290(3), 179-187.
- Cho, J. W., Kim, J. W., Jung, Y. C., & Goo, N. S. (2005). Electroactive shape-memory polyurethane composites incorporating carbon nanotubes. *Macromolecular Rapid Communications*, 26(5), 412-416.
- Chun, B. C., Cho, T. K., Chong, M. H., Chung, Y. C., Chen, J., Martin, D., & Cieslinski, R. C. (2007). Mechanical properties of polyurethane/montmorillonite nanocomposite prepared by melt mixing. *Journal of applied polymer science*, 106(1), 712-721.
- Chung, D. D. L. (2001). Electromagnetic interference shielding effectiveness of carbon materials. *carbon*, 39(2), 279-285.
- Chung, D. D. L. (2002). Review graphite. *Journal of materials science*, 37(8), 1475-1489.

- Compton, O. C., & Nguyen, S. T. (2010). Graphene Oxide, Highly Reduced Graphene Oxide, and Graphene: Versatile Building Blocks for Carbon-Based Materials. *small*, 6(6), 711-723.
- Dasari, A., Yu, Z. Z., & Mai, Y. W. (2005). Effect of blending sequence on microstructure of ternary nanocomposites. *Polymer*, 46(16), 5986-5991.
- de Paiva, L. B., Morales, A. R., & Guimaraes, T. R. (2007). Structural and optical properties of polypropylene–montmorillonite nanocomposites. *Materials Science and Engineering: A*, 447(1), 261-265.
- Deng, S., Ran, Q., Wu, S., & She, J. (2008). Study on polyurethane/MDI-modified-organic montmorillonite nanocomposites. *Polymer-Plastics Technology and Engineering*, 47(12), 1200-1204.
- Dikin, D. A., Stankovich, S., Zimney, E. J., Piner, R. D., Dommett, G. H., Evmenenko, G., ... & Ruoff, R. S. (2007). Preparation and characterization of graphene oxide paper. *Nature*, 448(7152), 457-460.
- Dresselhaus, M. S., & Dresselhaus, G. (1981). Intercalation compounds of graphite. *Advances in Physics*, 30(2), 139-326.
- Dresselhaus, M. S., & Endo, M. (2001). Relation of carbon nanotubes to other carbon materials. In *Carbon nanotubes* (pp. 11-28). Springer Berlin Heidelberg.
- Du, X. S., Xiao, M., & Meng, Y. Z. (2004). Synthesis and characterization of polyaniline/graphite conducting nanocomposites. *Journal of Polymer Science Part B: Polymer Physics*, 42(10), 1972-1978.
- Du, X. S., Xiao, M., & Meng, Y. Z. (2004). Synthesis and characterization of polyaniline/graphite conducting nanocomposites. *Journal of Polymer Science Part B: Polymer Physics*, 42(10), 1972-1978.
- Du, X. S., Xiao, M., Meng, Y. Z., & Hay, A. S. (2004). Synthesis and properties of poly(4, 4'-oxybis (benzene) disulfide)/graphite nanocomposites via in situ ring-opening polymerization of macrocyclic oligomers. *Polymer*, 45(19), 6713-6718.
- EMC-TutorialsShielding, "http://www.learnemc.com/tutorials/Shielding01/Shielding_Theory.html
- EMI shielding calculator, "http://www.cvel.clemson.edu/emc/calculators/SE_Calculator/index.html

- Falcao, E. H., Blair, R. G., Mack, J. J., Viculis, L. M., Kwon, C. W., Bendikov, M., ... & Wudl, F. (2007). Microwave exfoliation of a graphite intercalation compound. *Carbon*, 45(6), 1367-1369.
- Fukuda, K., Kikuya, K., Isono, K., & Yoshio, M. (1997). Foliated natural graphite as the anode material for rechargeable lithium-ion cells. *Journal of power sources*, 69(1), 165-168.
- Gall, K., Kreiner, P., Turner, D., & Hulse, M. (2004). Shape-memory polymers for microelectromechanical systems. *Microelectromechanical Systems, Journal of*, 13(3), 472-483.
- Ganster, J., & Fink, H. P. (2010). PLA-based bio-and nanocomposites. *Nano-and Biocomposites*, 275-290.
- Geim, A. K. (2011). Nobel Lecture: Random walk to graphene. *Reviews of Modern Physics*, 83(3), 851.
- Geim, A. K., & Novoselov, K. S. (2007). The rise of graphene. *Nature materials*, 6(3), 183-191.
- Geng, Y., Wang, S. J., & Kim, J. K. (2009). Preparation of graphite nanoplatelets and graphene sheets. *Journal of colloid and interface science*, 336(2), 592-598.
- Geng, Y., Zheng, Q., & Kim, J. K. (2011). Effects of stage, intercalant species and expansion technique on exfoliation of graphite intercalation compound into graphene sheets. *Journal of nanoscience and nanotechnology*, 11(2), 1084-1091.
- Goettler, L. A., Lee, K. Y., & Thakkar, H. (2007). Layered silicate reinforced polymer nanocomposites: development and applications. *Polymer Reviews*, 47(2), 291-317.
- Green, M., Marom, G., Li, J., & Kim, J. K. (2008). The electrical conductivity of graphite nanoplatelet filled conjugated polyacrylonitrile. *Macromolecular rapid communications*, 29(14), 1254-1258.
- Gurunathan, T., Rao, C. R., Narayan, R., & Raju, K. V. S. N. (2013). Polyurethane conductive blends and composites: synthesis and applications perspective. *Journal of Materials Science*, 48(1), 67-80.
- Han, J. H. "Current Status on Synthesis of Carbon Nanotubes and Their Applications to Conducting Polymer." *Polym. Sci. Technol* 16.2 (2005): 162-175.

- Harikrishnan, G., Lindsay, C. I., Arunagirinathan, M. A., & Macosko, C. W. (2009). Probing Nanodispersions of Clays for Reactive Foaming. *ACS applied materials & interfaces*, 1(9), 1913-1918.
- Harikrishnan, G., Singh, S. N., Kiesel, E., & Macosko, C. W. (2010). Nanodispersions of carbon nanofiber for polyurethane foaming. *Polymer*, 51(15), 3349-3353.
- He, F., Lau, S., Chan, H. L., & Fan, J. (2009). High dielectric permittivity and low percolation threshold in nanocomposites based on poly (vinylidene fluoride) and exfoliated graphite nanoplates. *Advanced Materials*, 21(6), 710-715.
- Hu, H., Wang, X., Wang, J., Liu, F., Zhang, M., & Xu, C. (2011). Microwave-assisted covalent modification of graphene nanosheets with chitosan and its electrorheological characteristics. *Applied Surface Science*, 257(7), 2637-2642.
- Hu, Y., Song, L., Xu, J., Yang, L., Chen, Z., & Fan, W. (2001). Synthesis of polyurethane/clay intercalated nanocomposites. *Colloid and Polymer Science*, 279(8), 819-822.
- Huang, S., Peng, H., Tjiu, W. W., Yang, Z., Zhu, H., Tang, T., & Liu, T. (2010). Assembling exfoliated layered double hydroxide (LDH) nanosheet/carbon nanotube (CNT) hybrids via electrostatic force and fabricating nylon nanocomposites. *The Journal of Physical Chemistry B*, 114(50), 16766-16772.
- Hummers Jr, W. S., & Offeman, R. E. (1958). Preparation of graphitic oxide. *Journal of the American Chemical Society*, 80(6), 1339-1339.
- Hwang, D. M., Kirczenow, G., Lagrange, P., Magerl, A., Moret, R., Moss, S. C., ... & Solin, S. A. (2013). Graphite intercalation compounds I: Structure and dynamics (Vol. 14). H. Zabel, & S. A. Solin (Eds.). Springer Science & Business Media.
- Igathinathane, C., Pordesimo, L. O., Columbus, E. P., Batchelor, W. D., & Methuku, S. R. (2008). Shape identification and particles size distribution from basic shape parameters using ImageJ. *computers and electronics in agriculture*, 63(2), 168-182.
- Jeong, E. H., Yang, J., Lee, H. S., Seo, S. W., Baik, D. H., Kim, J., & Youk, J. H. (2008). Effective preparation and characterization of montmorillonite/poly (ϵ -caprolactone)-based polyurethane nanocomposites. *Journal of applied polymer science*, 107(2), 803-809.
- Jiang, H., Lee, P. S., & Li, C. (2013). 3D carbon based nanostructures for advanced supercapacitors. *Energy & Environmental Science*, 6(1), 41-53.

- Jiang, X., Bin, Y., & Matsuo, M. (2005). Electrical and mechanical properties of polyimide–carbon nanotubes composites fabricated by in situ polymerization. *Polymer*, 46(18), 7418-7424.
- Jung, Y. C., Kim, H. H., Kim, Y. A., Kim, J. H., Cho, J. W., Endo, M., & Dresselhaus, M. S. (2010). Optically active multi-walled carbon nanotubes for transparent, conductive memory-shape polyurethane film. *Macromolecules*, 43(14), 6106-6112.
- Kalaitzidou, K., Fukushima, H., & Drzal, L. T. (2007). A new compounding method for exfoliated graphite–polypropylene nanocomposites with enhanced flexural properties and lower percolation threshold. *Composites Science and Technology*, 67(10), 2045-2051.
- Kato, A. U. I. N. H. M., & Usik, A. (2005). Polymer-clay nanocomposites. *Inorganic Polymeric Nanocomposites and Membranes*, 179, 135-195.
- Khanam, P. N., Ponnamma, D., & AL-Madeed, M. A. (2015). Electrical Properties of Graphene Polymer Nanocomposites. In *Graphene-Based Polymer Nanocomposites in Electronics* (pp. 25-47). Springer International Publishing.
- Khudyakov, I. V., Zopf, D. R., & Turro, N. J. (2009). Polyurethane nanocomposites. *Designed Monomers and Polymers*, 12(4), 279-290.
- Kim, H., & Macosko, C. W. (2008). Morphology and properties of polyester/exfoliated graphite nanocomposites. *Macromolecules*, 41(9), 3317-3327.
- Kim, H., Abdala, A. A., & Macosko, C. W. (2010). Graphene/polymer nanocomposites. *Macromolecules*, 43(16), 6515-6530.
- Kim, H., Miura, Y., & Macosko, C. W. (2010). Graphene/polyurethane nanocomposites for improved gas barrier and electrical conductivity. *Chemistry of Materials*, 22(11), 3441-3450.
- Kim, M., Lee, C., Seo, Y. D., Cho, S., Kim, J., & Jang, J. (2015). Fabrication of Various Conducting Polymers Using Graphene Oxide as a Chemical Oxidant. *Chemistry of Materials*.
- Kim, S., & Drzal, L. T. (2009). Comparison of exfoliated graphite nanoplatelets (xGnP) and CNTs for reinforcement of EVA nanocomposites fabricated by solution compounding method and three screw rotating systems. *Journal of Adhesion Science and Technology*, 23(12), 1623-1638.

- Kondawar, S. B., Deshpande, M. D., & Agrawal, S. P. (2012). Transport properties of conductive polyaniline nanocomposites based on carbon nanotubes. *International Journal of Composite Materials*, 2(3), 32-36.
- Kotal, M., Srivastava, S. K., & Paramanik, B. (2011). Enhancements in conductivity and thermal stabilities of polypyrrole/polyurethane nanoblends. *The Journal of Physical Chemistry C*, 115(5), 1496-1505.
- Krause, R. W., Mamba, B. B., Dlamini, L. N., & Durbach, S. H. (2010). Fe–Ni Nanoparticles supported on carbon nanotube-co-cyclodextrin polyurethanes for the removal of trichloroethylene in water. *Journal of Nanoparticle Research*, 12(2), 449-456.
- Kuilla, T., Bhadra, S., Yao, D., Kim, N. H., Bose, S., & Lee, J. H. (2010). Recent advances in graphene based polymer composites. *Progress in polymer science*, 35(11), 1350-1375.
- Kumar, D., Singh, K., Verma, V., & Bhatti, H. S. (2015). Microwave assisted synthesis and characterization of graphene nanoplatelets. *Applied Nanoscience*, 1-7.
- Kwon, J. Y., Kim, E. Y., & Kim, H. D. (2004). Preparation and properties of waterborne-polyurethane coating materials containing conductive polyaniline. *Macromolecular Research*, 12(3), 303-310.
- Kwon, J. Y., Koo, Y. S., & Kim, H. D. (2004). Preparation and properties of waterborne polyurethane/polyaniline codoped with dodecyl benzene sulfonic acid and hydrochloric acid blends. *Journal of applied polymer science*, 93(2), 700-710.
- Lai, Z. (1993). *Elementary theory of electromagnetic shielding*.
- Lau AKT, Hussain F, Lafdi K. *Nano-and biocomposites*. CRC Press; 2010.
- Lee, H. F., & Yu, H. H. (2011). Study of electroactive shape memory polyurethane–carbon nanotube hybrids. *Soft Matter*, 7(8), 3801-3807.
- Li Jing, Peng Cheng MA, Kim JK. Percolation threshold of conducting polymer composites containing graphite nanoplates and carbon nanotube. *16th Int. Conf. on Compos. Mater. Kyoto (Jpan) 2007*; p.1-8.
- Li, C. Y., Chiu, W. Y., & Don, T. M. (2007). Polyurethane/polyaniline and polyurethane-poly (methyl methacrylate)/polyaniline conductive core-shell particles: Preparation, morphology, and conductivity. *Journal of Polymer Science Part A: Polymer Chemistry*, 45(17), 3902-3911.

- Li, D., Mueller, M. B., Gilje, S., Kaner, R. B., & Wallace, G. G. (2008). Processable aqueous dispersions of graphene nanosheets. *Nature nanotechnology*, 3(2), 101-105.
- Li, J., & Kim, J. K. (2007). Percolation threshold of conducting polymer composites containing 3D randomly distributed graphite nanoplatelets. *Composites Science and Technology*, 67(10), 2114-2120.
- Li, J., Sham, M. L., Kim, J. K., & Marom, G. (2007). Morphology and properties of UV/ozone treated graphite nanoplatelet/epoxy nanocomposites. *Composites Science and Technology*, 67(2), 296-305.
- Li, J., Vaisman, L., Marom, G., & Kim, J. K. (2007). Br treated graphite nanoplatelets for improved electrical conductivity of polymer composites. *Carbon*, 45(4), 744-750.
- Li, J., Wong, P. S., & Kim, J. K. (2008). Hybrid nanocomposites containing carbon nanotubes and graphite nanoplatelets. *Materials Science and Engineering: A*, 483, 660-663.
- Liu, J., Fu, M., Jing, M., & Li, Q. (2013). Flame retardancy and charring behavior of polystyrene-organic montmorillonite nanocomposites. *Polymers for Advanced Technologies*, 24(3), 273-281.
- Liu, Y. T., Dang, M., Xie, X. M., Wang, Z. F., & Ye, X. Y. (2011). Synergistic effect of Cu 2+-coordinated carbon nanotube/graphene network on the electrical and mechanical properties of polymer nanocomposites. *Journal of Materials Chemistry*, 21(46), 18723-18729.
- Liu, Z., Bai, G., Huang, Y., Ma, Y., Du, F., Li, F., ... & Chen, Y. (2007). Reflection and absorption contributions to the electromagnetic interference shielding of single-walled carbon nanotube/polyurethane composites. *Carbon*, 45(4), 821-827.
- Mai, Y. W., & Yu, Z. Z. (2006). *Polymer nanocomposites*. Woodhead publishing.
- Mao, Q. (2007). *Synthesis and characterization of structurally well-defined polymer-layered silicate nanocomposites* (Doctoral dissertation, Max-Planck-Institute for Polymer Research).
- McAllister, M. J., Li, J. L., Adamson, D. H., Schniepp, H. C., Abdala, A. A., Liu, J., ... & Aksay, I. A. (2007). Single sheet functionalized graphene by oxidation and thermal expansion of graphite. *Chemistry of Materials*, 19(18), 4396-4404.

- McNally, T., Pötschke, P., Halley, P., Murphy, M., Martin, D., Bell, S. E., ... & Quinn, J. P. (2005). Polyethylene multiwalled carbon nanotube composites. *Polymer*, 46(19), 8222-8232.
- Menendez JA, Arenillas A, Fidalgo B, Fernandez Y, Zubizarreta L, Calvo EG, Bermudez JM (2010) Review: microwave heating processes involving carbon materials. *Fuel Process Technol* 91:1–8
- Meng, J., Kong, H., Han, Z., Wang, C., Zhu, G., Xie, S., & Xu, H. (2009). Enhancement of nanofibrous scaffold of multiwalled carbon nanotubes/polyurethane composite to the fibroblasts growth and biosynthesis. *Journal of Biomedical Materials Research Part A*, 88(1), 105-116.
- Mo, Z., Shi, H., Chen, H., Niu, G., Zhao, Z., & Wu, Y. (2009). Synthesis of graphite nanosheets/polyaniline nanorods composites with ultrasonic and conductivity. *Journal of applied polymer science*, 112(2), 573-578.
- Nasiri, S. H., Moravvej-Farshi, M. K., & Faez, R. (2012). Time domain analysis of graphene nanoribbon interconnects based on transmission line model. *Iranian Journal of Electrical and Electronic Engineering*, 8, 37-44.
- Navratilova, Z., Wojtowicz, P., Vaculikova, L., & Sugarkova, V. (2007). Sorption of alkylammonium cations on montmorillonite. *Acta Geodynamica et Geomaterialia*, 4(3), 59.
- Ni, P., Li, J., Suo, J., & Li, S. (2004). Novel polyether polyurethane/clay nanocomposites synthesized with organic-modified montmorillonite as chain extenders. *Journal of applied polymer science*, 94(2), 534-541.
- Novoselov, K. S., Jiang, D., Schedin, F., Booth, T. J., Khotkevich, V. V., Morozov, S. V., & Geim, A. K. (2005). Two-dimensional atomic crystals. *Proceedings of the National Academy of Sciences of the United States of America*, 102(30), 10451-10453.
- Nuruddin^{1a}, M., Gupta^{2b}, R., Tcherbi-Narteh^{1c}, A., Hosur^{1d}, M., & Jeelanile, S. (2015). Synergistic Effect of Graphene Nanoplatelets and Nanoclay on Epoxy Polymer Nanocomposites.
- Pal, S., Chandra, S., Phan, M. H., Mukherjee, P., & Srikanth, H. (2009). Carbon nanostraws: nanotubes filled with superparamagnetic nanoparticles. *Nanotechnology*, 20(48), 485604.

- Panupakorn, P., Chaichana, E., Praserttham, P., & Jongsomjit, B. (2013). Polyethylene/clay nanocomposites produced by in situ polymerization with zirconocene/MAO catalyst. *Journal of Nanomaterials*, 2013, 2.
- Panwar, V., & Mehra, R. M. (2008). Study of electrical and dielectric properties of styrene-acrylonitrile/graphite sheets composites. *European Polymer Journal*, 44(7), 2367-2375.
- Park, S. B., Lee, M. S., & Park, M. (2014). Study on lowering the percolation threshold of carbon nanotube-filled conductive polypropylene composites. *Carbon Letters*, 15(2), 117-124.
- Park, S., & Ruoff, R. S. (2009). Chemical methods for the production of graphenes. *Nature nanotechnology*, 4(4), 217-224.
- Paul, D. R., & Robeson, L. M. (2008). Polymer nanotechnology: nanocomposites. *Polymer*, 49(15), 3187-3204.
- Pawar, S. J., Kuo, W. S., & Huang, J. H. Exfoliated Graphite/Graphite Nanosheet-Epoxy Nanocomposites Revealed from the View Point of Synthesis Bottleneck. *Maharakham International Journal of Engineering Technology*, 22.
- Peeterbroeck, S., Alexandre, M., Nagy, J. B., Pirlot, C., Fonseca, A., Moreau, N., ... & Dubois, P. (2004). Polymer-layered silicate-carbon nanotube nanocomposites: unique nanofiller synergistic effect. *Composites Science and Technology*, 64(15), 2317-2323.
- Peng, H., Miao, Y. E., Tjiu, W. W., & Shen, L. (2014). Synergistic effect of carbon nanotubes and layered double hydroxides on the mechanical reinforcement of nylon-6 nanocomposites. *Chinese Journal of Polymer Science*, 32(10), 1276-1285.
- Potts, J. R., Dreyer, D. R., Bielawski, C. W., & Ruoff, R. S. (2011). Graphene-based polymer nanocomposites. *Polymer*, 52(1), 5-25.
- Q. Fu, C. Tang, H. Deng, Q. Zhang, Wiley/Scrivener Publishing, Hoboken, NJ/Salem, MA, 83(2010).
- Qin, F., & Peng, H. X. (2013). Ferromagnetic microwires enabled multifunctional composite materials. *Progress in Materials Science*, 58(2), 183-259.
- Quan, H., Zhang, B. Q., Zhao, Q., Yuen, R. K., & Li, R. K. (2009). Facile preparation and thermal degradation studies of graphite nanoplatelets (GNPs) filled thermoplastic polyurethane (TPU) nanocomposites. *Composites Part A: Applied Science and Manufacturing*, 40(9), 1506-1513.

- Ramanathan, T., Abdala, A. A., Stankovich, S., Dikin, D. A., Herrera-Alonso, M., Piner, R. D., ... & Brinson, L. C. (2008). Functionalized graphene sheets for polymer nanocomposites. *Nature nanotechnology*, 3(6), 327-331.
- Raulo, A., Suin, S., Paria, S., & Khatua, B. B. (2015). Expanded graphite (EG) as a potential filler in the reduction of percolation threshold of multiwall carbon nanotubes (MWCNT) in the PMMA/HDPE/EG/MWCNT nanocomposites. *Polymer Composites*.
- Ray, S. S. (2014). Recent Trends and Future Outlooks in the Field of Clay-Containing Polymer Nanocomposites. *Macromolecular Chemistry and Physics*, 215(12), 1162-1179.
- Rehab, A., & Salahuddin, N. (2005). Nanocomposite materials based on polyurethane intercalated into montmorillonite clay. *Materials Science and Engineering: A*, 399(1), 368-376.
- Rodrigues, P. C., & Akcelrud, L. (2003). Networks and blends of polyaniline and polyurethane: correlations between composition and thermal, dynamic mechanical and electrical properties. *Polymer*, 44(22), 6891-6899.
- Safdari, M., & Al-Haik, M. S. (2013). Synergistic electrical and thermal transport properties of hybrid polymeric nanocomposites based on carbon nanotubes and graphite nanoplatelets. *Carbon*, 64, 111-121.
- Sahay, H., Kumar, S., Upadhyay, S. N., & Upadhyay, Y. D. (1980). Solubility of benzoic acid in aqueous polyethylene glycol solutions. *Journal of Chemical and Engineering Data*, 25(4), 383-384.
- Sahoo, N. G., Jung, Y. C., Yoo, H. J., & Cho, J. W. (2007). Influence of carbon nanotubes and polypyrrole on the thermal, mechanical and electroactive shape-memory properties of polyurethane nanocomposites. *Composites Science and Technology*, 67(9), 1920-1929.
- Sandler, J. K. W., Kirk, J. E., Kinloch, I. A., Shaffer, M. S. P., & Windle, A. H. (2003). Ultra-low electrical percolation threshold in carbon-nanotube-epoxy composites. *Polymer*, 44(19), 5893-5899.
- Sari, B., Talu, M., Yildirim, F., & Balci, E. K. (2003). Synthesis and characterization of polyurethane/polythiophene conducting copolymer by electrochemical method. *Applied Surface Science*, 205(1), 27-38.
- Sarto, M. S., D'Aloia, A. G., Tamburrano, A., & De Bellis, G. (2012). Synthesis, modeling, and experimental characterization of graphite nanoplatelet-based composites

for EMC applications. *Electromagnetic Compatibility, IEEE Transactions on*, 54(1), 17-27.

- Schelkunoff, S. A. (1934). The electromagnetic theory of coaxial transmission lines and cylindrical shields. *Bell System Technical Journal*, 13(4), 532-579.
- Sengupta, R., Bhattacharya, M., Bandyopadhyay, S., & Bhowmick, A. K. (2011). A review on the mechanical and electrical properties of graphite and modified graphite reinforced polymer composites. *Progress in polymer science*, 36(5), 638-670.
- Shang, S., Zeng, W., & Tao, X. M. (2011). High stretchable MWNTs/polyurethane conductive nanocomposites. *Journal of Materials Chemistry*, 21(20), 7274-7280.
- Shanmuganathan, K., Deodhar, S., Dembsey, N., Fan, Q., Calvert, P. D., Warner, S. B., & Patra, P. K. (2007). Flame retardancy and char microstructure of nylon-6/layered silicate nanocomposites. *Journal of applied polymer science*, 104(3), 1540-1550.
- Shen, J. W., Chen, X. M., & Huang, W. Y. (2003). Structure and electrical properties of grafted polypropylene/graphite nanocomposites prepared by solution intercalation. *Journal of applied polymer science*, 88(7), 1864-1869.
- Solarski, S., Benali, S., Rochery, M., Devaux, E., Alexandre, M., Monteverde, F., & Dubois, P. (2005). Synthesis of a polyurethane/clay nanocomposite used as coating: Interactions between the counterions of clay and the isocyanate and incidence on the nanocomposite structure. *Journal of applied polymer science*, 95(2), 238-244.
- Song, L., Hu, Y., Li, B., Wang, S., Fan, W., & Chen, Z. (2003). A study on the synthesis and properties of polyurethane/clay nanocomposites. *International Journal of Polymer Analysis and Characterization*, 8(5), 317-326.
- Srivastava, N. K., & Mehra, R. M. (2008). Study of structural, electrical, and dielectric properties of polystyrene/foiated graphite nanocomposite developed via in situ polymerization. *Journal of applied polymer science*, 109(6), 3991-3999.
- Stankovich, S., Dikin, D. A., Compton, O. C., Dommett, G. H., Ruoff, R. S., & Nguyen, S. T. (2010). Systematic post-assembly modification of graphene oxide paper with primary alkylamines. *Chemistry of Materials*, 22(14), 4153-4157.
- Stankovich, S., Dikin, D. A., Dommett, G. H., Kohlhaas, K. M., Zimney, E. J., Stach, E. A., ... & Ruoff, R. S. (2006). Graphene-based composite materials. *Nature*, 442(7100), 282-286.

- Stankovich, S., Dikin, D. A., Piner, R. D., Kohlhaas, K. A., Kleinhammes, A., Jia, Y., ... & Ruoff, R. S. (2007). Synthesis of graphene-based nanosheets via chemical reduction of exfoliated graphite oxide. *Carbon*, 45(7), 1558-1565.
- Steffan, P., Vrba, R., & Drinovsky, J. (2010, April). A New Measuring Method Suitable for Measuring Shielding Efficiency of Composite Materials with Carbon Fibers. In *Systems (ICONS), 2010 Fifth International Conference on* (pp. 186-189). IEEE.
- Tang, C., Xiang, L., Su, J., Wang, K., Yang, C., Zhang, Q., & Fu, Q. (2008). Largely improved tensile properties of chitosan film via unique synergistic reinforcing effect of carbon nanotube and clay. *The Journal of Physical Chemistry B*, 112(13), 3876-3881.
- Thirumal, M., Khastgir, D., Singha, N. K., Manjunath, B. S., & Naik, Y. P. (2009). Effect of a nanoclay on the mechanical, thermal and flame retardant properties of rigid polyurethane foam. *Journal of Macromolecular Science®*, Part A: Pure and Applied Chemistry, 46(7), 704-712.
- Thomassin, J. M., Jérôme, C., Pardoën, T., Bailly, C., Huynen, I., & Detrembleur, C. (2013). Polymer/carbon based composites as electromagnetic interference (EMI) shielding materials. *Materials Science and Engineering: R: Reports*, 74(7), 211-232.
- Uhl, F. M., Yao, Q., Nakajima, H., Manias, E., & Wilkie, C. A. (2005). Expandable graphite/polyamide-6 nanocomposites. *Polymer Degradation and Stability*, 89(1), 70-84.
- Valentini, M., Piana, F., Pionteck, J., Lamastra, F. R., & Nanni, F. (2015). Electromagnetic properties and performance of exfoliated graphite (EG)-Thermoplastic polyurethane (TPU) nanocomposites at microwaves. *Composites Science and Technology*, 114, 26-33.
- Vicentini, D. S., Barra, G. M., Bertolino, J. R., & Pires, A. T. (2007). Polyaniline/thermoplastic polyurethane blends: Preparation and evaluation of electrical conductivity. *European Polymer Journal*, 43(10), 4565-4572.
- Viculis, L. M., Mack, J. J., Mayer, O. M., Hahn, H. T., & Kaner, R. B. (2005). Intercalation and exfoliation routes to graphite nanoplatelets. *Journal of Materials Chemistry*, 15(9), 974-978.
- Wakabayashi, K., Pierre, C., Dikin, D. A., Ruoff, R. S., Ramanathan, T., Brinson, L. C., & Torkelson, J. M. (2008). Polymer-graphite nanocomposites: effective dispersion and major property enhancement via solid-state shear pulverization. *Macromolecules*, 41(6), 1905-1908.

- Wang, G., Yang, J., Park, J., Gou, X., Wang, B., Liu, H., & Yao, J. (2008). Facile synthesis and characterization of graphene nanosheets. *The Journal of Physical Chemistry C*, 112(22), 8192-8195.
- Wang, H. L., Gopalan, A., & Wen, T. C. (2003). A novel lithium single ion based polyurethane electrolyte for light-emitting electrochemical cell. *Materials chemistry and physics*, 82(3), 793-800.
- Wang, H., Xu, P., Meng, S., Zhong, W., Du, W., & Du, Q. (2006). Poly (methyl methacrylate)/silica/titania ternary nanocomposites with greatly improved thermal and ultraviolet-shielding properties. *Polymer degradation and stability*, 91(7), 1455-1461.
- Wang, S. J., Geng, Y., Zheng, Q., & Kim, J. K. (2010). Fabrication of highly conducting and transparent graphene films. *Carbon*, 48(6), 1815-1823.
- Wang, T. L., Yang, C. H., Shieh, Y. T., & Yeh, A. C. (2009). Synthesis and properties of conducting organic/inorganic polyurethane hybrids. *European Polymer Journal*, 45(2), 387-397.
- Wang, Z., & Pinnavaia, T. J. (1998). Hybrid organic-inorganic nanocomposites: exfoliation of magadiite nanolayers in an elastomeric epoxy polymer. *Chemistry of Materials*, 10(7), 1820-1826.
- Wei, T., Fan, Z., Luo, G., Zheng, C., & Xie, D. (2009). A rapid and efficient method to prepare exfoliated graphite by microwave irradiation. *Carbon*, 47(1), 337-339.
- Wei, T., Luo, G., Fan, Z., Zheng, C., Yan, J., Yao, C., ... & Zhang, C. (2009). Preparation of graphene nanosheet/polymer composites using in situ reduction-extractive dispersion. *Carbon*, 47(9), 2296-2299.
- Weng, W., Chen, G., Wu, D., Chen, X., Lu, J., & Wang, P. (2004). Fabrication and characterization of nylon 6/foiled graphite electrically conducting nanocomposite. *Journal of Polymer Science Part B: Polymer Physics*, 42(15), 2844-2856.
- Wu, H., Li, X., Chen, J., Shao, L., Huang, T., Shi, Y., & Wang, Y. (2013). Reinforcement and toughening of polypropylene/organic montmorillonite nanocomposite using β -nucleating agent and annealing. *Composites Part B: Engineering*, 44(1), 439-445.
- Wycisk, R., Poźniak, R., & Pasternak, A. (2002). Conductive polymer materials with low filler content. *Journal of electrostatics*, 56(1), 55-66.

- Xiao, M., Sun, L., Liu, J., Li, Y., & Gong, K. (2002). Synthesis and properties of polystyrene/graphite nanocomposites. *Polymer*, 43(8), 2245-2248.
- Xiong, J., Liu, Y., Yang, X., & Wang, X. (2004). Thermal and mechanical properties of polyurethane/montmorillonite nanocomposites based on a novel reactive modifier. *Polymer Degradation and Stability*, 86(3), 549-555.
- Xiong, P., Huang, H., & Wang, X. (2014). Design and synthesis of ternary cobalt ferrite/graphene/polyaniline hierarchical nanocomposites for high-performance supercapacitors. *Journal of Power Sources*, 245, 937-946.
- Xu, Y. J., Zhuang, Y., & Fu, X. (2010). New insight for enhanced photocatalytic activity of TiO₂ by doping carbon nanotubes: a case study on degradation of benzene and methyl orange. *The Journal of Physical Chemistry C*, 114(6), 2669-2676.
- Xu, Z., Tang, X., Gu, A., & Fang, Z. (2007). Novel preparation and mechanical properties of rigid polyurethane foam/organoclay nanocomposites. *Journal of applied polymer science*, 106(1), 439-447.
- Yan, D. X., Dai, K., Xiang, Z. D., Li, Z. M., Ji, X., & Zhang, W. Q. (2011). Electrical conductivity and major mechanical and thermal properties of carbon nanotube-filled polyurethane foams. *Journal of applied polymer science*, 120(5), 3014-3019.
- Yang, Y., Wang, X., Liu, L., Xie, X., Yang, Z., Li, R. K. Y., & Mai, Y. W. (2007). Structure and photoresponsive behaviors of multiwalled carbon nanotubes grafted by polyurethanes containing azobenzene side chains. *The Journal of Physical Chemistry C*, 111(30), 11231-11239.
- Yasmin, A., Luo, J. J., & Daniel, I. M. (2006). Processing of expanded graphite reinforced polymer nanocomposites. *Composites Science and Technology*, 66(9), 1182-1189.
- Yasmin, A., Luo, J. J., & Daniel, I. M. (2006). Processing of expanded graphite reinforced polymer nanocomposites. *Composites Science and Technology*, 66(9), 1182-1189.
- Yerawar, G.R. (2012). Characterization of Chemically Synthesized Polyaniline-Zinc Oxide Nanocomposites. *Der Pharma Chemica*, 4 (3), 1288-1291.
- Yoshida, A., Hishiyama, Y., & Inagaki, M. (1991). Exfoliated graphite from various intercalation compounds. *Carbon*, 29(8), 1227-1231.

- Yousefi, N., Gudarzi, M. M., Zheng, Q., Lin, X., Shen, X., Jia, J., ... & Kim, J. K. (2013). Highly aligned, ultralarge-size reduced graphene oxide/polyurethane nanocomposites: mechanical properties and moisture permeability. *Composites Part A: Applied Science and Manufacturing*, 49, 42-50.
- Yu, C., & Li, B. (2008). Preparation and characterization of carboxymethyl polyvinyl alcohol-graphite nanosheet composites. *Polymer Composites*, 29(9), 998-1005.
- Yu, H., Ran, Q., Wu, S., & Shen, J. (2008). Structure and property of PU/MMT nanocomposites by in-situ polymerization. *Polymer-Plastics Technology and Engineering*, 47(6), 619-622.
- Zeng, Q. H., Yu, A. B., Lu, G. Q., & Paul, D. R. (2005). Clay-based polymer nanocomposites: research and commercial development. *Journal of nanoscience and nanotechnology*, 5(10), 1574-1592.
- Zhang, C. S., Ni, Q. Q., Fu, S. Y., & Kurashiki, K. (2007). Electromagnetic interference shielding effect of nanocomposites with carbon nanotube and shape memory polymer. *Composites Science and Technology*, 67(14), 2973-2980.
- Zhang, X. F., Guan, P. F., & Dong, X. L. (2010). Multidielectric polarizations in the core/shell Co/graphite nanoparticles. *Applied Physics Letters*, 96(22), 223111.
- Zhang, X., Shen, L., Xia, X., Wang, H., & Du, Q. (2008). Study on the interface of phenolic resin/expanded graphite composites prepared via in situ polymerization. *Materials Chemistry and Physics*, 111(2), 368-374.
- Zhang, Y. X., Gao, B., Li Puma, G., Ray, A. K., & Zeng, H. C. (2010). Self-assembled Au/TiO₂/CNTs ternary nanocomposites for photocatalytic applications. *Science of Advanced Materials*, 2(4), 503-513.
- Zhao, Y. F., Xiao, M., Wang, S. J., Ge, X. C., & Meng, Y. Z. (2007). Preparation and properties of electrically conductive PPS/expanded graphite nanocomposites. *Composites science and technology*, 67(11), 2528-2534.
- Zheng, G., Wu, J., Wang, W., & Pan, C. (2004). Characterizations of expanded graphite/polymer composites prepared by in situ polymerization. *Carbon*, 42(14), 2839-2847.
- Zheng, W., Lu, X., & Wong, S. C. (2004). Electrical and mechanical properties of expanded graphite-reinforced high-density polyethylene. *Journal of Applied Polymer Science*, 91(5), 2781-2788.

LIST OF PUBLICATIONS

SCI Indexed Journals:

1. Pooja Puri, Rajeev Mehta, and Sunita Rattan “Synthesis of Conductive Polyurethane/Graphite Composites for Electromagnetic Interference Shielding” *Journal of Electronic Materials*, Springer Vol. 44, No. 11, pp 4255-4268. **Published**
2. Pooja Puri, Rajeev Mehta, and Sunita Rattan “Synthesis and Mechanical Properties of Polyurethane/Clay Nanocomposites” *Journal of Optoelectronics and Advanced Materials*, Vol. 16, No. 9-10, September - October 2014, pp 1126 – 1130. **Published.**
3. Pooja Puri, Rajeev Mehta, and Sunita Rattan “Synergistic Effects of Clay and GNPs on Electrical and Mechanical Properties of PU/GNP/OMMT Ternary Composite” *Journal of Optoelectronics and Advanced Materials*, Vol. 17, No. 3-4, March - April 2015, pp 477-483. **Published.**

Conference Proceeding:

1. Pooja Puri, Rajeev Mehta, and Sunita Rattan “Polymer Nanocomposite with High Conductivity and Mechanical Strength” ICPPC-2010 Second International Conference on Polymer Processing and Characterization Kottayam, Kerala, India 2010 **Published.**